

สมบัติเชิงกายภาพของอนุภาคฮิกส์โบซอนที่ไม่อิสระต่อมวลมีซอน
แบบสเกลาร์เทียมในแบบจำลองเพอร์เทอร์เบทีฟไคแรลควาร์ก

ชลัมภ์ อุ่นอารีย์

วิทยานิพนธ์นี้เป็นส่วนหนึ่งของการศึกษาตามหลักสูตรปริญญาวิทยาศาสตรดุษฎีบัณฑิต
สาขาฟิสิกส์
มหาวิทยาลัยเทคโนโลยีสุรนารี
ปีการศึกษา 2550

**DEPENDENCE OF BARYON OCTET
PROPERTIES ON PSEUDOSCALAR MESON
MASSES IN THE PERTURBATIVE CHIRAL
QUARK MODEL**

Chalump Oonariya

**A Thesis Submitted in Partial Fulfillment of the Requirements for the
Degree of Doctor of Philosophy in Physics
Suranaree University of Technology
Academic Year 2007**

**DEPENDENCE OF BARYON OCTET PROPERTIES
ON PSEUDOSCALAR MESON MASSES IN THE
PERTURBATIVE CHIRAL QUARK MODEL**

Suranaree University of Technology has approved this thesis submitted in partial fulfillment of the requirements for the Degree of Doctor of Philosophy.

Thesis Examining Committee

(Asst. Prof. Col. Dr. Worasit Uchai)

Chairperson

(Assoc. Prof. Dr. Yupeng Yan)

Member (Thesis Advisor)

(Assoc. Prof. Dr. Puangratana Pairor)

Member

(Asst. Prof. Dr. Chinorat Kobdaj)

Member

(Asst. Prof. Dr. Viroj Limkaisang)

Member

(Prof. Dr. Pairote Sattayatham)

Vice Rector for Academic Affairs

(Assoc. Prof. Dr. Prapan Manyum)

Dean of Institute of Science

ชลัมภ์ อุ่นอารีย์: สมบัติเชิงกายภาพของอนุภาคอัฐแบรียอนที่ไม่อิสระต่อมวลมี-
ซอนแบบสเกลาร์เทียมในแบบจำลองเพอร์เทอร์เบทีฟไครเรลควาร์ก.

(DEPENDENCE OF BARYON OCTET PROPERTIES ON PSEUDOSCALAR
MESON MASSES IN THE PERTURBATIVE CHIRAL QUARK MODEL)

อาจารย์ที่ปรึกษา: รองศาสตราจารย์ ดร.ยูเป็ง แยน, 95 หน้า.

แบบจำลองเพอร์เทอร์เบทีฟไครเรลควาร์กได้รับการพิสูจน์แล้วว่ามีความเหมาะสม
ในการอธิบายสมบัติของแบรียอนหลายมุมมอง เช่น ฟอรัมแพกเตอร์เชิงแกน ฟอรัม-
แพกเตอร์เชิงแม่เหล็กและเชิงประจุ ไพออน-นิวคลีออน ซิกมาเทอม มวลแบรียอนที่
สถานะพื้นและอื่น ๆ แบบจำลองเพอร์เทอร์เบทีฟไครเรลถูกอธิบายด้วยกลุ่มควาร์กเปล่า
สามตัวแบบสัมพัทธภาพกักอยู่ภายใต้ศักย์สถิตย และถูกเสริมด้วยกลุ่มหมอกของโกลด์-
สโตนโบซอนแบบสเกลาร์เทียม(หมอกมีซอน) ซึ่งเป็นไปตามเงื่อนไขสมมาตรแบบไครเรล
อันตรกิริยาของควาร์กกับโกลด์สโตนโบซอน ถูกนำมาเป็นฐานของแบบจำลองแบบไม่เป็น
เชิงเส้น เมื่อพิจารณาสมามมีซอนว่าเป็นความผันผวนเพียงเล็กน้อย แบบจำลองจะ มี
การจำกัดอันตรกิริยาควาร์ก-มีซอนแบบเชิงเส้น ในงานวิจัยนี้ แบบจำลองเพอร์เทอร์-
เบทีฟไครเรลควาร์กที่หนึ่งรูป ถูกประยุกต์ขึ้นเพื่ออธิบายกระแสมวลควาร์ก (มวลไพออน)
ที่ไม่เป็นอิสระของฟอรัมแพกเตอร์เชิงแม่เหล็กและประจุ รัศมีเชิงประจุและค่าโมเมนต์
แม่เหล็ก ขอบเขตงานวิจัยได้กำหนดมวลของควาร์กที่ค่ามากสัมพันธ์กับมวลของไพออน
ที่ระดับ 0.6 จีอีวีขึ้นไป และลดลงสู่ค่ามวลไพออนเชิงกายภาพ (มวลที่ตรวจวัดได้ในห้อง
ปฏิบัติการ) ในขีดจำกัดแบบไครเรล กล่าวคือมวลไพออนที่มีค่าเข้าสู่ศูนย์ คิวซีดีที่พลังงาน
ต่ำถูกทำให้ใกล้เคียงจริงมากขึ้นในทฤษฎีสนามแบบยังผล ประกอบกับการแตกของ
สมมาตรแบบไครเรลที่เกิดขึ้นเองด้วยการสมมติสถานะไพออนแบบไร้มวล (ถือเป็นองค์
ประกอบที่สำคัญของโครงสร้างฮาดรอนที่พลังงานต่ำ ๆ)

งานวิจัยนี้พบว่า ผลการคำนวณทางทฤษฎีสำหรับ มวล ฟอรัมแพกเตอร์เชิงแม่-
เหล็กไฟฟ้าและโมเมนต์แม่เหล็กของอนุภาคอัฐแบรียอน เผยให้เห็นหน้าที่ที่สำคัญของ
หมอกมีซอนในบริเวณที่มีการถ่ายโอนโมเมนต์ต่ำ ๆ ความสอดคล้องดังกล่าวเป็นผลมา

จากหมอกมีซอนรอบนอกแบร็ออน ดังนั้นหมอกมีซอนจึงมีความสำคัญสำหรับการถ่ายโอนโมเมนตัมที่ค่าน้อย ๆ เท่านั้น การทำนายผลเชิงทฤษฎีสำหรับการขึ้นกับมวลมีซอนที่มีต่อสมบัติของอนุภาคอัลู แบร็ออนให้ผลพอใช้กับการคำนวณแบบแลตทิซควีซีดีในปัจจุบัน และการประมาณค่าแบบโคแรล งานวิจัยอาจสรุปได้ว่าการประมาณค่าที่หนึ่งดูมีความเหมาะสมเพื่ออธิบายสมบัติของอนุภาคอัลูแบร็ออนที่ขึ้นกับมวลมีซอน

สาขาฟิสิกส์

ปีการศึกษา 2550

ลายมือชื่อนักศึกษา _____

ลายมือชื่ออาจารย์ที่ปรึกษา _____

ลายมือชื่ออาจารย์ที่ปรึกษาร่วม _____

CHALUMP OONARIYA : DEPENDENCE OF BARYON OCTET
PROPERTIES ON PSEUDOSCALAR MESON MASSES IN THE
PERTURBATIVE CHIRAL QUARK MODEL. THESIS ADVISOR :
ASSOC. PROF. YUPENG YAN, Ph.D. 95 PP.

PERTURBATIVE CHIRAL QUARK MODEL/ MAGNETIC MOMENTS/
ELECTROMAGNETIC FORM FACTORS/ MESON CLOUD.

The Perturbative Chiral Quark Model (PCQM) has been verified successful in describing many aspects of baryon properties such as axial form factors, electromagnetic form factors, pion-nucleon sigma term, ground-state masses of baryons and other baryon properties. In the PCQM baryons are described by three relativistic valence quarks confined in a static potential, which are supplemented by a cloud of pseudoscalar Goldstone bosons (meson cloud), as required by chiral symmetry. The interaction of quarks with Goldstone bosons (π, K, η) is introduced on the basis of the nonlinear model. When considering mesons fields as small fluctuations we restrict ourselves to the linear form of the meson-quark interaction.

In this thesis PCQM at one loop is applied to describe the current quark mass (pion mass) dependence of the electromagnetic form factors, charge radii and magnetic moments, so far determined at relatively large quark masses corresponding to pion masses of $m_\pi \geq 0.6$ GeV, down to physical values of m_π (≈ 0.14 GeV). In the chiral limit, with $m_\pi \rightarrow 0$, QCD at low energies is realized in the form of an effective field theory with spontaneously broken chiral symmetry, with massless pions as the primary active degrees of freedom (an important component of hadron structure at low energy and low momentum scales).

It is found that the theoretical results for the masses, electromagnetic form factors and magnetic moments of the octet baryons display a significant role of the

meson cloud at low momentum transfers. This is consistent with that meson clouds form the outskirts of baryons and hence the meson cloud contributions should be significant for only small momentum transfers. The theoretical predictions for the meson mass dependence of baryon octet properties are fairly consistent with present lattice QCD calculation and chiral extrapolations of these results. Given also the simplicity of the PCQM approach, this work may conclude that the evaluation at one loop is sufficient to correctly describe the pion mass dependence of the discussed observables.

School of Physics

Academic Year 2007

Student's Signature_____

Advisor's Signature_____

Co-advisor's Signature_____

ACKNOWLEDGEMENTS

First of all, I am very grateful to Assoc. Prof. Dr. Yupeng Yan for being my thesis advisor and Asst. Prof. Dr. Chinorat Kobdaj as my co-advisor for their guidance, taught me the scientific thought and attitude of a physicist thinking. I have enhanced very important experiences during my work.

I am ultimately grateful to Prof. Dr. Dr. h.c. mult. Amand Faessler for his guidance and support my work. Prof. Dr. Thomas Gutsche and Dr. Valery E. Lyubovitskij for their constant guidance and substantial discussions at the Tuebingen time.

I would like to thank Asst. Prof. Col. Dr. Worasit Uchai, Assoc. Prof. Dr. Puangratana Pairor, and Asst. Prof. Dr. Viroj Limkaisang for sitting at the thesis committee and giving me advices during my study at SUT.

I would like to special thank Mr. Songvudhi Chimchinda for discussions and his helpfulness in physics when we stayed in Germany and Mr. Suppiya Siranan for his suggestions in \LaTeX . Thanks Mr. Chakrit Nualchimplee for discussions and his helpfulness here. Thanks Mr. Ayut Limpirat, Mr. Daris Samart, and Mr. Kritsada Kittimanapun are young brothers when we became the colleague in working group.

The research is supported in part by Thai Meteorological Department and the fellowship was supported by the Deutscher Akademischer Austausch Dienst when I stayed to work my research in Tuebingen, Germany.

Finally, I am extremely grateful to my parents for understanding encouragement from yesterday until today and beyond tomorrow absolutely.

Chalump Oonariya

Contents

ABSTRACT IN THAI	4
ABSTRACT IN ENGLISH	6
ACKNOWLEDGEMENTS	8
Contents	9
List of Tables	11
List of Figures	12
Chapter	
I INTRODUCTION	1
1.1 Introduction to Quantum Chromodynamics	1
1.2 Introduction to Lattice QCD	5
1.3 Introduction to Chiral Effective Field Theory	7
1.4 Thesis Arrangement	10
II PERTURBATIVE CHIRAL QUARK MODEL	12
III BARYON PROPERTIES IN PCQM	19
3.1 Nucleon Mass	19
3.2 Electromagnetic Form Factors in PCQM	22
IV RESULTS	28
V DISCUSSION AND CONCLUSIONS	44
REFERENCES	46

CONTENTS (Continued)

	Page
APPENDICES	
Appendix A SOLUTIONS OF THE DIRAC EQUATION FOR THE EFFECTIVE POTENTIAL	56
Appendix B γ -MATRICES AND TRACE TECHNOLOGY	63
Appendix C BASIC NOTATIONS OF THE SU(3) GROUP	67
Appendix D THE ELECTROMAGNETIC FORM FACTORS IN BREIT FRAME	70
Appendix E PUBLICATION PAPER	80
CURRICULUM VITAE	95

List of Tables

Table		Page
4.1	Nucleon mass (in GeV) in the SU(2) and SU(3) versions and at different values for M_π^2	29
4.2	Nucleon magnetic moments in SU(2)	30
4.3	Nucleon magnetic moments in SU(3) for fixed masses M_K^2 and M_η^2	30
4.4	Nucleon charge and magnetic radii (fm ²)	31

List of Figures

Figure		Page
1.1	The coupling of strong interactions $\alpha_s(\mu)$ and its dependence on the energy scale: taken from the Particle Data Group	3
3.1	Diagrams contributing to the nucleon mass shift: meson cloud (a) and meson exchange diagram (b)	19
3.2	Diagrams contributing to the electromagnetic form factors of the baryon octet: three-quark diagram (a), three-quark counter-term diagram (b), meson cloud diagram (c), vertex correction diagram (d), and meson-in-flight diagram (e)	26
4.1	Dependence of nucleon mass m_N on meson masses M_Φ^2 : $m_N(M_\pi^2)$ in SU(2) (dotted line) and $m_N(M_\pi^2)$, $m_N(M_K^2)$ $m_N(M_\eta^2)$ in SU(3) (the other lines)	32
4.2	Dependence of nucleon mass m_N on pion mass M_π^2 : $m_N(M_\pi^2)$ in SU(2) (dotted line), SU(3) (solid line) and from lattice QCD (Procura et al., 2006b) (the others) at order p^3 and p^4	33
4.3	Pion-mass dependence of nucleon mass $m_N(M_\pi^2)$ in SU(2) (dotted line) and in SU(3)(solid line) compared to lattice data from various collaborations	34

LIST OF FIGURES (Continued)

Figure		Page
4.4	M_π^2 -dependence of the proton magnetic moment $\mu_p(M_\pi^2)$ to one-loop from sum rules (Holstein et al., 2005) (dotted curve), lattice QCD (Wang et al., 2007) (dashed curve) and our results in SU(3) (solid curve)	35
4.5	M_π^2 -dependence of the neutron magnetic moment $\mu_n(M_\pi^2)$ to one-loop from QCD sum rules (Holstein et al., 2005) (dotted curve), lattice QCD (Wang et al., 2007) (dashed curve) and our results in SU(3) (solid curve)	35
4.6	M_π^2 -dependence of the nucleon magnetic moment $\mu_N(M_\pi^2)$, with $m_s = 50 - 200$ MeV: (a) for proton and (b) for neutron	36
4.7	Current quarks mass \hat{m} -dependence of the proton magnetic moment $\mu_p(M_\pi^2)$, with $m_s = 50 - 200$ MeV: (a) for proton and (b) for neutron	37
4.8	Nucleon magnetic moments as functions of M_π^2 , with various scale parameter: (a) for proton μ_p in SU(2), (b) for neutron μ_n in SU(2), (c) for proton μ_p in SU(3) and (d) for neutron μ_n in SU(3)	38
4.9	Proton charge form factor $G_E^p(Q^2)$ with various M_π^2 : (a) in SU(2) and (b) in SU(3)	39
4.10	Proton magnetic form factor $G_M^p(Q^2)$ for various M_π^2 (a) in SU(2) and (b) in SU(3). Neutron magnetic form factor $G_M^n(Q^2)$ for various M_π^2 (c) in SU(2) and (d) in SU(3)	40

LIST OF FIGURES (Continued)

Figure		Page
4.11	Dependence of μ_N on pion mass M_π^2 in SU(2): quark core dressed with cloud (solid line), bare quarks (dashed line), meson cloud (dotted line) and lattice QCD [solid squares taken from (Hackett-Jones et al., 2000b), and solid circle taken from (Lee et al., 2005a,b)] (a) for μ_p and (b) for μ_n	41
4.12	Dependence of μ_B on M_π^2 in SU(2): quark core dressed with cloud (solid line), quark core (dashed line), meson cloud (dotted line) and lattice QCD [solid squares taken from (Hackett-Jones et al., 2000b), and solid circle taken from (Lee et al., 2005a,b)] (a) μ_{Σ^+} , (b) μ_{Σ^-} , (c) μ_{Ξ^0} , (d) μ_{Ξ^-} , (e) μ_{Σ^0} , and (f) μ_Λ	42
D.1	Three-quark diagram	75
D.2	Three-quark counter-term diagram	76
D.3	Meson cloud diagram	76
D.4	Vertex correction diagram	78
D.5	Meson-in-flight diagram	79

Chapter I

INTRODUCTION

The work investigates the dependence of static properties of the octet baryons, such as masses, charge radii, electromagnetic form factors and magnetic moments on the pseudoscalar meson masses in the Perturbative Chiral Quark Model (PCQM) and compare the theoretical results with experimental data and lattice QCD (Quantum Chromodynamics) data and chiral extrapolations. Since the PCQM is one of the effect field theories derived in the spirit of QCD and the lattice QCD is a numerical approach to evaluate physical obserables in the framework of QCD, we would like first to give a brief description of QCD before we go to PCQM and lattice QCD.

1.1 Introduction to Quantum Chromodynamics

Fundamental particles like electron, photon and neutrinos are structureless and pointlike. In the 1960s a growing number of new particles was being discovered, and it became clear that they could not all be elementary. Physicists were looking for the true theory to explain this phenomenon. In 1964 Gell-Mann and Zweig provided a simple idea which solved the problem, they proposed that all mesons comprised of a quark and an antiquark and all baryons comprised of three quarks. Up to now, it has been accepted that quarks come in six flavors: u (up), d (down), s(strange), c (charm), b (bottom) and t (top), and carry fractional electric charge (up, charm and top quarks carry charge $+\frac{2}{3}e$, and down, strange and bottom carry charge $-\frac{1}{3}e$). Quarks also carry another property called color charge

which was introduced by (Greenberg, 1964), and by (Han and Nambu, 1965). Quarks and antiquarks combine together to form hadrons in such a way that all observed hadrons are color neutral and carry integer electric charge.

Quantum Chromodynamics (QCD) was proposed in the 1970s as a theory of the strong interactions, describing the quarks and gluons degree of freedoms in the Standard Model. The theory of QCD has a remarkable simplicity and elegance at the classical level, with its under-lying non-Abelian SU(3) color symmetry as revealed by a whole spectrum of contrasting behaviors over a wide range of energy scales, from confinement to asymptotic freedom, in addition to various possible phase transitions under extreme conditions. It was widely accepted after the discovery of asymptotic freedom by (Gross and Wilczek, 1973) and (Politzer, 1973) as it offered a satisfying explanation to some of the puzzling experimental results. Asymptotic freedom turned out to be a very useful property for studying high energy QCD. It allows one to treat the coupling constant perturbatively for sufficiently small distances and therefore calculate physical properties under consideration in a systematic and controlled manner. Confinement is an important property of the strong interaction that is widely accepted and incorporated into any model claiming to imitate strong QCD. Quark confinement is often defined as the absence of isolated quarks in nature as they have never been experimentally observed. Seeking for free quarks normally focus on free particles with fractional electrical charge. But the observation of a particle with fractional charge does not necessarily mean that a free quark has been observed. Although, at high energies it is perturbative, i.e. observables can be expanded in terms of the strong coupling constant α_s . However the theory becomes highly non-perturbative at low energies since α_s becomes large. The dependence of the coupling on the energy scale and the experimental data are shown in Fig. 1.1.

Quantum Chromodynamics (QCD), the nonabelian gauge theory of interacting

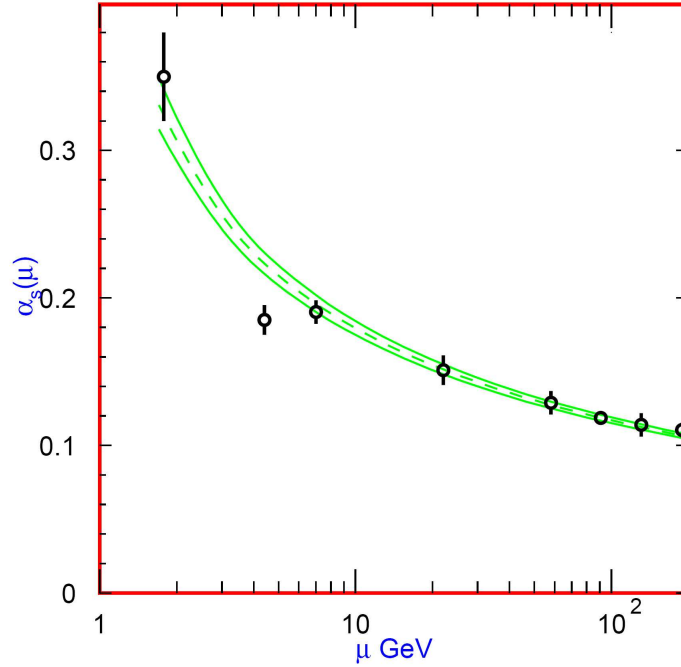


Figure 1.1 The coupling of strong interactions $\alpha_s(\mu)$ and its dependence on the energy scale: taken from the Particle Data Group

quarks and gluons, can be described by the QCD Lagrangian;

$$\mathcal{L} = \bar{\psi}_q(i\gamma^\mu D_\mu - m_q)\psi_q - \frac{1}{4}\mathcal{G}_{\mu\nu}^a\mathcal{G}^{a\mu\nu} \quad (1.1)$$

where $\mathcal{G}_{\mu\nu}^a$ is the non-abelian field strength tensor of the gluons, ψ_q is the quark wave function, D_μ is the covariant derivative, m_q is the quark mass, and a is an index for the three color charges. The field strength tensor of the gluons is given by

$$\mathcal{G}_{\mu\nu}^a = \partial_\mu A_\nu^a - \partial_\nu A_\mu^a - gf^{abc}A_\nu^b A_\mu^c \quad (1.2)$$

where A_μ^j ($j = a, b, c$) are the gauge potentials of the gluon fields, g is coupling con-

stant for the gluon, and f^{abc} are the complete antisymmetric structure constants of the gauge group SU(3). The covariant derivative is given by

$$D_\mu = \partial_\mu - ig \sum_a A_\mu^a T^a \quad (1.3)$$

where T^i are the gauge group generators in the representation matrices and the generators obey the commutation relation $[T^a, T^b] = if^{abc}T^c$. The coupling constant g is normally rewritten in terms of the strong coupling constant $\alpha_s = g^2/4\pi$.

Nowadays, it is widely believed that the true theory of strong interaction is QCD. The main confirmation of QCD comes from considering the processes at high energies and high momentum transfers, because of asymptotic freedom regime, the high precision of theoretical calculation is achieved and comparison with experimental data confirms QCD with a very good accuracy. In the domain of low energies and momentum transfers, because of confinement regime, the situation is more complicated: the strong coupling constant α_s is large and many loops perturbative calculations are needed. Understanding of their properties and structure will probably lead us to a deeper understanding of the mechanism of the strong interaction in nature. Experiments indicate that the nucleon is not a point-like particle but contains a subtle structure. First evidence has taken from investigating of the magnetic moment of the nucleon in which a strong deviation from the value of the point-like particle, because of an anomalous magnetic moment, was observed. An information of the spatial distribution of the electromagnetic current in the nucleon was achieved by elastic electron scattering on the nucleon. Deep inelastic scatterings of electrons on the nucleon, leads to the evidence for point-like scattering centers in the nucleon and consequently to the knowledge of the quarks and gluons degree of freedom. Other evidence for the structure of the

nucleon is taken from the enhance excitation spectrum of the nucleon. The searching for and the determination of the structure of the nucleon is one crucial task in nuclear and particle physics. Among all the fundamental interactions, the electromagnetic interaction of the nucleon gives an ultimate information. This leads to the knowledge of the electromagnetic structure of the nucleon which gives us the information of charge and current distribution in the nucleon. The important one for fulfilling measurement of the electromagnetic form factors of the nucleon from various laboratories leads to more precise data, which is significant for the theoretical study. QCD is still far from the final state of the strong interactions. One of the main problems is the difficulty to explain much of the experimental data on the particle properties from the first principles. In particularly QCD at low energies regime, a central role is played by the spontaneously and explicitly broken chiral symmetry, has been and still is the framework from the theoretical as well as experimental approach. The framework is actively studied both on theoretical and experimental sides. The useful methods are: the chiral effective theory, lattice calculations and various model approaches. The framework is desirable to have a compatibility of all these approaches with QCD calculations at low energy and momentum transfer square Q^2 about 1 GeV^2 .

1.2 Introduction to Lattice QCD

The lattice formulation of gauge theory was firstly proposed in 1974 by Wilson and individually by Polyakov and Wegner. They propose the implement of continuous SU(3) gauge symmetry of QCD and lattice field theory provided a non-perturbative definition of the functional integral. The basic idea was to replace continuous finite volume space-time with a four dimensional lattice size L^3T . The cells are separated by the lattice spacing a . The quarks and gluons

fields are supposed at discrete points. A theoretical point of view, the lattice and finite volume provide local gauge-invariant ultraviolet and infrared cutoffs regions, respectively. A great advantage of the lattice formulation of gauge theory is that the limit of strong coupling. It is particularly simple and revealed a confinement phenomenon. The lattice QCD calculation is needed the extremely high performance computing technology and incorporated with the efficiency of Monte Carlo simulations. There are still main problems in approximations must be done in order to obtain results and good accuracy in the technology of today. The lattice formulation of QCD is well established and is a powerful tool for studying the structure of nucleons. The computation of nucleon properties in lattice QCD is progressing with steadily increasing accuracy (Procura et al., 2006b)-(Ali Khan et al., 2004). Accurate computations of the nucleon mass with dynamical fermions and two active flavors are now possible (Ali Khan et al., 2002; Aoki et al., 2003) in lattice QCD. In practice, these computations are so far limited to relatively large quark masses. Direct simulations of QCD for light current quark masses, near the chiral limit, remain computationally intensive. To extract predictions for observables, lattice data generated at high current quark masses have to be extrapolated to the point of physical quark or pion mass. Therefore, one of the current aims in lattice QCD is to establish the quark mass dependence of quantities of physical interest, such as the nucleon mass, magnetic moments and form factors. The major tool in establishing the current quark mass dependence of lattice QCD results are methods based on chiral effective field theory. Recent extrapolation studies of lattice results concern the nucleon mass (Procura et al., 2006b, 2004; Young et al., 2003; Bernard et al., 2004; Frink et al., 2005), its axial vector coupling constant and magnetic moments (Young et al., 2003; Bernard et al., 2004; Holstein et al., 2005), the pion-nucleon sigma term, charge radii (Hackett-Jones et al., 2000a),

form factors (Hemmer and Weise, 2002; Hemmer et al., 2003b; Leinweber et al., 2000; Wang et al., 2007), and moments of structure functions (Detmold et al., 2001). Lattice QCD is still limited in the lattice spacing and size of volume used in the calculations due to the performance of computer. In last decade, there has been an improvement of chiral extrapolations within ChPT as well as techniques to try to get a handle on the systematic errors inherent to the lattice QCD calculation.

1.3 Introduction to Chiral Effective Field Theory

This thesis will report here on some of these in the framework of Chiral perturbation theory (ChPT) to the case when nucleons are presented and extended to a whole baryon octet with the quark states point of view. The ideas underlying ChPT have been generalized to the nucleon sector where one has to deal with a nonperturbative problem. The central idea of the effective field theory (EFT) approach was formulated by Weinberg in 1979. It is formulated in terms of the asymptotically observed states replacing the quark and gluon degrees of freedom of the fundamental theory. It requires both the knowledge of the general Lagrangian up to and including the given order one is interested in as well as an expansion scheme for observables. EFT has been used to study the low energies domain physical properties and is also able to describe and predict hadron spectrum, namely dynamical properties. The EFT is chiral perturbation theory which is governed by chiral symmetry, a symmetry of QCD. It has been considered as an approximate symmetry of the strong interactions. One of the most interesting features of QCD reveals spontaneous, explicit, and anomalous symmetry breaking which these broken symmetries can be analyzed underneath an effective field theory formulations. An important consequence of the spontaneous breakdown of a symmetry is the

existence of a massless mode, the so called Goldstone-boson (meson cloud). In our case, the Goldstone bosons are the pseudoscalar mesons, namely pion, kaon and η -meson (in the case of two-flavor sector is only pion). If chiral symmetry was a perfect symmetry of QCD, the mesons should be massless. Since chiral symmetry is only approximated, we expect the pion to have a finite value but small mass. This is the basic idea of chiral perturbation theory, which is very successful to describe physical pion mass. It is the chiral effective field theory (χ EFT) of the strong interactions at low energies. In the context of the strong interactions these ideas have been applied to the interactions among the Goldstone bosons of spontaneous symmetry breaking.

Chiral Quark Models were proposed early 1980s, describing the nucleon as a bound state of valence quarks with a surrounding pion cloud, have played an important role in the description of low-energy nucleon physics. These models include the two main features of low-energy hadron structure, confinement and chiral symmetry. The original type of chiral quark models assumes that the valence quarks content dominates the nucleon, thereby treating pion contributions perturbatively. Originally, this idea was formulated in the context of the cloudy bag model. By imposing chiral symmetry the MIT bag model was extended to include the interaction of the confined quarks with the pion fields on the bag surface. With the pion cloud treated as a perturbation on the basic features of the MIT bag, pionic effects generally improve the description of nucleon observables. By introducing a static quark potential of general form, these quark models contain a set of free parameters characterizing the confinement and/or the quark masses. The perturbative technique allows a fully quantized treatment of the pion field up to a given order in accuracy. Perturbative chiral quark models are formally close to chiral perturbation theory on the hadron level. Alternatively, when the pion

cloud is assumed to dominate the nucleon structure this effect has to be treated nonperturbatively. This model is based on the concept that the QCD instant on vacuum is responsible for the spontaneous breaking of chiral symmetry, which in turn leads to an effective chiral Lagrangian at low energy as derived from QCD. As a further development of chiral quark models with a perturbative treatment of the pion cloud. The Perturbative Chiral Quark Model (PCQM) is based on an effective chiral Lagrangian describing quarks as relativistic fermions moving in a self-consistent field (static potential). The model potential defines unperturbed wave functions of quarks which are subsequently used in the calculation of baryon properties. In the PCQM baryons are described by three relativistic valence quarks confined in a static potential, which are supplemented by a cloud of pseudoscalar Goldstone bosons (π , K and η -meson), as required by chiral symmetry. The interaction of quarks with Goldstone bosons is introduced on the basis of the nonlinear model. When considering mesons fields as small fluctuations we restrict ourselves to the linear form of the meson-quark interaction. With the derived interaction Lagrangian we do our perturbation theory in the expansion parameter $1/F$ (where F is the pion leptonic decay constant in the chiral limit).

The basic ideal of building blocks of the atomic nuclei, namely the nucleon is treated as identical particles of proton and neutron, has been playing an importance role in physics. In recent years nucleon properties have been in the focus of manifestly Lorentz covariant Chiral Perturbation Theory (ChPT), improved lattice QCD computations and chiral extrapolations (see e.g. Refs. (Becher and Leutwyler, 1999)-(Hemmert et al., 2003a)). The chiral expansion in chiral effective field theory (χ EFT) has been used to study the quark mass (pion mass) dependence of the magnetic moments, magnetic form factors and the axial-vector coupling constant (Hemmert et al., 2003b; Procura et al., 2006a) of the nucleon

for extrapolations of lattice QCD results, so far determined at relatively large quark masses corresponding to pion masses of $m_\pi \geq 0.8$ GeV, down to physical values of m_π . In the chiral limit, with $m_\pi \rightarrow 0$, QCD at low energies is realized in the form of an effective field theory with spontaneously broken chiral symmetry, with massless pions as the primary active degrees of freedom. The coupling of the chiral Goldstone bosons to these spin-1/2 matter field produces the so-called "pion-cloud" of the nucleon, an important component of nucleon structure at low energy and low momentum scales.

1.4 Thesis Arrangement

In this thesis we firstly investigate the dependence of nucleon properties (mass, magnetic moments and electromagnetic form factors) on pseudoscalar meson masses applying the perturbative chiral quark model (PCQM) (Lyubovitskij et al., 2001a,b,c, 2002a,b; Simkovic et al., 2002; Cheedket et al., 2004) and extend this work to a whole baryon octet. This simple phenomenological model has already been successfully applied to the charge and magnetic form factors of baryons, sigma terms, ground state masses of baryons, the electromagnetic $N \rightarrow \Delta$ transition, and other baryon properties (Lyubovitskij et al., 2001a,b,c, 2002a,b; Simkovic et al., 2002; Cheedket et al., 2004), and it has been extended, in Refs. (Faessler et al., 2006c,b), by constructing a framework which is manifestly Lorentz covariant and aims for consistency with ChPT.

Our strategy is as follows. First, we study the dependence of nucleon properties (mass, magnetic moments and electromagnetic form factors) on the pion mass in the two-flavor sector (only u and d quarks involved). Second, we extend our formalism to the three-flavor sector including kaon and η -meson degrees of freedom with fixed masses. Finally, we probe the static properties of the whole

baryon octet. All calculations are performed at one loop. The chiral limit, where current quark masses approach zero with $\hat{m}, m_s \rightarrow 0$, is well defined. We compare the obtained quark mass dependence of the nucleon observables with the results of other approaches (lattice QCD results and chiral extrapolations).

The thesis is organized as follows. In Chapter II we give a short overview of our approach, namely Perturbative Chiral Quark Model. In Chapter III we give the formula development of static properties (charge radii, electromagnetic form factors and magnetic moments) of the nucleon and other octet baryons in the PCQM. The numerical results are given in Chapter IV for the dependence of octet baryon properties on the pion mass in the two- and three-flavor pictures (included K and η meson) in the PCQM and are compared with other theoretical approaches, namely chiral extrapolation and lattice QCD calculations. In Chapter V we discuss and conclude our works.

Chapter II

PERTURBATIVE CHIRAL QUARK MODEL

The perturbative chiral quark model (Lyubovitskij et al., 2001a,b,c, 2002a,b; Simkovic et al., 2002; Cheedket et al., 2004) is based on an effective chiral Lagrangian describing baryons by a core of three valence quarks, moving in a central Dirac field with $V_{\text{eff}}(r) = S(r) + \gamma^0 V(r)$, where $r = |\vec{x}|$. In order to respect chiral symmetry, a cloud of Goldstone bosons (π , K and η) is included, which are treated as small fluctuations around the three-quark core. The effective Lagrangian \mathcal{L}_{eff} , derived in Ref. (Lyubovitskij et al., 2001b), is

$$\mathcal{L}_{\text{eff}} = \mathcal{L}_{\text{inv}}^{\text{lin}} + \mathcal{L}_{\chi SB}, \quad (2.1)$$

where $\mathcal{L}_{\text{inv}}^{\text{lin}}$ is the chiral-invariant Lagrangian

$$\mathcal{L}_{\text{inv}}^{\text{lin}} = \bar{\psi}(x)[i \not{\partial} - S(r) - \gamma^0 V(r)]\psi(x) + \mathcal{L}_{\Phi} - \mathcal{L}_{\text{int}}, \quad (2.2)$$

and a term $\mathcal{L}_{\chi SB}$ is the explicitly breaks chiral symmetry which arises from the nonvanishing of the quarks mass matrix \mathcal{M}

$$\mathcal{L}_{\chi SB} = -\bar{\psi}(x)\mathcal{M}\psi(x) - \frac{B}{8}\text{Tr}\{\hat{\Phi}(x), \{\hat{\Phi}(x), \mathcal{M}\}\}, \quad (2.3)$$

corresponding to the mass terms for quarks and of the octet of Goldstone boson (Lyubovitskij et al., 2001b).

The chiral-invariant interaction Lagrangian is introduced as

$$\begin{aligned}\mathcal{L}_{int} &= -\bar{\psi}(x)S(r)\left[\frac{U+U^\dagger}{2} + \gamma^5\frac{U-U^\dagger}{2}\right]\psi(x), \\ &= -\bar{\psi}(x)S(r)\exp\left[i\gamma^5\frac{\hat{\Phi}}{F}\right]\psi(x),\end{aligned}\tag{2.4}$$

and kinetic term of the meson fields

$$\mathcal{L}_\Phi = \frac{F^2}{4}\text{Tr}[\partial_\mu U\partial^\mu U^\dagger].\tag{2.5}$$

The eight Goldstone bosons are most conveniently summarized in a matrix $U \in SU(3)$, the chiral field can be represented by the exponential parameterization

$$U = \exp\left[i\frac{\hat{\Phi}}{F}\right] \simeq 1 + i\frac{\hat{\Phi}}{F} + o\left(\frac{\hat{\Phi}}{F}\right),\tag{2.6}$$

the octet matrix $\hat{\Phi}$ of pseudoscalar mesons is defined as

$$\hat{\Phi} = \sum_{i=1}^8 \Phi_i \lambda_i = \sqrt{2} \begin{pmatrix} \frac{\pi^0}{\sqrt{2}} + \frac{\eta}{\sqrt{6}} & \pi^+ & K^+ \\ \pi^- & \frac{-\pi^0}{\sqrt{2}} + \frac{\eta}{\sqrt{6}} & K^0 \\ K^- & \bar{K}^0 & \frac{-2\eta}{\sqrt{6}} \end{pmatrix}.\tag{2.7}$$

We rely on the standard picture of chiral symmetry breaking (Gasser and Leutwyler, 1985) and for the masses of pseudoscalar mesons we use the leading term in their chiral expansion (i.e., linear in the current quark mass):

$$M_\pi^2 = 2\hat{m}B, \quad M_K^2 = (\hat{m} + m_s), \quad M_\eta^2 = \frac{2}{3}(\hat{m} + 2m_s)B.\tag{2.8}$$

Meson masses obviously satisfy the "Gell-Mann-OakesRenner" and the "Gell-MannOkubo" relation as well,

$$3M_\eta^2 + M_\pi^2 = 4M_K^2, \quad (2.9)$$

in the evaluation we use the following set of QCD parameters (Gasser and Leutwyler, 1982):

$$\hat{m} = 7\text{MeV}, \quad \frac{m_s}{\hat{m}} = 25, \quad B = \frac{M_{\pi^+}^2}{2\hat{m}} = 1.4\text{GeV}. \quad (2.10)$$

Therefore, the model Lagrangian is

$$\begin{aligned} \mathcal{L}(x) = & \bar{\psi}(x)[i \not{\partial} - \gamma^0 V(r) - \mathcal{M}]\psi(x) \\ & + \frac{F^2}{4} \text{Tr} \left[\partial^\mu U(x) \partial^\mu U^\dagger(x) + 2\mathcal{M}B(U(x) + U^\dagger(x)) \right] \\ & - \bar{\psi}(x)S(r) \left[\frac{U(x) + U^\dagger(x)}{2} + \gamma^5 \frac{U(x) - U^\dagger(x)}{2} \right] \psi(x), \end{aligned} \quad (2.11)$$

where $\psi = (u, d, s)$ is the triplet of quark fields, $U = \exp[i\hat{\Phi}/F]$ is the chiral field in the exponential parametrization, $F = 88 \text{ MeV}$ is the pion decay constant in the chiral limit (Gasser et al., 1988), $\mathcal{M} = \text{diag}\{m_u, m_d, m_s\}$ is the mass matrix of current quarks and $B = -\langle 0|\bar{u}u|0\rangle/F^2 = -\langle 0|\bar{d}d|0\rangle/F^2$ is the quark condensate constant. In the numerical calculations we restrict to the isospin symmetry limit $m_u = m_d = \hat{m}$. We rely on the standard picture of chiral symmetry breaking (Gasser and Leutwyler, 1982) and for the masses of pseudoscalar mesons we use the leading term in their chiral expansion (i.e. linear in the current quark mass). By construction, our effective chiral Lagrangian is consistent with the known low-energy theorems (Gell-Mann-Okubo and Gell-Mann-Oakes-Renner re-

lations, partial conservation of axial current (PCAC), Feynman-Hellmann relation between pion-nucleon σ -term and the derivative of the nucleon mass, etc.). The electromagnetic field is included into the effective Lagrangian Eq. (2.11) using the standard procedure, i.e. the interaction of quarks and charged mesons with photons is introduced using minimal substitution.

To derive the properties of baryons, which are modeled as bound states of valence quarks surrounded by a meson cloud, we formulate perturbation theory and restrict the quark states to the ground-state contribution with $\psi(x) = b_0 u_0(\vec{x}) \exp(-i\mathcal{E}_0 t)$, where b_0 is the corresponding single-quark annihilation operator. The quark wave function $u_0(\vec{x})$ belongs to the basis of potential eigenstates used for expanding the quark field operator $\psi(\vec{x})$. In our calculation of matrix elements, we project quark diagrams on the respective baryon states. The baryon states are conventionally set up by the product of the SU(6) spin-flavor and SU(3)_c color wave functions, where the nonrelativistic single quark spin wave function is simply replaced by the relativistic solution $u_0(\vec{x})$ of the Dirac equation

$$\left[-i\gamma^0 \vec{\gamma} \cdot \vec{\nabla} + \gamma^0 S(r) + V(r) - \mathcal{E}_0 \right] u_0(\vec{x}) = 0, \quad (2.12)$$

where \mathcal{E}_0 is the single-quark ground-state energy. For the description of baryon properties, we use the effective potential $V_{\text{eff}}(r)$ with a quadratic radial dependence (Lyubovitskij et al., 2001a,b):

$$S(r) = M_1 + c_1 r^2, \quad V(r) = M_2 + c_2 r^2, \quad (2.13)$$

with the particular choice

$$M_1 = \frac{1 - 3\rho^2}{2\rho R}, \quad M_2 = \mathcal{E}_0 - \frac{1 + 3\rho^2}{2\rho R}, \quad c_1 \equiv c_2 = \frac{\rho}{2R^3}. \quad (2.14)$$

Here, R and ρ are parameters related to the ground-state quark wave function u_0 :

$$u_0(\vec{x}; i) = N_0 \exp\left[-\frac{\vec{x}^2}{2R^2}\right] \begin{pmatrix} 1 \\ i\rho\vec{\sigma}(i) \cdot \vec{x}/R \end{pmatrix} \chi_s(i)\chi_f(i)\chi_c(i), \quad (2.15)$$

where $N_0 = [\pi^{3/2}R^3(1 + 3\rho^2/2)]^{-1/2}$ is a normalization constant; χ_s , χ_f , χ_c are the spin, flavor and color quark wave functions, respectively. The index "i" stands for the i -th quark. The constant part of the scalar potential M_1 can be interpreted as the constituent mass of the quark, which is simply the displacement of the current quark mass due to the potential $S(r)$. The parameter ρ is related to the axial charge g_A of the nucleon calculated in zeroth-order (or 3q-core) approximation:

$$g_A = \frac{5}{3} \left(1 - \frac{2\rho^2}{1 + \frac{3}{2}\rho^2}\right). \quad (2.16)$$

Therefore, ρ can be replaced by g_A using the matching condition Eq. (2.16). Note that since PCAC is fulfilled in our model (Lyubovitskij et al., 2001b), on the tree level the axial charge g_A is on the tree level related to the pion-nucleon coupling constant $G_{\pi NN}$ by the Goldberger-Treiman relation

$$G_{\pi NN} = \frac{m_N}{3F} \left(1 - \frac{2\rho^2}{1 + \frac{3}{2}\rho^2}\right) \equiv \frac{m_N}{F} g_A, \quad (2.17)$$

where m_N is the physical nucleon mass. The same condition holds even for their form factors. The analytical expression for the pion-nucleon form factor in the chiral limit is given by

$$\begin{aligned} G_{\pi NN}(Q^2) &= \frac{m_N}{F} g_A(Q^2), \\ &\equiv \frac{m_N}{F} g_A(Q^2) F_{\pi NN}(Q^2), \end{aligned} \quad (2.18)$$

where Q^2 is the squared Euclidean momentum of the pion and $F_{\pi NN}(Q^2)$ is the πNN form factor normalized to unity at zero recoil $Q^2 = 0$:

$$F_{\pi NN}(Q^2) = \exp\left(-\frac{Q^2 R^2}{4}\right) \left\{ 1 + \frac{Q^2 R^2}{8} \left(1 - \frac{5}{3g_A}\right) \right\}. \quad (2.19)$$

The parameter R is related to the charge radius of the proton in the zeroth-order approximation as

$$\langle r_E^2 \rangle_{\text{LO}}^p = \int d^3x u_0^\dagger(\vec{x}) \vec{x}^2 u_0(\vec{x}) = \frac{3R^2}{2} \frac{1 + \frac{5}{2}\rho^2}{1 + \frac{3}{2}\rho^2}. \quad (2.20)$$

In our calculations we use the value $g_A=1.25$. Therefore, we have only one free parameter in our model, that is R or $\langle r_E^2 \rangle_{\text{LO}}^p$. In previous publications R was varied in the region from 0.55 fm to 0.65 fm, which corresponds to a change of $\langle r_E^2 \rangle_{\text{LO}}^p$ from 0.5 to 0.7 fm². Note that for the given form of the effective potential Eq. (2.13) the Dirac equation Eq. (2.12) can be solved analytically [for the ground state see Eq. (2.15), for excited states see Ref. (Cheedket et al., 2004)]. The expectation value of an operator \hat{A} is then set up as:

$$\langle \hat{A} \rangle = {}^B \langle \phi_0 | \sum_{n=1}^{\infty} \frac{i^n}{n!} \int d^4x_1 \dots \int d^4x_n T[\mathcal{L}_I(x_1) \dots \mathcal{L}_I(x_n) \hat{A}] | \phi_0 \rangle_c^B, \quad (2.21)$$

where the state vector $|\phi_0\rangle$ corresponds to the unperturbed three-quark state (3q-core). Superscript "B" in the equation indicates that the matrix elements have to be projected onto the respective baryon states, whereas subscript "c" refers to contributions from connected graphs only. Here $\mathcal{L}_I(x)$ is the appropriate interaction Lagrangian. For the purpose of the present paper, we include in $\mathcal{L}_I(x)$ the linearized coupling of pseudoscalar fields with quarks and the corresponding coupling of quarks and mesons to the electromagnetic field (see details in Ref. (Lyubovitskij

et al., 2001a)):

$$\begin{aligned} \mathcal{L}_I(x) = & -\bar{\psi}(x)i\gamma^5\frac{\hat{\Phi}(x)}{F}S(r)\psi(x) - eA_\mu(x)\bar{\psi}(x)\gamma^\mu Q\psi(x) \\ & - eA_\mu(x)\sum_{i,j=1}^8\left[f_{3ij} + \frac{f_{8ij}}{\sqrt{3}}\right]\Phi_i(x)\partial^\mu\Phi_j(x) + \dots, \end{aligned} \quad (2.22)$$

where f_{ijk} are the SU(3) antisymmetric structure constants. For the evaluation of Eq. (2.21) we apply Wick's theorem with the appropriate propagators for the quarks and pions. For the quark propagator we use the vacuum Feynman propagator for a fermion in a binding potential restricted to the ground-state quark wave function with

$$iG_0(x, y) = u_0(\vec{x})\bar{u}_0(\vec{y})e^{-i\mathcal{E}_0(x_0-y_0)}\theta(x_0 - y_0). \quad (2.23)$$

For the meson field we use the free Feynman propagator for a boson field with

$$i\Delta_{ij}(x - y) = \langle 0|T\{\Phi_i(x)\Phi_j(y)\}|0\rangle = \delta_{ij}\int\frac{d^4k}{(2\pi)^4i}e^{-ik(x-y)}\Delta_\Phi(k), \quad (2.24)$$

where $\Delta_\Phi(k) = [M_\Phi^2 - k^2 - i0^+]^{-1}$ is the meson propagator in momentum space and M_Φ is the meson mass.

Chapter III

BARYON PROPERTIES IN PCQM

3.1 Nucleon Mass

We first define and discuss the quantities relevant for mass and wave function renormalization. Following the Gell-Mann and Low theorem we define the mass shift of the nucleonic three-quark ground state Δm_N due to the interaction with Goldstone mesons as

$$\Delta m_N = {}^B \langle \phi_0 | \sum_{n=1}^{\infty} \frac{i^n}{n!} \int i\delta(t_1) d^4x_1 \dots \int d^4x_n T[\mathcal{L}_I(x_1) \dots \mathcal{L}_I(x_n) \hat{A}] | \phi_0 \rangle_c^B. \quad (3.1)$$

At one-loop, with an order of accuracy $o(1/F^2)$, the diagrams that contribute to the mass shift are shown in Fig. 3.1. The so-called "meson cloud" (MC) diagram of Fig. 3.1(a) describes the emission and reabsorption of the meson on the same quark, whereas the "meson exchange" (ME) diagram of Fig. 3.1(b) connects two quark lines.

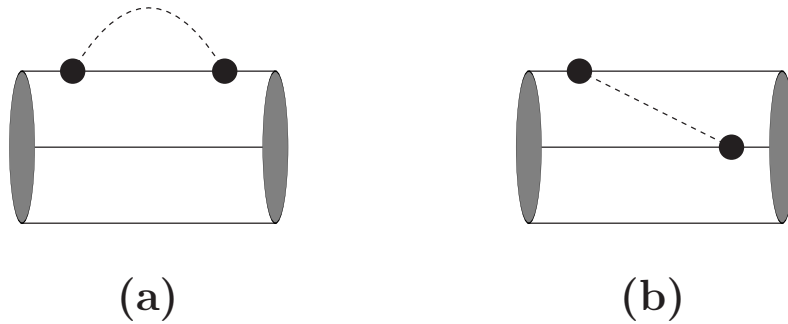


Figure 3.1 Diagrams contributing to the nucleon mass shift: meson cloud (a) and meson exchange diagram (b)

The MC and ME diagrams are examples of one and two-body operator, respectively. The nucleon wave function is conventionally set up by the product of the SU(6) spin-flavor WF and SU(3)_c color WF, where the nonrelativistic single quark spin WF is replaced by the relativistic ground-state solution of Eq. (2.15). Projection of "one-body" diagrams on the nucleon state refers to

$$\chi_{f'}^\dagger \chi_{s'}^\dagger I^{f'f} J^{s's} \chi_f \chi_s \rightarrow \langle B | \sum_{n=1}^3 (IJ)^{(i)} | B \rangle, \quad (3.2)$$

where the single-particle matrix element of the operators I and J , acting in flavor and spin space, is replaced by the one embedded in the nucleon state. For "two-body" diagrams with two independent quark indices i and j the projection prescription reads as

$$\chi_{f'}^\dagger \chi_{s'}^\dagger I_1^{f'f} J_1^{s's} \chi_f \chi_s \otimes \chi_{k'}^\dagger \chi_{\sigma'}^\dagger I_2^{k'k} J_2^{\sigma'\sigma} \chi_k \chi_\sigma \rightarrow \langle B | \sum_{n \neq 1}^3 (I_1 J_1)^{(i)} \otimes (I_2 J_2)^{(i)} | B \rangle. \quad (3.3)$$

The physical nucleon mass at one loop is given by

$$m_N = m_N^{core} + \Delta m_N, \quad (3.4)$$

where

$$m_N^{core} = 3 \left\{ \mathcal{E}_0 + \gamma \hat{m} \right\} = 3 \left\{ \mathcal{E}_0 + \frac{\gamma}{2B} M_\pi^2 \right\}, \quad (3.5)$$

is the contribution of the three-quark core (the second term in the r.h.s. of Eq. (3.5) is the contribution of the current quark mass) and

$$\Delta m_N = \Pi^{\text{MC}} + \Pi^{\text{ME}}, \quad (3.6)$$

is the nucleon mass shift due to the meson cloud contribution. The diagrams that contribute to the nucleon mass shift Δm_N at one loop are shown in Fig. 3.1 (see details in Refs. (Lyubovitskij et al., 2001a,b)). Fig. 3.1(a) corresponds to the so-called meson-cloud (MC) contribution and Fig. 3.1(b) is the meson-exchange (ME) contribution. The operators Π^{MC} and Π^{ME} are functions of the meson masses and are expressed in terms of the universal self-energy operator

$$\Pi(M_\Phi^2) = -I_\Phi^{24}, \Phi = \pi, K, \eta. \quad (3.7)$$

Here we introduce a notation for the structure integral in terms of which all further formulas can be expressed:

$$I_\Phi^{MN} = \left(\frac{g_A}{\pi F}\right)^2 \int_0^\infty \frac{dp p^N F_{\pi NN}^2(p^2)}{(M_\Phi^2 + p^2)^{\frac{M}{2}}}, M, N = 0, 1, 2, \dots \quad (3.8)$$

and

$$I_\Phi^{0N} \equiv I_N \equiv \left(\frac{g_A}{\pi F}\right)^2 \int_0^\infty dp p^N F_{\pi NN}^2(p^2) = \left(\frac{g_A}{\pi F}\right)^2 \left(\frac{2}{R^2}\right)^{\frac{N+1}{2}} \\ \times \Gamma\left(\frac{N+1}{2}\right) \left(\frac{1}{2} - \frac{N+1}{4}\beta + \frac{(N+1)(N+3)}{32}\beta^2\right), \quad (3.9)$$

where $\beta = 2\rho^2/(2-\rho^2)$. The function $F_{\pi NN}(p^2)$ is the πNN form factor normalized to unity at zero recoil ($p^2 = 0$):

$$F_{\pi NN}(Q^2) = \exp\left(-\frac{Q^2 R^2}{4}\right) \left\{1 - \frac{Q^2 R^2}{4}\beta\right\}. \quad (3.10)$$

The meson cloud contributions to the mass shift are then given

1) in SU(2) as

$$\Pi^{\text{MC}} = \frac{81}{400}\Pi(M_\pi^2), \quad (3.11)$$

$$\Pi^{\text{ME}} = \frac{90}{400}\Pi(M_\pi^2). \quad (3.12)$$

2) in SU(3) as

$$\Pi^{\text{MC}} = \frac{81}{400}\Pi(M_\pi^2) + \frac{54}{400}\Pi(M_K^2) + \frac{9}{400}\Pi(M_\eta^2), \quad (3.13)$$

$$\Pi^{\text{ME}} = \frac{90}{400}\Pi(M_\pi^2) - \frac{6}{400}\Pi(M_\eta^2). \quad (3.14)$$

Finally, the effect of a finite current quark mass \hat{m} on the nucleon mass shift is taken into account perturbatively, resulting in the linear term $3\gamma\hat{m}$ in Eq. (3.5).

3.2 Electromagnetic Form Factors in PCQM

The measurements of the electromagnetic form factors of the proton and the neutron gave the first hints at an internal structure of the nucleon, and a theory of the nucleon cannot be considered satisfactory if it is not able to reproduce the form factor data. The overall trend of the experimental results for small and moderate values of the momentum transfer Q^2 could be described reasonably well by phenomenological (dipole) fits

$$G_D(Q^2) = \frac{1}{(1 + Q^2/0.71\text{GeV}^2)^2}. \quad (3.15)$$

Recently, the form factors of the nucleon have been studied experimentally with high precision and deviations from this uniform dipole form have been observed,

both at very small Q^2 and in the region above 1 GeV². It is therefore of great interest to derive the nucleon form factors from QCD. Since form factors are typical low-energy quantities, perturbation theory in terms of quarks and gluons is useless for this purpose and a non-perturbative method is needed. If one wants to avoid additional assumptions or models, one is essentially restricted to lattice QCD and Monte Carlo simulations. In view of the importance of nucleon form factors and the amount of experimental data available, it is surprising that there are only a few lattice investigations of form factors Refs. (Richards, 2007; Leinweber et al., 2005; Suganuma et al., 2001). The structure of the nucleon is encoded in several form factors. For example, the electromagnetic Dirac and Pauli form factors $F_1(Q^2)$ and $F_2(Q^2)$, or equivalently the electric and magnetic Sachs form factors $G_E(Q^2)$ and $G_M(Q^2)$, parameterize the matrix elements of the electromagnetic current operator and are well-known over a wide region of momentum transfer squared Q^2 . The electromagnetic form factors are matrix elements of the current operator, $J^\mu(x)$, between nucleon states of different momentum (exact expressions for the nucleon electromagnetic form factors can be found in Ref. (Lyubovitskij et al., 2001a)):

$$\langle N'(p') | J^\mu(0) | N(p) \rangle = \bar{u}_{N'}(p') \left\{ \gamma^\mu F_1^B(Q^2) + \frac{i\sigma^{\mu\nu} q_\nu}{2m_N} F_2^B(Q^2) \right\} u_N(p), \quad (3.16)$$

where $q = p' - p$ is taken as space-like momentum transfer squared given as $Q^2 = -q^2 = \vec{q}^2$. According to the Lagrangian, the one loop Feynman diagrams which contribute to the nucleon magnetic moments are draw in Fig. 3.2. The charge (Dirac) form factor is F_1^N , normalized such that $F_1^N(0)$ is the nucleon charge, and the magnetic (Pauli) form factor is F_2^N , normalized such that $F_2^N(0)$ is the anomalous magnetic moment. Instead of working with $F_1^N(Q^2)$ and $F_2^N(Q^2)$, it

is convenient to consider linear combination constructed as electromagnetic form factors in the definitions of physical properties are given from the Sachs form factors with the space-like. The nucleon charge G_E^N and magnetic G_M^N form factors can be written in the form of the Dirac and Pauli form factors by

$$G_E^N(Q^2) \equiv F_1^N(q^2) + \left\{ \frac{q^2}{4m_N^2} \right\} F_2^N(q^2), \quad (3.17)$$

$$G_M^N(Q^2) \equiv F_1^N(q^2) + F_2^N(q^2). \quad (3.18)$$

At zero recoil ($q^2 = 0$) the Sachs form factors satisfy the following normalization conditions:

$$G_E^p(0) = 1, \quad G_E^n(0) = 0, \quad G_M^p(0) = \mu_p, \quad G_M^n = \mu_n, \quad (3.19)$$

where the magnetic moments $\mu_p \sim 2.793$ and $\mu_n \sim -1.913$ in units of nuclear magnetons. In the Breit frame coincides with the center-of-mass frame, in particular frame the energy transfer vanishes and thus the photon carries the four-momentum $q^\mu = (0, \vec{q})$ and therefore $Q^2 = \vec{q}^2$, the initial momentum of the nucleon is $p = (E, -\vec{q}/2)$, the final momentum is $p' = (E, \vec{q}/2)$ and the four-momentum of the photon is $q = (0, \vec{q})$ with $p' = p + q$.

$$\langle N'_s(\vec{q}/2) | J^0(0) | N_s(-\vec{q}/2) \rangle = G_E^N(Q^2) \chi_{N'_s}^\dagger \chi_{N_s}, \quad (3.20)$$

$$\langle N'_s(\vec{q}/2) | \vec{J}(0) | N_s(-\vec{q}/2) \rangle = G_M^N(Q^2) \chi_{N'_s}^\dagger \frac{i\vec{\sigma}_N \times \vec{q}}{2m_N} \chi_{N_s}. \quad (3.21)$$

where $J^0(0)$ and $\vec{J}(0)$ are the time and space component of the electromagnetic current operators; χ_{N_s} and $\chi_{N'_s}^\dagger$ are the nucleon spin WFs in the initial and final state; $\vec{\sigma}_N$ is the nucleon spin matrix. The charge radii of the nucleons are given

by

$$\begin{aligned} \langle r^2 \rangle_E^p &= -6 \frac{dG_E^p(Q^2)}{dQ^2} \Big|_{Q^2=0}, \quad \langle r^2 \rangle_E^n = -6 \frac{dG_E^n(Q^2)}{dQ^2} \Big|_{Q^2=0}, \\ \langle r^2 \rangle_M^N &= -\frac{6}{G_M^N(0)} \frac{dG_M^N(Q^2)}{dQ^2} \Big|_{Q^2=0}. \end{aligned} \quad (3.22)$$

In the framework of the PCQM and in the Breit frame, the Sachs form factors of the nucleon evaluated at one loop are defined by

$$\begin{aligned} \chi_{N_{s'}}^\dagger \chi_{N_s}^\dagger G_E^N(Q^2) &=^N \langle \phi_0 | \sum_{n=0}^2 \frac{i^n}{n!} \int \delta(t) d^4x d^4x_1 \dots d^4x_n e^{-iqx} \\ &\quad \times T[\mathcal{L}_r^{str}(x_1) \dots \mathcal{L}_r^{str}(x_n) j_r^0(x)] | \phi_0 \rangle_c^N, \end{aligned} \quad (3.23)$$

$$\begin{aligned} \chi_{N_{s'}}^\dagger \frac{i\vec{\sigma}_N \times \vec{q}}{2m_N} \chi_{N_s}^\dagger G_M^N(Q^2) &=^N \langle \phi_0 | \sum_{n=0}^2 \frac{i^n}{n!} \int \delta(t) d^4x d^4x_1 \dots d^4x_n e^{-iqx} \\ &\quad \times T[\mathcal{L}_r^{str}(x_1) \dots \mathcal{L}_r^{str}(x_n) \vec{j}_r(x)] | \phi_0 \rangle_c^N. \end{aligned} \quad (3.24)$$

Exact expressions for the nucleon electromagnetic form factors can be found in Ref. (Lyubovitskij et al., 2001a). Here we just present the typical results for the magnetic moments in SU(2) and SU(3). The two-flavor result is obtained from the three-flavor one when neglecting kaon and η -meson contributions.

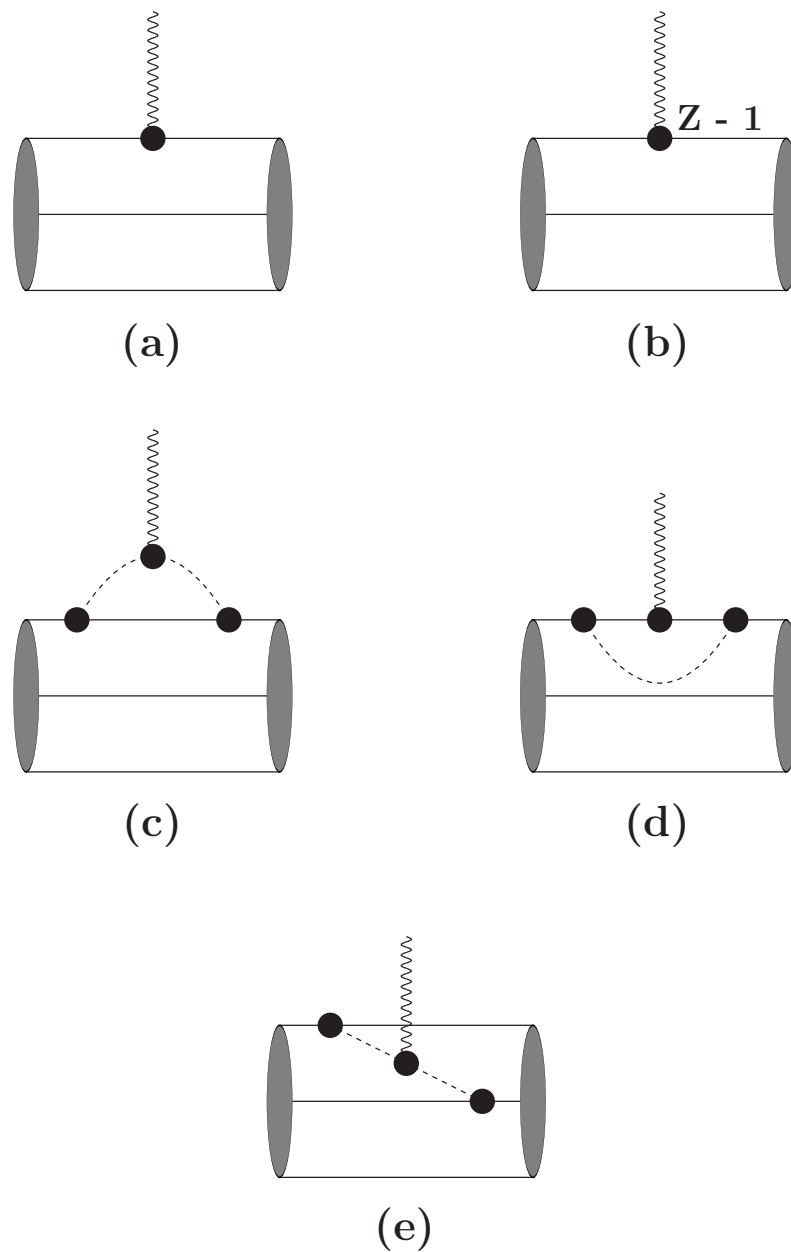


Figure 3.2 Diagrams contributing to the electromagnetic form factors of the baryon octet: three-quark diagram (a), three-quark counter-term diagram (b), meson cloud diagram (c), vertex correction diagram (d), and meson-in-flight diagram (e)

The magnetic moments of the nucleons, μ_p and μ_n , are given by the expressions

$$\begin{aligned}\mu_p &= \mu_p^{LO} \left[1 + \delta - \frac{1}{400} \left\{ 26I_\pi^{34} + 16I_K^{34} + 4I_\eta^{34} \right\} \right] + \frac{m_N}{50} \left\{ 11I_\pi^{44} + I_K^{44} \right\}, \\ \mu_n &= -\frac{2}{3}\mu_p^{LO} \left[1 + \delta - \frac{1}{400} \left\{ 21I_\pi^{34} + 21I_K^{34} + 4I_\eta^{34} \right\} \right] - \frac{m_N}{50} \left\{ 11I_\pi^{44} + I_K^{44} \right\},\end{aligned}\quad (3.25)$$

where

$$\mu_p^{LO} = \frac{2m_N\rho R}{1 + \frac{3}{2}\rho^2}, \quad (3.26)$$

is the leading-order contribution to the proton magnetic moment. The factor

$$\delta = -\left(\hat{m} + \frac{\Pi^{\text{MC}}}{3} \cdot \frac{1 + \frac{3}{2}\rho^2}{1 - \frac{3}{2}\rho^2} \right) \frac{2 - \frac{3}{2}\rho^2}{\left(1 + \frac{3}{2}\rho^2 \right)^2} R\rho, \quad (3.27)$$

defines the NLO correction to the nucleon magnetic moments due to the modification of the quark wave function (Lyubovitskij et al., 2001a). Note that the well-known SU_6 relation between nucleon magnetic moments $\mu_n/\mu_p = -2/3$ can be easily deduced from Eq. (3.25). If (i) we restrict to contributions from one-body diagrams in Figs. 3.2(a) - 3.2(d), corresponding to the additive quark picture and (ii) apply the $SU(3)$ -flavor limit ($M_\pi = M_K = M_\eta = M_\Phi$). In particular, we have

$$\begin{aligned}\mu_p^{(SU_6)} &\equiv -\frac{2}{3}\mu_n^{(SU_6)}, \\ &= \mu_p^{LO} \left(1 + \delta - \frac{23}{200} I_\Phi^{34} \right) + \frac{9}{50} m_N I_\Phi^{44}.\end{aligned}\quad (3.28)$$

Taking into account the meson-in-flight diagram Fig. 3.2(e) generated by two-body forces leads to a deviation of the ratio μ_n/μ_p from the naive SU_6 result.

Chapter IV

RESULTS

In this section we present our numerical results of octet baryon properties in PCQM. Shown in Table 4.1 are the evaluated nucleon mass with various values of the pion mass. Both the SU(2) version, considering only the pion cloud contribution, and the SU(3) one, including in addition kaon and η -meson cloud contributions, are considered. The total result is normalized to the physical value (coinciding with the proton mass treated as the reference point) $m_N \equiv m_p = 938.27$ MeV by fixing the ground-state quark energy to $\mathcal{E}_0 \simeq 397$ MeV [in case of SU(2)] and $\mathcal{E}_0 \simeq 411$ MeV [in case of SU(3)]. We also indicate the separate contributions of the 3q-core and the meson cloud. It is found that the values obtained in the chiral limit are consistent with the results of Refs. (Faessler et al., 2006c; Borasoy and Meissner, 1997; Frink et al., 2005). For the dependence on the pion mass we choose mass values in the range of $M_\pi^2 \simeq 0.15 - 1.2$ GeV² and the resulting nucleon mass is directly compared to both chiral extrapolations and lattice data (Orth et al., 2005; Ali Khan et al., 2004). It is found that our results are consistent with the corresponding values of the extrapolations and the lattice QCD results.

Table 4.1 Nucleon mass (in GeV) in the SU(2) and SU(3) versions and at different values for M_π^2

Nucleon mass	SU(2)	SU(3)	Other approaches
$3q$ -core	1.203	1.247	-
Meson loops (total)	-0.265	-0.309	-
π loops	-0.265	-0.265	-
K loops	-	-0.042	-
η loops	-	-0.002	-
Total	0.93827	0.93827	-
Chiral limit	0.887	0.831	0.880 (Procura et al., 2004); 0.890 (Frink et al., 2005); 0.832 (Faessler et al., 2006c) 0.883 (Procura et al., 2006b); 0.770 (Borasoy and Meissner, 1997);
M_π^2 (in GeV ²)			
0.153	1.122	1.128	1.182(26) (Orth et al., 2005)
0.162	1.133	1.138	1.195(42) (Orth et al., 2005)
0.175	1.148	1.154	1.104(20) (Orth et al., 2005)
0.240	1.212	1.220	1.228(31) (Orth et al., 2005)
0.348	1.310	1.320	1.356(21) (Orth et al., 2005)
0.413	1.360	1.371	1.377(19) (Orth et al., 2005)
0.462	1.400	1.412	1.410(17) (Orth et al., 2005)
0.557	1.475	1.490	1.533(28) (Orth et al., 2005)
0.588	1.500	1.515	1.509(16) (Orth et al., 2005)
0.678	1.566	1.582	1.637(27) (Orth et al., 2005)
0.774	1.638	1.656	1.631(30) (Orth et al., 2005)
0.810	1.664	1.682	1.619(16) (Orth et al., 2005)
0.258	1.231	1.239	1.253(15) (Ali Khan et al., 2004)
0.271	1.240	1.248	1.275(82) (Ali Khan et al., 2004)
0.297	1.266	1.275	1.300(22) (Ali Khan et al., 2004)
0.310	1.275	1.284	1.320(19) (Ali Khan et al., 2004)
0.314	1.280	1.288	1.412(61) (Ali Khan et al., 2004)
0.354	1.314	1.324	1.348(13) (Ali Khan et al., 2004)
0.502	1.431	1.444	1.497(77) (Ali Khan et al., 2004)
0.514	1.442	1.456	1.506(94) (Ali Khan et al., 2004)
0.536	1.458	1.742	1.509(18) (Ali Khan et al., 2004)
0.540	1.462	1.476	1.519(11) (Ali Khan et al., 2004)
0.578	1.493	1.507	1.657(26) (Ali Khan et al., 2004)
0.607	1.515	1.530	1.629(20) (Ali Khan et al., 2004)
0.776	1.640	1.658	1.679(36) (Ali Khan et al., 2004)
0.874	1.710	1.730	1.741(29) (Ali Khan et al., 2004)
0.883	1.717	1.736	1.781(15) (Ali Khan et al., 2004)
0.894	1.725	1.744	1.878(28) (Ali Khan et al., 2004)
0.901	1.730	1.749	1.785(35) (Ali Khan et al., 2004)
0.913	1.738	1.758	1.798(85) (Ali Khan et al., 2004)
0.921	1.744	1.764	1.801(14) (Ali Khan et al., 2004)
0.940	1.758	1.778	1.809(17) (Ali Khan et al., 2004)
1.201	1.943	1.965	2.063(26) (Ali Khan et al., 2004)

Presented in Table 4.2 are our results for the nucleon magnetic moments in the SU(2) version for different values of the model scale parameter R at $M_\pi = 0$ and at the physical pion mass. In Table 4.3 we give the analogous results for the SU(3) version with fixed masses M_K^2 and M_η^2 . The results show that the scalar parameter R around 0.6 fm gives the best fits to the nucleon magnetic moments experimental data, $\mu_p^{exp} \cong 2.793$ and $\mu_n^{exp} \cong -1.913$. It is found that the theoretical results for the neutron magnetic moment are almost the same for both the SU(2) and SU(3) versions though the results for the proton magnetic moment are a little bit larger in the SU(2) version.

Table 4.2 Nucleon magnetic moments in SU(2)

R (fm)	μ_p		μ_n	
	$M_\pi = 0$	M_π^{phys}	$M_\pi = 0$	M_π^{phys}
0.50	3.896	2.984	-2.948	-2.015
0.55	3.828	2.947	-2.871	-1.970
0.60	3.796	2.945	-2.823	-1.952
0.65	3.792	2.969	-2.797	-1.954
0.70	3.803	3.012	-2.789	-1.973

Table 4.3 Nucleon magnetic moments in SU(3) for fixed masses M_K^2 and M_η^2

R (fm)	μ_p		μ_n	
	$M_\pi = 0$	M_π^{phys}	$M_\pi = 0$	M_π^{phys}
0.50	3.512	2.598	-2.976	-2.043
0.55	3.466	2.585	-2.984	-1.993
0.60	3.456	2.605	-2.843	-1.972
0.65	3.471	2.648	-2.815	-1.972
0.70	3.505	2.709	-2.804	-1.988

Shown in Table 4.4 are the pion mass dependence of the nucleon charge and magnetic radius. By choosing $\rho = 0.39(g_A = 1.5)$ and scale parameter $R = 0.6$ fm, we obtain $\langle r^2 \rangle_E^p = 0.74$ fm, $\langle r^2 \rangle_M^p = 0.74$ fm and $\langle r^2 \rangle_M^n = 0.79$ fm, which are consistent to the experimental data. The predicted values for the proton and neutron charge and magnetic radii are also presented for larger pion masses. Our results indicate that the nucleon charge radii are almost independent of the pion mass.

Table 4.4 Nucleon charge and magnetic radii (fm²)

	Slope	3q-core	Meson cloud	Total	Data
$M_\pi^2 = (M_\pi^{\text{phys}})^2$	$\langle r^2 \rangle_E^p$	0.603	0.133	0.736	0.74
	$\langle r^2 \rangle_M^p$	0.412	0.330	0.742	0.74
	$\langle r^2 \rangle_M^n$	0.362	0.431	0.793	0.77
$M_\pi^2 = 0$	$\langle r^2 \rangle_E^p$	0.589	-	-	-
	$\langle r^2 \rangle_M^p$	0.407	-	-	-
	$\langle r^2 \rangle_M^n$	0.358	-	-	-
$M_\pi^2 = 0.1 \text{ GeV}^2$	$\langle r^2 \rangle_E^p$	0.614	0.065	0.678	-
	$\langle r^2 \rangle_M^p$	0.411	0.076	0.487	-
	$\langle r^2 \rangle_M^n$	0.361	0.093	0.454	-
$M_\pi^2 = 0.2 \text{ GeV}^2$	$\langle r^2 \rangle_E^p$	0.616	0.049	0.665	-
	$\langle r^2 \rangle_M^p$	0.408	0.038	0.446	-
	$\langle r^2 \rangle_M^n$	0.358	0.042	0.400	-
$M_\pi^2 = 0.3 \text{ GeV}^2$	$\langle r^2 \rangle_E^p$	0.617	0.043	0.660	-
	$\langle r^2 \rangle_M^p$	0.405	0.025	0.430	-
	$\langle r^2 \rangle_M^n$	0.356	0.025	0.381	-
$M_\pi^2 = 0.4 \text{ GeV}^2$	$\langle r^2 \rangle_E^p$	0.617	0.034	0.657	-
	$\langle r^2 \rangle_M^p$	0.403	0.019	0.422	-
	$\langle r^2 \rangle_M^n$	0.354	0.017	0.371	-
$M_\pi^2 = 0.5 \text{ GeV}^2$	$\langle r^2 \rangle_E^p$	0.616	0.031	0.654	-
	$\langle r^2 \rangle_M^p$	0.402	0.016	0.418	-
	$\langle r^2 \rangle_M^n$	0.353	0.013	0.366	-
$M_\pi^2 = 0.6 \text{ GeV}^2$	$\langle r^2 \rangle_E^p$	0.616	0.028	0.644	-
	$\langle r^2 \rangle_M^p$	0.401	0.014	0.415	-
	$\langle r^2 \rangle_M^n$	0.352	0.010	0.362	-
$M_\pi^2 = 0.7 \text{ GeV}^2$	$\langle r^2 \rangle_E^p$	0.616	0.026	0.642	-
	$\langle r^2 \rangle_M^p$	0.400	0.013	0.413	-
	$\langle r^2 \rangle_M^n$	0.351	0.008	0.359	-

In Fig. 4.1 we show the dependence of nucleon mass on meson masses both in SU(2) [M_π^2 -dependence only] and in SU(3) [M_K^2 and M_η^2 -dependence included]. It is found that the pion-mass dependence of the nucleon mass is considerable and the results are almost the same for the SU(2) (dotted curve) and SU(3) (solid curve) cases. In the SU(3) case Kaon and η -meson contributions have been included with their physical masses.

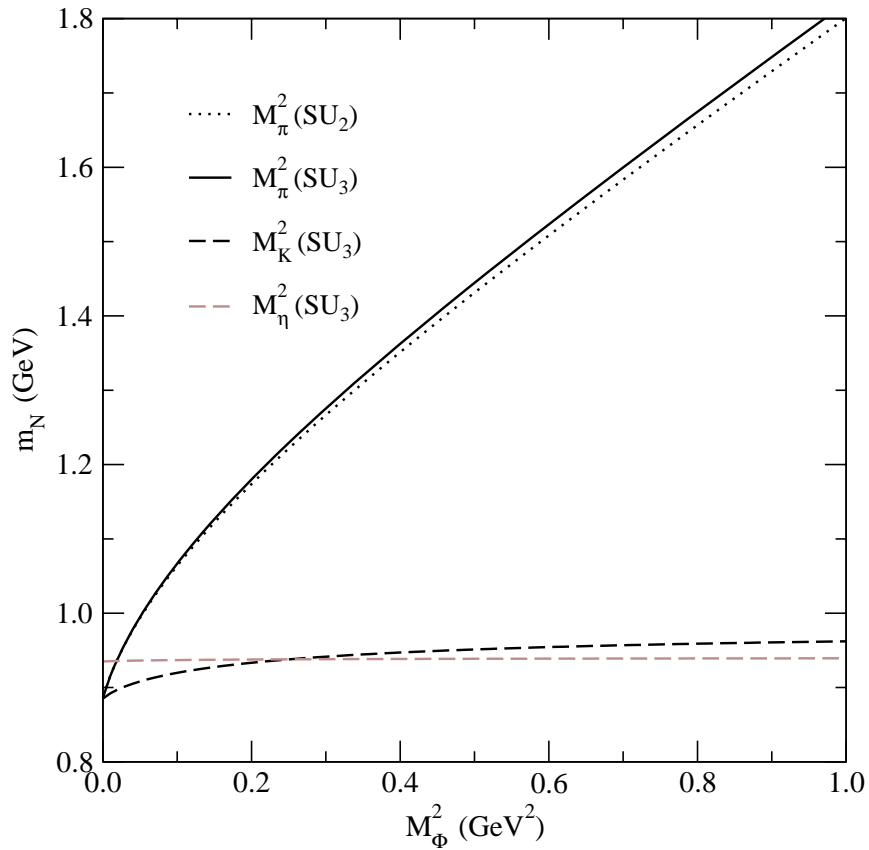


Figure 4.1 Dependence of nucleon mass m_N on meson masses M_Φ^2 : $m_N(M_\pi^2)$ in SU(2) (dotted line) and $m_N(M_\pi^2)$, $m_N(M_K^2)$, $m_N(M_\eta^2)$ in SU(3) (the other lines)

The M_K^2 and M_η^2 -dependence of nucleon mass, separately shown in Fig. 4.1, indicates that their contributions, especially for the η meson, are negligible.

Our results for the M_π^2 -dependence of the nucleon mass in both the SU(2) and SU(3) cases are compared with lattice QCD calculations at order p^3 and p^4 of Ref. (Procura et al., 2006b) in Fig. 4.2. Again, it is found that the pion-mass dependence is dominated over the Kaon and η ones. Note that, in Fig. 4.2, our results are closer to the lattice QCD results at order p^4 (Procura et al., 2006b).

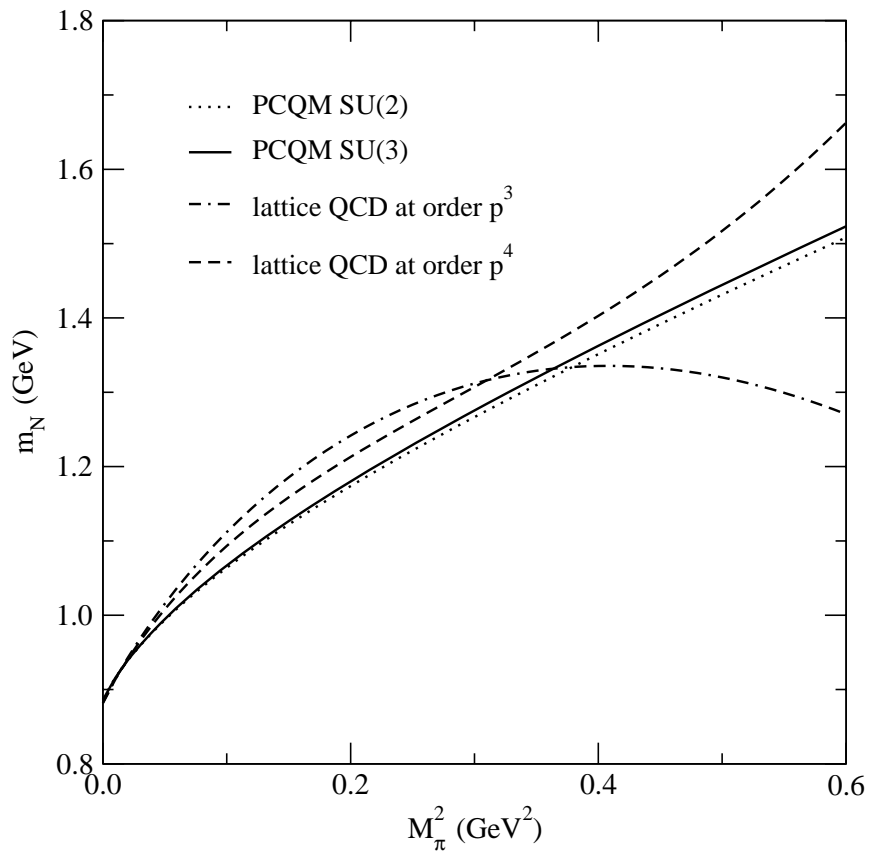


Figure 4.2 Dependence of nucleon mass m_N on pion mass M_π^2 : $m_N(M_\pi^2)$ in SU(2) (dotted line), SU(3) (solid line) and from lattice QCD (Procura et al., 2006b) (the others) at order p^3 and p^4

Shown in Fig. 4.3 are our results for the pion-mass dependence of nucleon mass in both the SU(2) and SU(3) cases, compared to lattice QCD calculations from various collaborations (Orth et al., 2005; Ali Khan et al., 2004). The

curves show a good consistence with various lattice QCD results, especially at low M_π^2 regime ($\leq 0.4 \text{ GeV}^2$). At large M_π^2 regime our results are generally lower than the lattice QCD predictions. Our results may be improved by including contributions from excited quark/antiquark states in the meson loop.

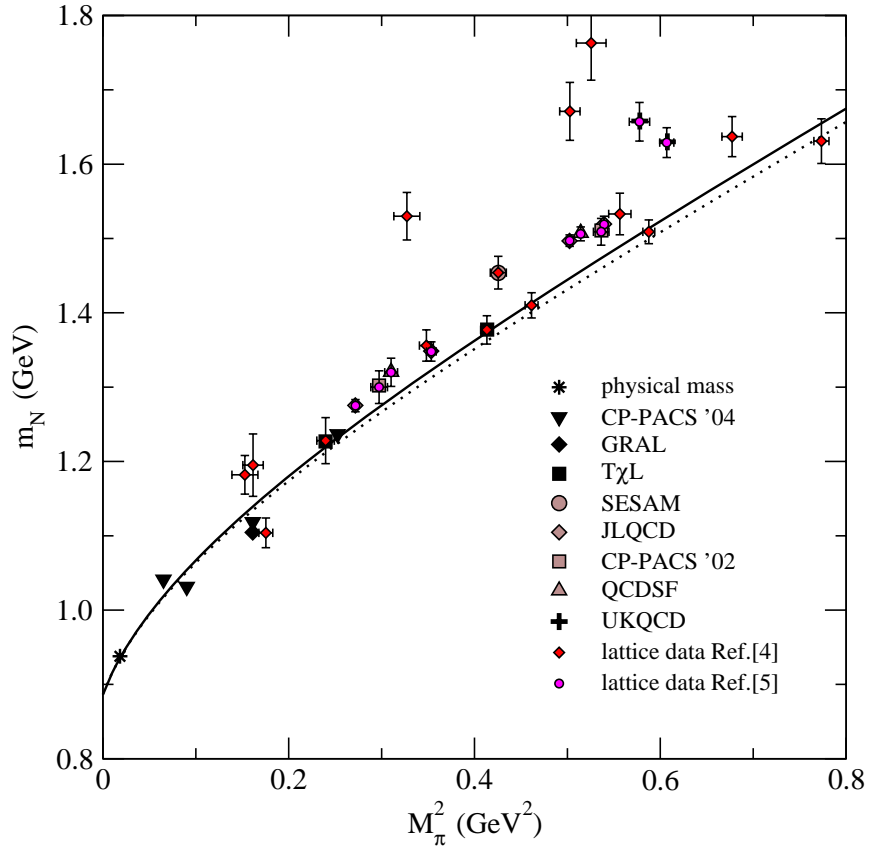


Figure 4.3 Pion-mass dependence of nucleon mass $m_N(M_\pi^2)$ in SU(2) (dotted line) and in SU(3)(solid line) compared to lattice data from various collaborations

Shown in Figs. 4.4 and 4.5 are our results for the nucleon magnetic moments as functions of M_π^2 , compared with lattice QCD calculations (Holstein et al., 2005) and sum rules (Wang et al., 2007). Our results, shown as the solid curve, are close to the results from other approaches at small M_π^2 masses.

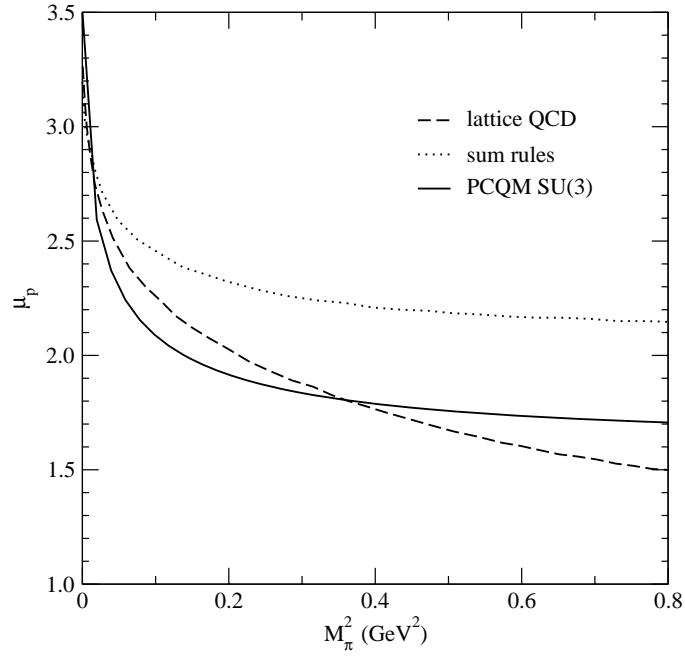


Figure 4.4 M_π^2 -dependence of the proton magnetic moment $\mu_p(M_\pi^2)$ to one-loop from sum rules (Holstein et al., 2005) (dotted curve), lattice QCD (Wang et al., 2007) (dashed curve) and our results in SU(3) (solid curve)

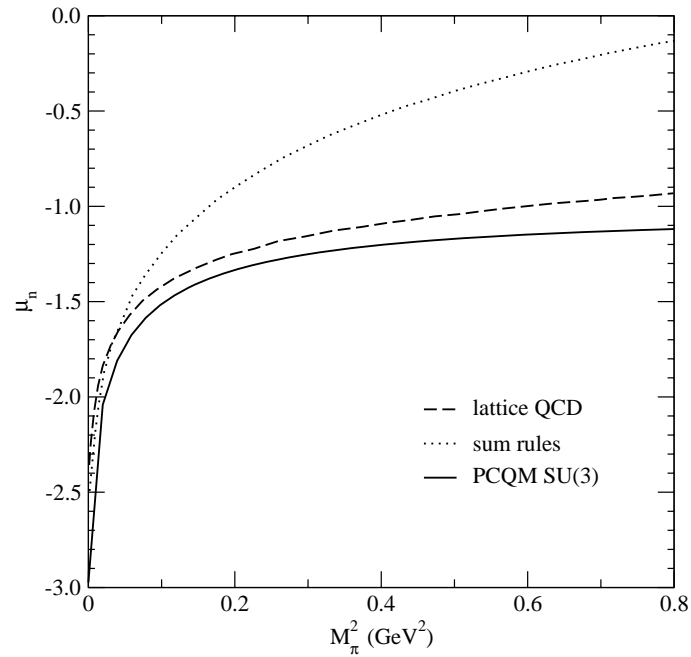


Figure 4.5 M_π^2 -dependence of the neutron magnetic moment $\mu_n(M_\pi^2)$ to one-loop from QCD sum rules (Holstein et al., 2005) (dotted curve), lattice QCD (Wang et al., 2007) (dashed curve) and our results in SU(3) (solid curve)

We probe also the strange quark mass m_s -dependence of the nucleon magnetic moments. Shown in Figs. 4.6(a) and 4.6(b) are our results of the nucleon magnetic moments as functions of M_π^2 at different values of the strange current quark mass m_s . It can be seen that the nucleon magnetic moments are not sensitive to a variation of m_s .

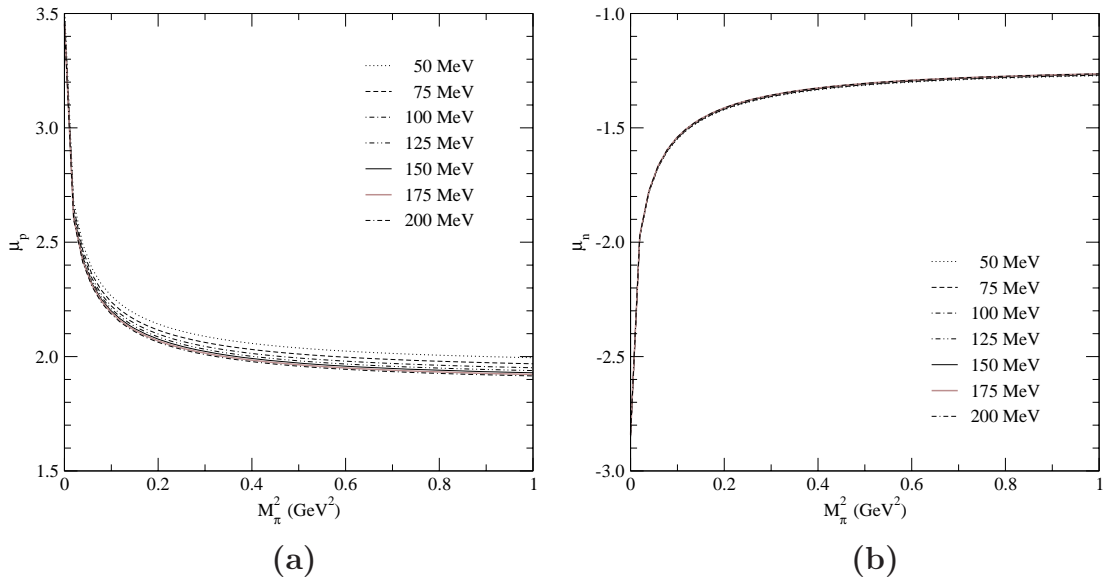


Figure 4.6 M_π^2 -dependence of the nucleon magnetic moment $\mu_N(M_\pi^2)$, with $m_s = 50 - 200$ MeV: (a) for proton and (b) for neutron

In Figs. 4.7(a) and 4.7(b), we show our results for the nucleon magnetic moments as functions of current quarks mass \hat{m} at different values of m_s (50 - 200 MeV). The results are not sensitive to m_s , the same as the previous plots of M_π^2 -dependence. Note that, the relation of \hat{m} and M_π^2 can be approximated by Eq. 3.5 ($\hat{m} \equiv M_\pi^2$).

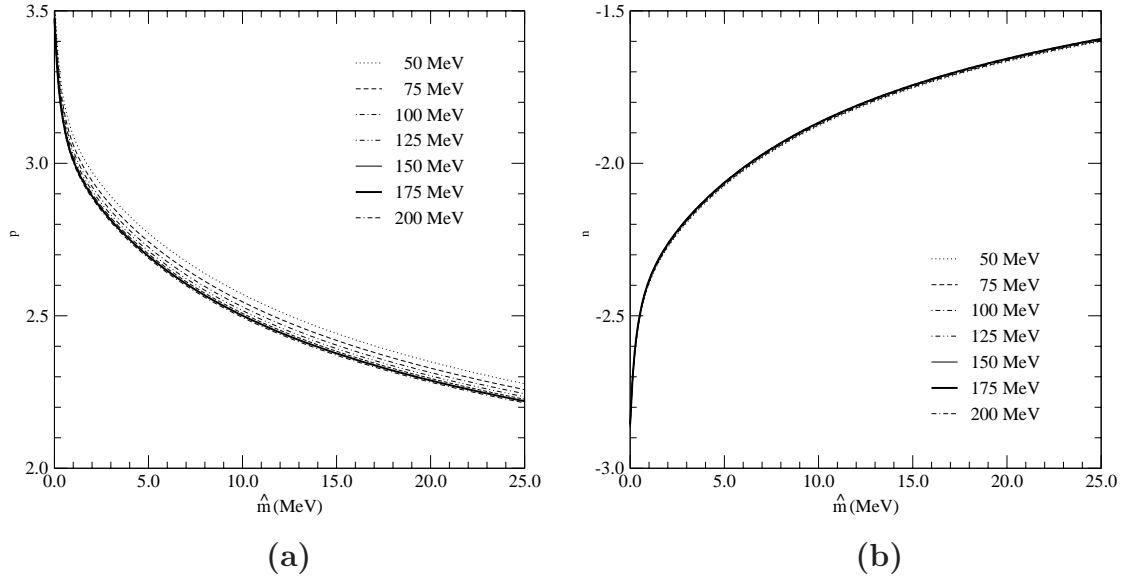


Figure 4.7 Current quarks mass \hat{m} -dependence of the proton magnetic moment $\mu_p(M_\pi^2)$, with $m_s = 50 - 200$ MeV: (a) for proton and (b) for neutron

In Figs. 4.8(a) - 4.8(d) we demonstrate the dependence of the nucleon magnetic moments on the scale parameter R . It is found that the theoretical results are not sensitive to the parameter at low M_π^2 region (below the physical mass), but at high pion mass region the scale parameter R plays an important role.

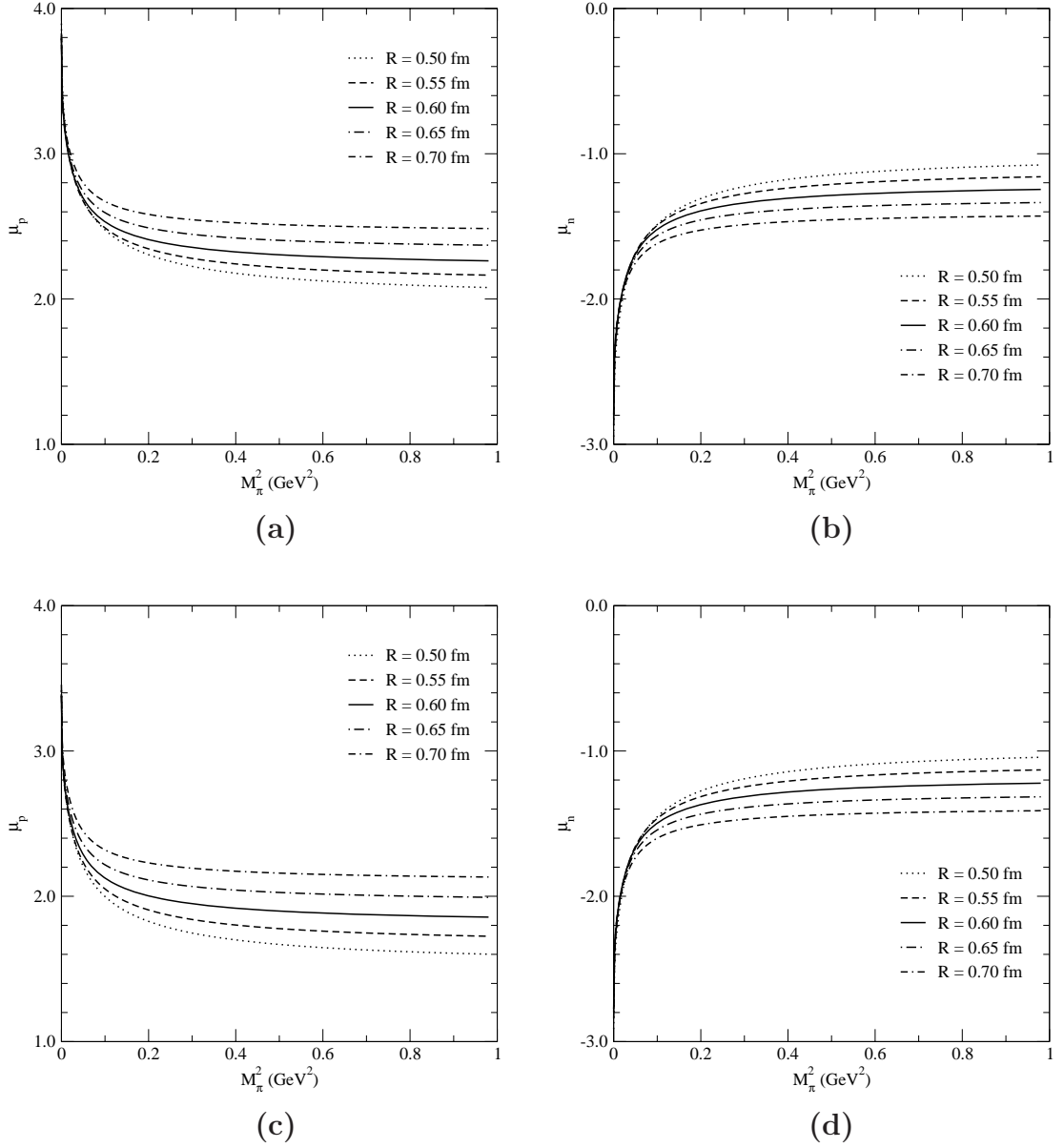


Figure 4.8 Nucleon magnetic moments as functions of M_π^2 , with various scale parameter: (a) for proton μ_p in SU(2), (b) for neutron μ_n in SU(2), (c) for proton μ_p in SU(3) and (d) for neutron μ_n in SU(3)

The proton charge form factors $G_E^p(Q^2)$ are presented in Figs. 4.9(a) and 4.9(b) for the two-flavor sector SU(2) and three-flavor sector SU(3), respectively, for various values of pion mass M_π^2 . It is clear that the M_π^2 -dependence of the form

factors is very slightly. Note that we have normalized the Sachs form factors to 1 at zero momentum transfer, for example, $G_E^p(0) = 1$. It is also found that the proton charge form factors are almost the same in SU(2) and SU(3) sectors.

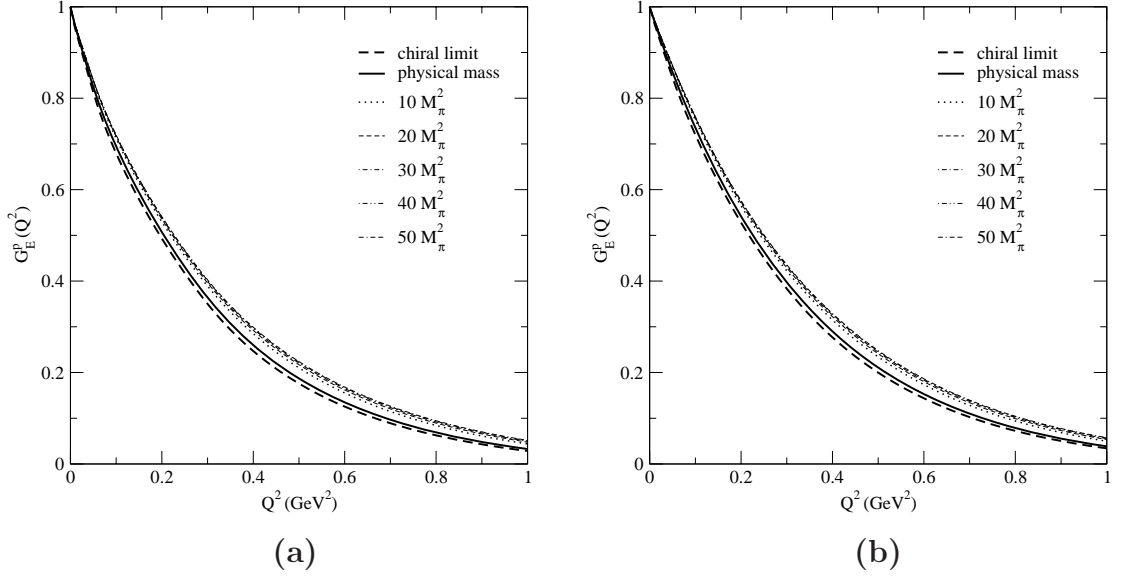


Figure 4.9 Proton charge form factor $G_E^p(Q^2)$ with various M_π^2 : (a) in SU(2) and (b) in SU(3)

Presented in Figs. 4.10(a) - 4.10(d) are our results of the nucleon magnetic form factors for various M_π^2 . The Sachs form factors are normalized to the nucleon magnetic moments at zero momentum transfer, that is, $G_E^p(0) = \mu_p$ and $G_M^n(0) = \mu_n$. It is found that the pion-mass dependence of the magnetic form factors is much stronger than for the proton charge form factor. And again the results from the SU(2) and SU(3) sectors are almost the same.

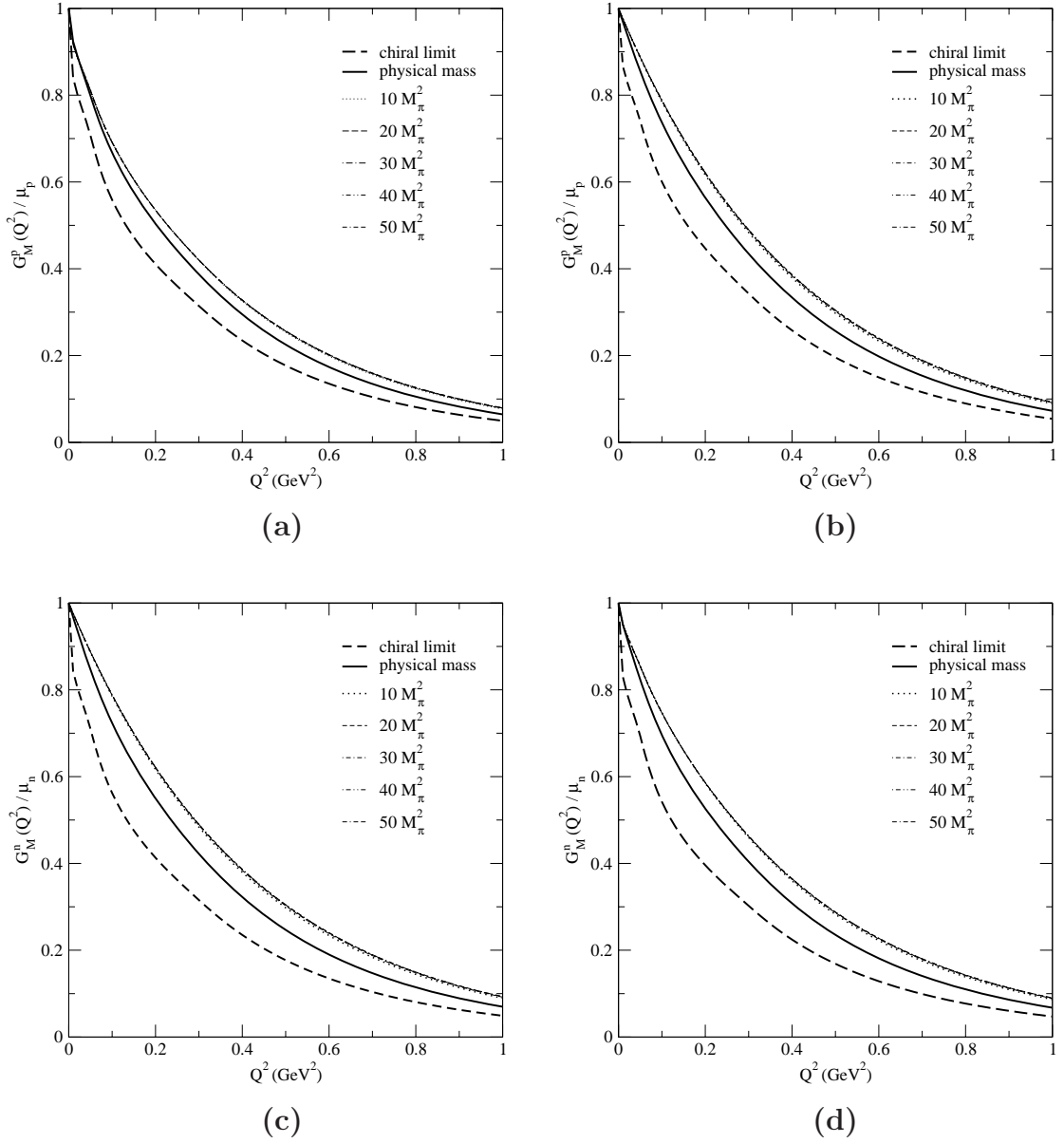


Figure 4.10 Proton magnetic form factor $G_E^p(Q^2)$ for various M_π^2 (a) in SU(2) and (b) in SU(3). Neutron magnetic form factor $G_M^n(Q^2)$ for various M_π^2 (c) in SU(2) and (d) in SU(3)

The pion-mass dependence of the nucleon magnetic moments is studied in the PCQM in the SU(2) case. Shown in Figs. 4.11(a) and 4.11(b) are the theoretical results of contributions of three-quarks core, meson cloud, and three-quarks core

plus meson cloud respectively. Our theoretical results are fairly consistent with lattice QCD calculations in Refs. (Hackett-Jones et al., 2000b) and (Lee et al., 2005a,b). It is also found that only the meson-cloud contribution to the nucleon magnetic moments is sensitive to the pion mass, especially at the low pion mass region ($M_\pi^2 \geq 0.2 \text{ GeV}^2$), and the meson-cloud contribution tends to zero when M_π^2 gets to 1.0 GeV^2 .

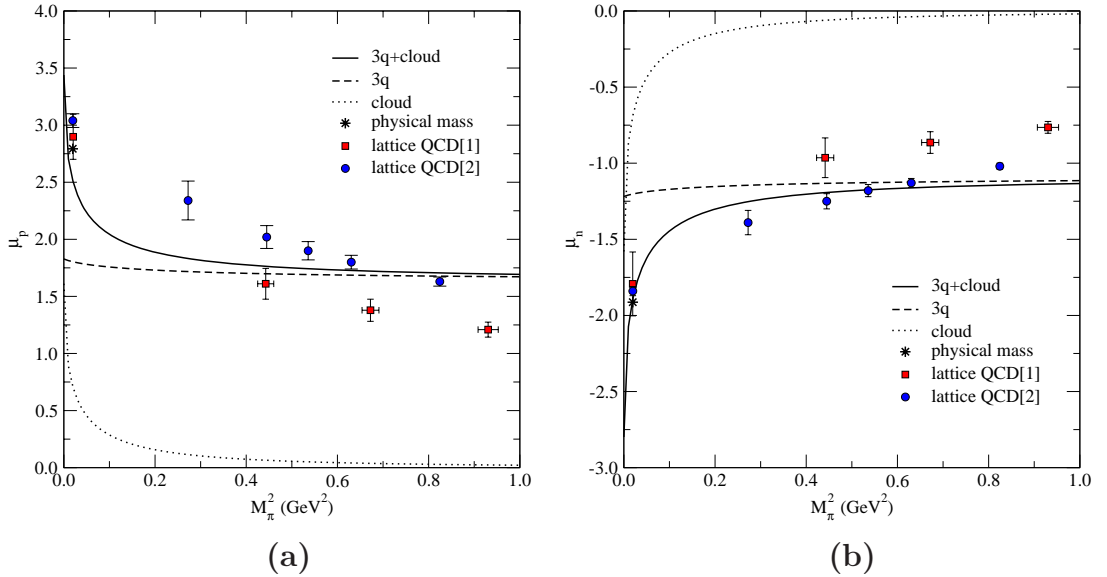


Figure 4.11 Dependence of μ_N on pion mass M_π^2 in $SU(2)$: quark core dressed with cloud (solid line), bare quarks (dashed line), meson cloud (dotted line) and lattice QCD [solid squares taken from (Hackett-Jones et al., 2000b), and solid circle taken from (Lee et al., 2005a,b)] (a) for μ_p and (b) for μ_n

As an extension, we have studied the pion-mass dependence of magnetic moments of the whole baryon octet in the $SU(3)$ sector. Presented in Figs. 4.12(a) - 4.12(f) are the theoretical results for μ_{Σ^+} , μ_{Σ^-} , μ_{Ξ^0} , μ_{Ξ^-} , μ_{Σ^0} , and μ_Λ , respectively. We obtain a fair consistence with lattice QCD calculations (Lee et al., 2005a,b), especially with the improved lattice QCD results (Lee et al., 2005a).

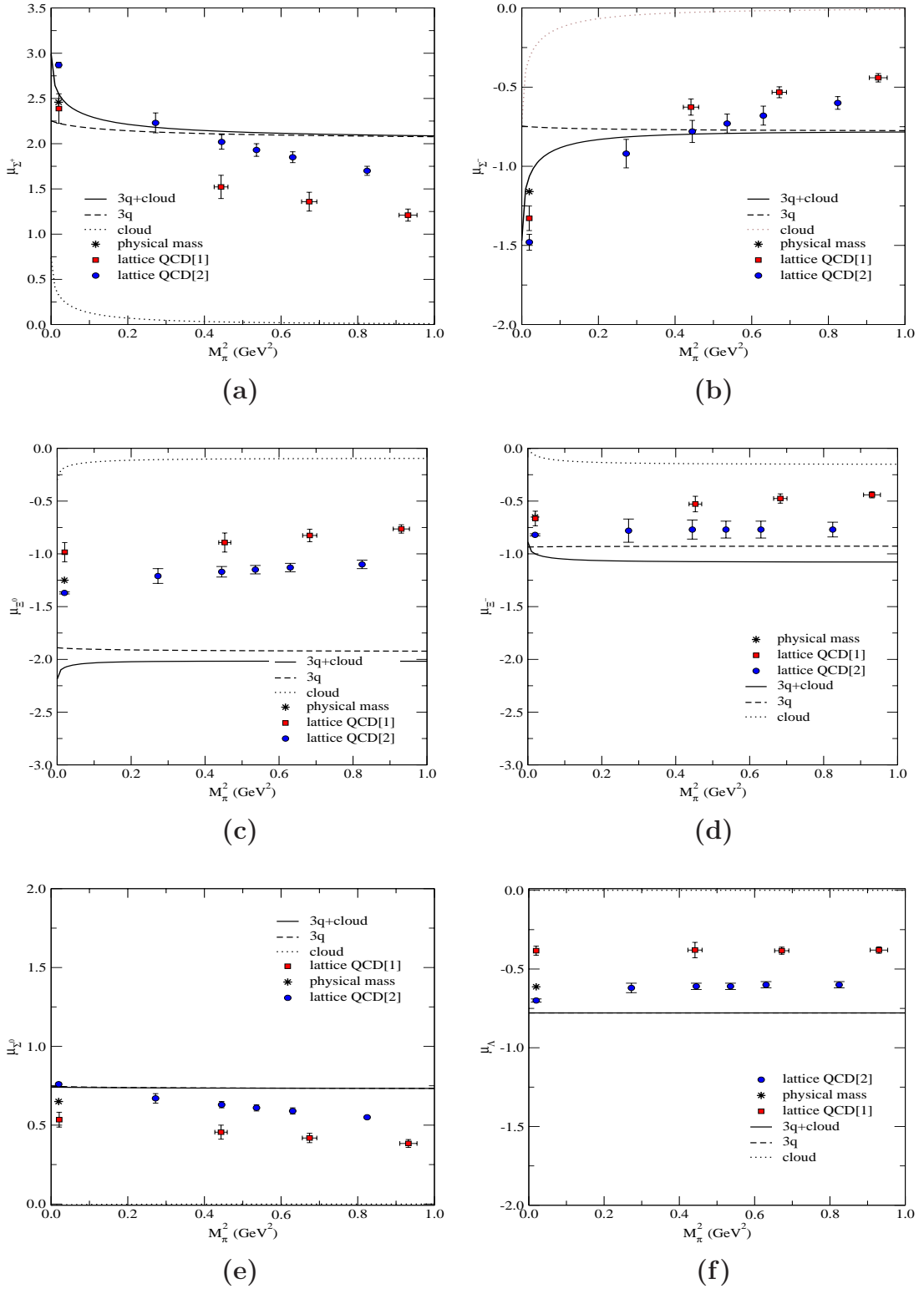


Figure 4.12 Dependence of μ_B on M_π^2 in SU(2): quark core dressed with cloud (solid line), quark core (dashed line), meson cloud (dotted line) and lattice QCD [solid squares taken from (Hackett-Jones et al., 2000b), and solid circle taken from (Lee et al., 2005a,b)] (a) μ_{Σ^+} , (b) μ_{Σ^-} , (c) μ_{Ξ^0} , (d) μ_{Ξ^-} , (e) μ_{Σ^0} , and (f) μ_Λ

Note in Figs. 4.12(e) and 4.12(f) that the meson cloud has no contribution to the μ_{Σ^0} and μ_{Λ} magnetic moments, and in Figs. 4.12(c) and 4.12(d) that the quark core contributions are independent of the pion mass at one-loop approximation of the PCQM.

Chapter V

DISCUSSION AND CONCLUSIONS

In this work we have applied the perturbative chiral quark model at one loop to describe the dependence of the baryon octet properties on the meson masses. It is found that the meson-mass dependence of the baryon octet properties such as the mass, magnetic moments, electromagnetic form factors, both for the two and three flavor sectors, are reasonably described in comparison to present lattice QCD and chiral extrapolation of these results. Given also the simplicity of this model approach, the evaluation at one loop seems sufficient to correctly describe the pion mass dependence of the discussed observables.

Starting point for the perturbative chiral quark model is based on the concept of effective chiral Lagrangian describing baryons by dressing the three valence quark operators by the chiral fields (the eight Goldstone mesons) which moving in a central Dirac field with a static potential. The underlying Lagrangian is motivated by the one of Chiral Perturbation Theory (ChPT), where the fundamental fermionic degrees of freedom are three valence quarks. The pseudoscalar mesons as additional degrees of freedom are included in our study as well. The supplementary of three valence quark operators by the chiral fields (a cloud of mesons) are projected on the baryonic level in order to obtain hadronic matrix elements. The parts concerning the meson cloud and three valence quarks factorize in the matrix element. Both parts can be separately calculated. The meson cloud part involves the chiral dynamics which arises from the chiral Lagrangian and can be calculated to the order of accuracy desired. The three valence quarks part in turn

can be relegated to a quark model with specific assumptions concerning confinement and hadronization, hence modelling three valence quarks structure. At this stage the factorization scheme can be viewed as a well-defined method to include chiral dynamics in a valence quark model. The chiral Lagrangian contains a set of low energy constants (LECs) which are parameters encoding short-distance effects and contributions due to heavy particle states. Incorporated with the impact of chiral symmetry breaking (e.g. spontaneous and explicit breaking) and chiral symmetry constraints (e.g. Gell-Mann-Oakes-Renner relations, Gell-Mann-Okubo relation, Goldberger-Treiman relation and partial conservation of axial current) are included.

In our framework we investigate the internal structure of the baryon octet, by probing the dependence of their static properties such as mass, charge radii, electromagnetic form factors and magnetic moments on the pseudoscalar meson masses. Our results of the electromagnetic form factors and magnetic moments for the baryon octet display a significant role of the meson cloud at low Q^2 , which is necessary to reproduce the detailed structure of these observables. The results may indicate that virtual mesons (meson-cloud) exist mainly outside the quark core.

REFERENCES

REFERENCES

- Ali Khan, A. et al. (2002). **Light hadron spectroscopy with two flavors of dynamical quarks on the lattice.** *Phys. Rev.*, D65:054505.
- Ali Khan, A. et al. (2004). **The nucleon mass in $N(f) = 2$ lattice QCD: Finite size effects from chiral perturbation theory.** *Nucl. Phys.*, B689:175–194.
- Aoki, S. et al. (2003). **Light hadron spectroscopy with two flavors of $O(a)$ -improved dynamical quarks.** *Phys. Rev.*, D68:054502.
- Becher, T. and Leutwyler, H. (1999). **Baryon chiral perturbation theory in manifestly Lorentz invariant form.** *Eur. Phys. J.*, C9:643–671.
- Becher, T. and Leutwyler, H. (2001). **Low energy analysis of $\pi N \rightarrow \pi N$.** *JHEP*, 06:017.
- Bernard, V. (2008). **Chiral Perturbation Theory and Baryon Properties.** *Prog. Part. Nucl. Phys.*, 60:82–160.
- Bernard, V., Hemmert, T. R., and Meissner, U.-G. (2004). **Cutoff schemes in chiral perturbation theory and the quark mass expansion of the nucleon mass.** *Nucl. Phys.*, A732:149–170.
- Borasoy, B. and Meissner, U.-G. (1997). **Chiral expansion of baryon masses and sigma-terms.** *Annals Phys.*, 254:192–232.
- Cheedket, S. et al. (2004). **Electromagnetic form factors of the baryon octet in the perturbative chiral quark model.** *Eur. Phys. J.*, A20:317–327.

- De Fazio, F. and Neubert, M. (1999). **$B \rightarrow X/u$ anti- ν/l decay distributions to order $\alpha(s)$.** *JHEP*, 06:017.
- DeGrand, T. A. (2004). **Lattice QCD at the end of 2003.** *Int. J. Mod. Phys.*, A19:1337–1394.
- Detmold, W., Melnitchouk, W., Negele, J. W., Renner, D. B., and Thomas, A. W. (2001). **Chiral extrapolation of lattice moments of proton quark distributions.** *Phys. Rev. Lett.*, 87:172001.
- Ellis, P. J. and Tang, H.-B. (1998). **Pion nucleon scattering in a new approach to chiral perturbation theory.** *Phys. Rev.*, C57:3356–3375.
- Faessler, A. et al. (2006a). **Electromagnetic properties of nucleons and hyperons in a Lorentz covariant quark model.**
- Faessler, A. et al. (2006b). **Light baryon magnetic moments and $N \rightarrow \Delta$ gamma transition in a Lorentz covariant chiral quark approach.** *Phys. Rev.*, D74:074010.
- Faessler, A., Gutsche, T., Lyubovitskij, V. E., and Pumsa-Ard, K. (2005). **Chiral dynamics of baryons in a covariant quark model.** *Prog. Part. Nucl. Phys.*, 55:12–22.
- Faessler, A., Gutsche, T., Lyubovitskij, V. E., and Pumsa-ard, K. (2006c). **Chiral dynamics of baryons in a Lorentz covariant quark model.** *Phys. Rev.*, D73:114021.
- Faessler, A., Gutsche, T., Lyubovitskij, V. E., and Pumsa-Ard, K. (2007). **Chiral dynamics of baryons in the quark model.** *AIP Conf. Proc.*, 884:43–51.

- Frink, M., Meissner, U.-G., and Scheller, I. (2005). **Baryon masses, chiral extrapolations, and all that.** *Eur. Phys. J.*, A24:395–409.
- Fuchs, T., Gegelia, J., and Scherer, S. (2004). **Structure of the nucleon in chiral perturbation theory.** *Eur. Phys. J.*, A19:35–42.
- Gasser, J. and Leutwyler, H. (1982). **Quark Masses.** *Phys. Rept.*, 87:77–169.
- Gasser, J. and Leutwyler, H. (1985). **Chiral Perturbation Theory: Expansions in the Mass of the Strange Quark.** *Nucl. Phys.*, B250:465.
- Gasser, J., Sainio, M. E., and Svarc, A. (1988). **Nucleons with Chiral Loops.** *Nucl. Phys.*, B307:779.
- Greenberg, O. W. (1964). **Spin and Unitary Spin Independence in a Paraquark Model of Baryons and Mesons.** *Phys. Rev. Lett.*, 13:598–602.
- Gross, D. J. and Wilczek, F. (1973). **Ultraviolet behavior of non-abelian gauge theories.** *Phys. Rev. Lett.*, 30:1343–1346.
- Gupta, R. (1997). **Introduction to lattice QCD.**
- Hackett-Jones, E. J., Leinweber, D. B., and Thomas, A. W. (2000a). **Incorporating chiral symmetry and heavy quark theory in extrapolations of octet baryon charge radii.** *Phys. Lett.*, B494:89–99.
- Hackett-Jones, E. J., Leinweber, D. B., and Thomas, A. W. (2000b). **Incorporating chiral symmetry in extrapolations of octet baryon magnetic moments.** *Phys. Lett.*, B489:143–147.
- Han, M. Y. and Nambu, Y. (1965). **Three-triplet model with double SU(3) symmetry.** *Phys. Rev.*, 139:B1006–B1010.

- Hemmert, T. R., Procura, M., and Weise, W. (2003a). **Chiral extrapolations of nucleon properties from lattice QCD.** *Nucl. Phys.*, A721:938–941.
- Hemmert, T. R., Procura, M., and Weise, W. (2003b). **Quark mass dependence of the nucleon axial-vector coupling constant.** *Phys. Rev.*, D68:075009.
- Hemmert, T. R. and Weise, W. (2002). **Chiral magnetism of the nucleon.** *Eur. Phys. J.*, A15:487–504.
- Holstein, B. R., Pascalutsa, V., and Vanderhaeghen, M. (2005). **Sum rules for magnetic moments and polarizabilities in QED and chiral effective-field theory.** *Phys. Rev.*, D72:094014.
- Inoue, T., Lyubovitskij, V. E., Gutsche, T., and Faessler, A. (2004). **Updated analysis of meson nucleon sigma terms in the perturbative chiral quark model.** *Phys. Rev.*, C69:035207.
- Khosonthongkee, K. et al. (2004). **Axial form factor of the nucleon in the perturbative chiral quark model.** *J. Phys.*, G30:793–810.
- Kubis, B. and Meissner, U. G. (2001a). **Baryon form factors in chiral perturbation theory.** *Eur. Phys. J.*, C18:747–756.
- Kubis, B. and Meissner, U.-G. (2001b). **Low energy analysis of the nucleon electromagnetic form factors.** *Nucl. Phys.*, A679:698–734.
- Lee, F. X., Kelly, R., Zhou, L., and Wilcox, W. (2005a). **Baryon magnetic moments in the background field method.** *Phys. Lett.*, B627:71–76.
- Lee, F. X., Kelly, R., Zhou, L., and Wilcox, W. (2005b). **Baryon magnetic moments in the external field method.** *Nucl. Phys. Proc. Suppl.*, 140:414–416.

- Lehnhart, B. C., Gegelia, J., and Scherer, S. (2005). **Baryon masses and nucleon sigma terms in manifestly Lorentz-invariant baryon chiral perturbation theory.** *J. Phys.*, G31:89–104.
- Leinweber, D. B., Lu, D.-H., and Thomas, A. W. (1999). **Nucleon magnetic moments beyond the perturbative chiral regime.** *Phys. Rev.*, D60:034014.
- Leinweber, D. B., Melnitchouk, W., Richards, D. G., Williams, A. G., and Zanotti, J. M. (2005). **Baryon spectroscopy in lattice QCD.** *Lect. Notes Phys.*, 663:71–112.
- Leinweber, D. B., Thomas, A. W., Tsushima, K., and Wright, S. V. (2000). **Baryon masses from lattice QCD: Beyond the perturbative chiral regime.** *Phys. Rev.*, D61:074502.
- Leinweber, D. B., Thomas, A. W., and Young, R. D. (2004). **Physical nucleon properties from lattice QCD.** *Phys. Rev. Lett.*, 92:242002.
- Luscher, M. (2003). **Lattice QCD: From quark confinement to asymptotic freedom.** *Annales Henri Poincare*, 4:S197–S210.
- Lyubovitskij, V. E., Gutsche, T., and Faessler, A. (2001a). **Electromagnetic structure of the nucleon in the perturbative chiral quark model.** *Phys. Rev.*, C64:065203.
- Lyubovitskij, V. E., Gutsche, T., Faessler, A., and Drukarev, E. G. (2001b). **Sigma-term physics in the perturbative chiral quark model.** *Phys. Rev.*, D63:054026.
- Lyubovitskij, V. E., Gutsche, T., Faessler, A., and Vinh Mau, R. (2001c). **π N scattering and electromagnetic corrections in the perturbative chiral quark model.** *Phys. Lett.*, B520:204–212.

- Lyubovitskij, V. E., Gutsche, T., Faessler, A., and Vinh Mau, R. (2002a). **Electromagnetic couplings of the ChPT Lagrangian from the perturbative chiral quark model.** *Phys. Rev.*, C65:025202.
- Lyubovitskij, V. E., Wang, P., Gutsche, T., and Faessler, A. (2002b). **Strange nucleon form factors in the perturbative chiral quark model.** *Phys. Rev.*, C66:055204.
- Meissner, U.-G. (2006a). **Quark mass dependence of baryon properties.** *PoS*, LAT2005:009.
- Meissner, U. G. (2006b). **Quark mass dependence of baryon properties: Foundations and applications.** *Nucl. Phys. Proc. Suppl.*, 153:170–184.
- Orth, B., Lippert, T., and Schilling, K. (2005). **Finite-size effects in lattice QCD with dynamical Wilson fermions.** *Phys. Rev.*, D72:014503.
- Petreczky, P. (2007). **Progress in finite temperature lattice QCD.**
- Politzer, H. D. (1973). **Reliable perturbative results for strong interactions?** *Phys. Rev. Lett.*, 30:1346–1349.
- Procura, M., Hemmert, T. R., and Weise, W. (2004). **Nucleon mass, sigma term and lattice QCD.** *Phys. Rev.*, D69:034505.
- Procura, M., Musch, B. U., Hemmert, T. R., and Weise, W. (2006a). **Quark mass dependence of nucleon observables and lattice QCD.** *AIP Conf. Proc.*, 842:240–242.
- Procura, M., Musch, B. U., Hemmert, T. R., and Weise, W. (2007). **Chiral extrapolation of $g(A)$ with explicit $\Delta(1232)$ degrees of freedom.** *Phys. Rev.*, D75:014503.

- Procura, M., Musch, B. U., Wollenweber, T., Hemmert, T. R., and Weise, W. (2006b). **Nucleon mass: From lattice QCD to the chiral limit.** *Phys. Rev.*, D73:114510.
- Pumsa-ard, K., Lyubovitskij, V. E., Gutsche, T., Faessler, A., and Cheedket, S. (2003). **Electromagnetic nucleon Delta transition in the perturbative chiral quark model.** *Phys. Rev.*, C68:015205.
- Richards, D. (2007). **Nucleon Structure from Lattice QCD.**
- Schindler, M. R., Djukanovic, D., Gegelia, J., and Scherer, S. (2007a). **Chiral expansion of the nucleon mass to order $O(q^6)$.** *Phys. Lett.*, B649:390–393.
- Schindler, M. R., Fuchs, T., Gegelia, J., and Scherer, S. (2007b). **Axial, induced pseudoscalar, and pion nucleon form factors in manifestly Lorentz-invariant chiral perturbation theory.** *Phys. Rev.*, C75:025202.
- Schindler, M. R., Gegelia, J., and Scherer, S. (2004). **Infrared regularization of baryon chiral perturbation theory reformulated.** *Phys. Lett.*, B586:258–266.
- Schindler, M. R., Gegelia, J., and Scherer, S. (2005). **Electromagnetic form factors of the nucleon in chiral perturbation theory including vector mesons.** *Eur. Phys. J.*, A26:1–5.
- Simkovic, F., Lyubovitskij, V. E., Gutsche, T., Faessler, A., and Kovalenko, S. (2002). **Neutrino mediated muon electron conversion in nuclei revisited.** *Phys. Lett.*, B544:121–126.
- Suganuma, H. et al. (2001). **Hadron Physics and Confinement Physics in Lattice QCD.** *AIP Conf. Proc.*, 594:376–386.

Wang, P., Leinweber, D. B., Thomas, A. W., and Young, R. D. (2007). **Chiral extrapolation of nucleon magnetic form factors.** *Phys. Rev.*, D75:073012.

Young, R. D., Leinweber, D. B., and Thomas, A. W. (2003). **Convergence of chiral effective field theory.** *Prog. Part. Nucl. Phys.*, 50:399–417.

APPENDICES

Appendix A

SOLUTIONS OF THE DIRAC EQUATION FOR THE EFFECTIVE POTENTIAL

In this section we indicate the solutions to the Dirac equation with the effective potential $V_{\text{eff}}(r) = S(r) + \gamma^0 V(r)$. The scalar $S(r)$ and time-like vector $V(r)$ parts are given by

$$\begin{aligned} S(r) &= M_1 + c_1 r^2, \\ V(r) &= M_2 + c_2 r^2, \end{aligned} \tag{A.1}$$

with the particular choice

$$M_1 = \frac{1 - 3\rho^2}{2\rho R}, \quad M_2 = \mathcal{E}_0 - \frac{1 + 3\rho^2}{2\rho R}, \quad c_1 \equiv c_2 = \frac{\rho}{2R^3}. \tag{A.2}$$

The quark wave function $u_\alpha(\vec{r})$ in state α with eigen-energy \mathcal{E}_α satisfies the Dirac equation

$$[-i\vec{\alpha}\vec{\nabla} + \beta S(r) + V(r) - \mathcal{E}_\alpha]u_\alpha(\vec{r}) = 0. \tag{A.3}$$

Solutions of the Dirac spinor $u_\alpha(\vec{r})$ can be written in the form (?)

$$u_\alpha(\vec{r}) = N_\alpha \begin{pmatrix} g_\alpha(r) \\ i\vec{\sigma} \cdot \hat{r} f_\alpha(r) \end{pmatrix} \mathcal{Y}_\alpha(\hat{r}) \chi_f \chi_c. \tag{A.4}$$

For the particular choice of the potential the radial functions g and f satisfy the

form

$$g_\alpha(r) = \left(\frac{r}{R_\alpha}\right)^l L_{n-1}^{l+1/2}\left(\frac{r^2}{R_\alpha^2}\right) e^{-\frac{r^2}{2R_\alpha^2}}, \quad (\text{A.5})$$

where for $j = l + \frac{1}{2}$

$$f_\alpha(r) = \rho_\alpha \left(\frac{r}{R_\alpha}\right)^{l+1} \left[L_{n-1}^{l+3/2}\left(\frac{r^2}{R_\alpha^2}\right) + L_{n-2}^{l+3/2}\left(\frac{r^2}{R_\alpha^2}\right) \right] e^{-\frac{r^2}{2R_\alpha^2}}, \quad (\text{A.6})$$

and for $j = l - \frac{1}{2}$

$$f_\alpha(r) = -\rho_\alpha \left(\frac{r}{R_\alpha}\right)^{l-1} \left[\left(n + l - \frac{1}{2}\right) L_{n-1}^{l-1/2}\left(\frac{r^2}{R_\alpha^2}\right) + n L_n^{l-1/2}\left(\frac{r^2}{R_\alpha^2}\right) \right] e^{-\frac{r^2}{2R_\alpha^2}}. \quad (\text{A.7})$$

The label $\alpha = (nljm)$ characterizes the state with principle quantum number $n = 1, 2, 3, \dots$, orbital angular momentum l , total angular momentum $j = l \pm \frac{1}{2}$ and projection m . Due to the quadratic nature of the potential the radial wave functions contain the associated Laguerre polynomials $L_n^k(x)$ with

$$L_n^k(x) = \sum_{m=0}^n (-1)^m \frac{(n+k)!}{(n-m)!(k+m)!m!} x^m. \quad (\text{A.8})$$

The angular dependence ($\mathcal{Y}_\alpha(\hat{r}) \equiv \mathcal{Y}_{lmj}(\hat{r})$) is defined by

$$\mathcal{Y}_{lmj}(\hat{r}) = \sum_{m_l, m_s} (lm_l \frac{1}{2} m_s | jm) Y_{lm_l}(\hat{r}) \chi_{\frac{1}{2} m_s} \quad (\text{A.9})$$

where $Y_{lm_l}(\hat{r})$ is the usual spherical harmonic. Flavor and color parts of the Dirac spinor are represented by χ_f and χ_c , respectively.

The normalization constant is obtained from the condition

$$\int_0^\infty d^3\vec{r} u_\alpha^\dagger(\vec{r}) u_\alpha(\vec{r}) = 1 \quad (\text{A.10})$$

which results in

$$N_\alpha = \left[2^{-2(n+l+1/2)} \pi^{1/2} R_\alpha^3 \frac{(2n+2l)!}{(n+l)!(n-1)!} \left\{ 1 + \rho_\alpha^2 \left(2n + l - \frac{1}{2} \right) \right\} \right]^{-1/2}, \quad (\text{A.11})$$

The two coefficients R_α and ρ_α are of the form

$$R_\alpha = R(1 + \Delta\mathcal{E}_\alpha \rho R)^{-1/4}, \quad (\text{A.12})$$

$$\rho_\alpha = \rho \left(\frac{R_\alpha}{R} \right)^3, \quad (\text{A.13})$$

and are related to the Gaussian parameters ρ and R of Eq. (2.15). The quantity $\Delta\mathcal{E}_\alpha = \mathcal{E}_\alpha - \mathcal{E}_0$ is the difference between the energy of state α and the ground state. $\Delta\mathcal{E}_\alpha$ depends on the quantum numbers n and l and is related to the parameters ρ and R by

$$\left(\Delta\mathcal{E}_\alpha + \frac{3\rho}{R} \right)^2 \left(\Delta\mathcal{E}_\alpha + \frac{1}{\rho R} \right) = \frac{\rho}{R^3} (4n + 2l - 1)^2. \quad (\text{A.14})$$

The potential of harmonic oscillator is widely employed to study the interaction in quark-antiquark system of mesons and three quarks system of baryon. The main character of potential considered to be harmonic is

$$V(r) \propto r^2. \quad (\text{A.15})$$

In the spherical coordinate, the radial schrödinger equation is

$$\left[\frac{d^2}{dr^2} + \frac{2\mu}{\hbar^2} \left(E - \frac{1}{2} \mu \omega^2 r^2 \right) - \frac{l(l+1)}{r^2} \right] u(r) = 0 \quad (\text{A.16})$$

where

$$u(r) = rR(r) \quad (\text{A.17})$$

Eq. (A.16) can be contracted to

$$\left[\frac{d^2}{d\rho^2} - \frac{l(l+1)}{\rho^2} + \lambda - \rho^2 \right] u(\rho) = 0 \quad (\text{A.18})$$

by introducing the dimensionless variable

$$\begin{aligned} \rho &= \alpha r \\ \lambda &= \frac{2E}{\hbar\omega} \end{aligned} \quad (\text{A.19})$$

where

$$\alpha = \left(\frac{\mu\omega}{\hbar} \right)^{1/2} \quad (\text{A.20})$$

The study of an asymptotic behavior of $u(\rho)$ leads to, when $\rho \rightarrow 0$,

$$u(\rho) \sim \rho^{l+1} \quad (\text{A.21})$$

and, when $\rho \rightarrow \infty$,

$$\left[\frac{d^2}{d\rho^2} - \rho^2 \right] u(\rho) = 0. \quad (\text{A.22})$$

The solution of asymptotic equation is

$$u(\rho) \sim e^{-\rho^2/2}. \quad (\text{A.23})$$

According to the asymptotic behaviors in eqs. (A.21) and (A.23), the solution of

$u(\rho)$ in (A.18) is assumed as

$$u(\rho) = e^{-\rho^2/2} \rho^{l+1} g(\rho). \quad (\text{A.24})$$

Introduced $y = \rho^2$ and inserted (A.24) into (A.18), equation of $g(\rho)$ becomes

$$y \frac{d^2 g(y)}{dy^2} + \left[\left(l + \frac{3}{2} \right) - y \right] \frac{dg(y)}{dy} - \left[\frac{1}{2} \left(l + \frac{3}{2} \right) - \frac{\lambda}{4} \right] g(y) = 0. \quad (\text{A.25})$$

This is the Kummer-Laplace differential equation whose solution, regular at the origin, is

$$g(y) = CF \left(\frac{l}{2} + \frac{3}{4} - \frac{\lambda}{4}, l + \frac{3}{2}, y \right) \quad (\text{A.26})$$

where C is a constant and F is the confluent hypergeometric function,

$$\begin{aligned} F(\alpha, \gamma, \rho) &= 1 + \frac{\alpha \rho}{\gamma 1!} + \frac{\alpha(\alpha+1) \rho^2}{\gamma(\gamma+1) 2!} + \dots \\ &= \sum_{k=0}^{\infty} \frac{(\alpha)_k \rho^k}{(\gamma)_k k!} \end{aligned} \quad (\text{A.27})$$

The spherical wave function or the simultaneous eigenfunction of the observables (H, L^2, L_z) reads

$$\psi_{nlm}(r, \theta, \phi) = R_{nl}(r) Y_{lm}(\theta, \phi) \quad (\text{A.28})$$

where $R_{nl}(r)$ is the radial wave functions and $Y_{lm}(\theta, \phi)$ is the spherical harmonics.

From (A.26), the radial wave function behaves

$$R_{nl}(r) \sim (\alpha r)^l e^{-\frac{1}{2}\alpha^2 r^2} F\left(-n, l + \frac{3}{2}, \alpha^2 r^2\right). \quad (\text{A.29})$$

The normalized wave function reads

$$R_{nl}(r) = \alpha^{3/2} \left[\frac{2^{l+2-n}(2l+2n+1)!!}{\sqrt{\pi}n![(2l+1)!!]^2} \right] (\alpha r)^l e^{-\frac{1}{2}\alpha^2 r^2} F(-n, l + \frac{3}{2}, \alpha^2 r^2). \quad (\text{A.30})$$

It is more often and convenient to write the above equation in terms of Laguerre polynomials,

$$R_{nl}(r) = \left[\frac{2\alpha^3 n!}{\Gamma(n+l+\frac{3}{2})} \right] (\alpha r)^l e^{-\frac{1}{2}\alpha^2 r^2} L_n^{l+1/2}(\alpha^2 r^2). \quad (\text{A.31})$$

where $L_n^{l+1/2}(\alpha^2 r^2)$ are the associated Laguerre polynomials

$$L_n^{l+1/2}(\alpha^2 r^2) = \sum_{k=0}^n \frac{(-1)^k}{k!} \frac{\Gamma(n+l+\frac{3}{2})}{(n-k)!\Gamma(k+l+\frac{3}{2})} r^{2k} \quad (\text{A.32})$$

The radial wave functions have the orthogonal property

$$\int_0^\infty r^2 dr R_{nl}(r) R_{n'l}(r) = \delta_{nn'} \quad (\text{A.33})$$

By the Fourier transformation, the analytical wave function of a harmonic oscillator in momentum space is shown

$$\psi_{nlm}(\vec{p}) = \frac{1}{(2\pi\hbar)^{\frac{3}{2}}} \int d\vec{r} \psi_{nlm}(\vec{r}) e^{-i\vec{p}\cdot\vec{r}} = (-i)^{2n+l} R_{nl}(p) Y_{lm}(\vec{p}) \quad (\text{A.34})$$

where

$$R_{nl}(r) = \left[\frac{2\beta^3 n!}{\Gamma(n+l+\frac{3}{2})} \right] (\beta r)^l e^{-\frac{1}{2}\beta^2 r^2} L_n^{l+1/2}(\beta^2 r^2). \quad (\text{A.35})$$

and

$$\beta = \frac{1}{\alpha\hbar} \quad (\text{A.36})$$

In our calculation, the spatial wave functions in momentum space are always used and β is interpreted as a size parameter in unit of GeV^{-1} . For mesons (quark-antiquark boundstates), \vec{p} is the momentum of the center of mass

$$\vec{p} = \frac{\vec{p}_1 - \vec{p}_2}{2} \quad (\text{A.37})$$

where \vec{p}_1 and \vec{p}_2 are momentums of quark and antiquark, respectively.

Appendix B

γ -MATRICES AND TRACE TECHNOLOGY

Four dimensional γ -matrices are defined by the anticommutation relation

$$\{\gamma^\mu, \gamma^\nu\} \equiv \gamma^\mu \gamma^\nu + \gamma^\nu \gamma^\mu = 2\gamma^{\mu\nu} + \mathbf{1}_{n \times n}. \quad (\text{B.1})$$

Definitions base on “An Introduction to Quantum Field Theory”* with priority.

Specific Weyl or chiral representations are

$$\gamma^0 = \begin{pmatrix} 0 & 1 \\ 1 & 0 \end{pmatrix}; \quad \gamma^i = \begin{pmatrix} 0 & \sigma^i \\ -\sigma^i & 0 \end{pmatrix} \quad (\text{B.2})$$

where σ^i is Pauli matrices,

$$\sigma^1 = \begin{pmatrix} 0 & 1 \\ 1 & 0 \end{pmatrix}; \quad \sigma^2 = \begin{pmatrix} 0 & -i \\ i & 0 \end{pmatrix}; \quad \sigma^3 = \begin{pmatrix} 1 & 0 \\ 0 & -1 \end{pmatrix}. \quad (\text{B.3})$$

To easily attack QED problems, the trace techniques produced by R. P. Feynman has been a very important tools. Here are some proves and properties. The prove

*Michael E. Peskin and Daniel V. Schroeder, 1995

of trace of one γ matrix is

$$\begin{aligned}
\text{tr}\gamma^\mu &= \text{tr}\gamma^5\gamma^5\gamma^\mu && \text{since } (\gamma^5)^2 = 1 \\
&= -\text{tr}\gamma^5\gamma^\mu\gamma^5 && \text{since } \{\gamma^\mu, \gamma^5\} = 0 \\
&= -\text{tr}\gamma^5\gamma^5\gamma^\mu && \text{using cyclic properties of trace} \\
&= -\text{tr}\gamma^\mu && \text{(B.4)}
\end{aligned}$$

where $\gamma^5 = \begin{pmatrix} -1 & 0 \\ 0 & 1 \end{pmatrix}$. Any parameter equal to minus itself must be vanished.

The result is also applied to trace of odd number of γ matrix. For the trace of two γ matrices, we use the anticommutation property and the cyclic property of trace,

$$\begin{aligned}
\text{tr}\gamma^\mu\gamma^\nu &= \text{tr}(2g^{\mu\nu} \cdot 1 - \gamma^\mu\gamma^\nu) && \text{(anticommutation)} \\
&= 8g^{\mu\nu} - \text{tr}\gamma^\mu\gamma^\nu && \text{(cyclicity) (B.5)}
\end{aligned}$$

Hence $\text{tr}\gamma^\mu\gamma^\nu = 4g^{\mu\nu}$. The trace of any even number of γ matrices are evaluated in the same way by anticommuting the first γ matrix all the way to right, then cycle it back to the left. For the trace of four γ matrices, we have

$$\begin{aligned}
\text{tr}(\gamma^\mu\gamma^\nu\gamma^\rho\gamma^\sigma) &= \text{tr}(2g^{\mu\nu}\gamma^\rho\gamma^\sigma - \gamma^\nu\gamma^\mu\gamma^\rho\gamma^\sigma) \\
&= \text{tr}(2g^{\mu\nu}\gamma^\rho\gamma^\sigma - \gamma^\nu 2g^{\mu\rho}\gamma^\sigma + \gamma^\nu\gamma^\rho 2g^{\mu\sigma} - \gamma^\nu\gamma^\rho\gamma^\sigma\gamma^\mu) && \text{(B.6)}
\end{aligned}$$

Using the cyclic property on the last term and move it to the left hand side, we obtain

$$\begin{aligned}
\text{tr}(\gamma^\mu\gamma^\nu\gamma^\rho\gamma^\sigma) &= g^{\mu\nu}\text{tr}\gamma^\rho\gamma^\sigma - g^{\mu\rho}\text{tr}\gamma^\mu\gamma^\sigma + g^{\mu\sigma}\text{tr}\gamma^\nu\gamma^\rho \\
&= 4(g^{\mu\nu}g^{\rho\sigma} - g^{\mu\rho}g^{\nu\sigma} + g^{\mu\sigma}g^{\nu\rho}) && \text{(B.7)}
\end{aligned}$$

For $\gamma^5 = i\gamma^0\gamma^1\gamma^2\gamma^3$, the trace of γ^5 and any odd number of other matrices is vanish. The trace of γ^5 itself, however, is also zero,

$$\text{tr}\gamma^5 = \text{tr}(\gamma^0\gamma^0\gamma^5) = -\text{tr}(\gamma^0\gamma^5\gamma^0) = -\text{tr}(\gamma^0\gamma^0\gamma^5) = -\text{tr}\gamma^5 = 0. \quad (\text{B.8})$$

These are summary of trace theorems;

$$\begin{aligned} \text{tr}(1) &= 4 \\ \text{tr}(\text{any odd \# of } \gamma^s) &= 0 \\ \text{tr}(\gamma^\mu\gamma^\nu) &= 4g^{\mu\nu} \\ \text{tr}(\gamma^\mu\gamma^\nu\gamma^\rho\gamma^\sigma) &= 4(g^{\mu\nu}g^{\rho\sigma} - g^{\mu\rho}g^{\nu\sigma} + g^{\mu\sigma}g^{\nu\rho}) \\ \text{tr}(\gamma^5) &= 0 \\ \text{tr}(\gamma^\mu\gamma^\nu\gamma^5) &= 0 \\ \text{tr}(\gamma^\mu\gamma^\nu\gamma^\rho\gamma^\sigma\gamma^5) &= -4i\epsilon^{\mu\nu\rho\sigma}. \end{aligned} \quad (\text{B.9})$$

The last formula can be simplified by

$$\begin{aligned} \epsilon^{\alpha\beta\gamma\delta}\epsilon_{\alpha\beta\gamma\delta} &= -24 \\ \epsilon^{\alpha\beta\gamma\mu}\epsilon_{\alpha\beta\gamma\nu} &= -6\delta_\nu^\mu \\ \epsilon^{\alpha\beta\gamma\delta}\epsilon_{\alpha\beta\rho\sigma} &= -2(\delta_\rho^\mu\delta_\sigma^\nu - \delta_\sigma^\mu\delta_\rho^\nu) \end{aligned} \quad (\text{B.10})$$

The order of all γ matrices can be reversed,

$$\text{tr}(\gamma^\mu\gamma^\nu\gamma^\rho\gamma^\sigma \dots) = \text{tr}(\dots\gamma^\sigma\gamma^\rho\gamma^\nu\gamma^\mu) \quad (\text{B.11})$$

Two γ matrices with similar indices dotted together can be reduced by

$$\gamma^\mu \gamma_\mu = g_{\mu\nu} \gamma^\mu \gamma^\nu = \frac{1}{2} g_{\mu\nu} \{\gamma^\mu, \gamma^\nu\} = g_{\mu\nu} g^{\mu\nu} = 4. \quad (\text{B.12})$$

In addition, several γ matrices dotted together and having the following form can be reduced by contraction identities, easily proved by using the anticommutation relations,

$$\begin{aligned} \gamma^\mu \gamma^\nu \gamma_\mu &= -2\gamma^\nu \\ \gamma^\mu \gamma^\nu \gamma^\rho \gamma_\mu &= -2g^{\nu\rho} \\ \gamma^\mu \gamma^\nu \gamma^\rho \gamma^\sigma \gamma_\mu &= -2\gamma^\sigma \gamma^\rho \gamma^\nu. \end{aligned} \quad (\text{B.13})$$

All these properties are important in the QED calculation of differential cross section.

Appendix C

BASIC NOTATIONS OF THE SU(3) GROUP

The group SU(3) is defined as the set of all unitary, unimodular and 3×3 matrices U i.e.

$$U^\dagger U = 1, \quad \det(U) = 1. \quad (\text{C.1})$$

In mathematical terms, SU(3) is an eight-parameter, compact Lie group. This implies that any group element can be parameterized by a set of eight independent real parameters $\theta = (\theta_1, \dots, \theta_8)$ varying over a continuous range. Elements of SU(3) can be obtained from the exponential representation:

$$U[\theta] = \exp\left(-i \sum_{a=1}^8 \theta_a \frac{\lambda_a}{2}\right) \quad (\text{C.2})$$

with θ_a real numbers, and where the eight linearly independent matrices λ_a are the so-called Gell-Mann matrices, satisfying

$$\lambda_a = \lambda_a^\dagger, \quad (\text{C.3})$$

$$\text{Tr}(\lambda_a \lambda_b) = 2\delta_{ab}, \quad (\text{C.4})$$

$$\text{Tr}(\lambda_a) = 0. \quad (\text{C.5})$$

where λ_a are the Gell-Mann matrices with the explicit forms

$$\begin{aligned}
\lambda_1 &= \begin{pmatrix} 0 & 1 & 0 \\ 1 & 0 & 0 \\ 0 & 0 & 0 \end{pmatrix}, \lambda_2 = \begin{pmatrix} 0 & -i & 0 \\ i & 0 & 0 \\ 0 & 0 & 0 \end{pmatrix}, \lambda_3 = \begin{pmatrix} 1 & 0 & 0 \\ 0 & -1 & 0 \\ 0 & 0 & 0 \end{pmatrix}, \\
\lambda_4 &= \begin{pmatrix} 0 & 0 & 1 \\ 0 & 0 & 0 \\ 1 & 0 & 0 \end{pmatrix}, \lambda_5 = \begin{pmatrix} 0 & 0 & -i \\ 0 & 0 & 0 \\ i & 0 & 0 \end{pmatrix}, \lambda_6 = \begin{pmatrix} 0 & 0 & 0 \\ 0 & 0 & 1 \\ 0 & 1 & 0 \end{pmatrix}, \\
\lambda_7 &= \begin{pmatrix} 0 & 0 & 0 \\ 0 & 0 & -i \\ 0 & i & 0 \end{pmatrix}, \lambda_8 = \sqrt{\frac{1}{3}} \begin{pmatrix} 1 & 0 & 0 \\ 0 & 1 & 0 \\ 0 & 0 & -2 \end{pmatrix}.
\end{aligned} \tag{C.6}$$

The commutation relations of the Gell-Mann matrices indicate the structure of the Lie group of SU(3) with

$$\left[\frac{\lambda_a}{2}, \frac{\lambda_b}{2} \right] = i f_{abc} \frac{\lambda_c}{2}, \tag{C.7}$$

where f_{abc} are the totally antisymmetry structure constants. The non-vanishing values of f_{abc} are

$$\begin{aligned}
f_{123} &= 1, \\
f_{147} &= -f_{156} = f_{246} = f_{257} = f_{345} = -f_{367} = 1/2, \\
f_{458} &= f_{678} = \sqrt{3}/2.
\end{aligned} \tag{C.8}$$

Other important relations of the Gell-Mann matrices are their anti-commutation relations

$$\{\lambda_a, \lambda_b\} = \frac{4}{3}\delta_{ab} + 2d_{abc}\lambda_c, \quad (\text{C.9})$$

where the totally symmetric real constants d_{abc} are

$$\begin{aligned} d_{118} = d_{228} = d_{338} = -d_{888} &= \frac{1}{\sqrt{3}}, \\ d_{146} = d_{157} = -d_{247} = -d_{256} = d_{344} = d_{355} = -d_{366} = -d_{377} &= \frac{1}{2}, \\ d_{488} = d_{588} = d_{688} = d_{788} &= -\frac{1}{2\sqrt{3}}. \end{aligned} \quad (\text{C.10})$$

Appendix D

THE ELECTROMAGNETIC FORM FACTORS IN BREIT FRAME

The electromagnetic current operator for the baryon J^μ can be written as

$$\begin{aligned}
\langle B'(p') | J^\mu(0) | B(p) \rangle &= \bar{u}_{B'}(p') [\gamma^\mu F_1^B(q^2) + \frac{i\sigma^{\mu\nu} q_\nu}{2m_B} F_2^B(q^2)] u_B(p) \\
&= \bar{u}_{B'}(p') [\gamma^\mu F_1^B(q^2) + \{ \gamma^\mu - \frac{1}{2m_B} (p' - p)^\mu \} F_2^B(q^2)] u_B(p) \\
&= \bar{u}_{B'}(p') [\gamma^\mu F_1^B(q^2) + F_2^B(q^2) - \frac{1}{2m_B} (p' - p)^\mu F_2^B(q^2)] u_B(p).
\end{aligned} \tag{D.1}$$

where

$$\begin{aligned}
\bar{u}_{B'}(p') i\sigma^{\mu\nu} q_\nu u_B(p) &= \bar{u}_{B'}(p') [-\frac{1}{2} (\gamma^\mu \gamma^\nu - \gamma^\nu \gamma^\mu) (p' - p)_\nu] u_B(p) \\
&= -\frac{1}{2} \bar{u}_{B'}(p') [\{ (2g^{\mu\nu} - \gamma^\nu \gamma^\mu) - \gamma^\nu \gamma^\mu \} p'_\nu \\
&\quad - \{ \gamma^\mu \gamma^\nu - (2g^{\nu\mu} - \gamma^\mu \gamma^\nu) \} p_\nu] u_B(p) \\
&= -\frac{1}{2} \bar{u}_{B'}(p') [2g^{\mu\nu} p'_\nu - 2\gamma^\nu p'_\nu \gamma^\mu - 2\gamma^\mu \gamma^\nu p_\nu + 2g^{\nu\mu} p_\nu] u_B(p) \\
&= -\bar{u}_{B'}(p') [p'^\mu - m_B \gamma^\mu - \gamma^\mu m_B + p^\mu] u_B(p) \\
&= \bar{u}_{B'}(p') [2m_B \gamma^\mu - (p' + p)^\mu] u_B(p).
\end{aligned} \tag{D.2}$$

and

$$\bar{u}_{B'}(\gamma^\nu p_\mu - m_B) = 0, \quad \bar{u}_{B'}\gamma^\nu p_\nu = m_B \bar{u}_{B'} \quad (\text{D.3})$$

$$(\gamma^\nu p_\nu - m_B)u_B = 0, \quad \gamma^\nu p_\nu u_B = m_B u_B. \quad (\text{D.4})$$

The Sachs form factors can be written by

$$G_E^B(Q^2) \equiv F_1^B(q^2) + \frac{q^2}{4m_B^2} F_2^B(q^2), \quad \text{time component} \quad (\text{D.5})$$

$$G_M^B(Q^2) \equiv F_1^B(q^2) + F_2^B(q^2). \quad \text{space component} \quad (\text{D.6})$$

The current matrix elements can be decomposed into two components, namely time and spatial component:

$$\begin{aligned} \langle B'(p') | J^0(0) | B(p) \rangle &= \{F_1^B(q^2) + F_2^B(q^2)\} \bar{u}_{B'}(p') \gamma^0 u_B(p) - \frac{E}{m_B} F_2^B(q^2) \bar{u}_{B'}(p') u_B(p) \\ &= \{F_1^B(q^2) + F_2^B(q^2)\} \chi_{s'}^\dagger \chi_s - \frac{E}{m_B} F_2^B(q^2) \frac{E}{m_B} \chi_{s'}^\dagger \chi_s \\ &= \{F_1^B(q^2) + (1 - \frac{E^2}{m_B^2}) F_2^B(q^2)\} \chi_{s'}^\dagger \chi_s \\ &= \{F_1^B(q^2) + \frac{q^2}{m_B^2} F_2^B(q^2)\} \chi_{s'}^\dagger \chi_s \\ &= G_E^B(Q^2) \chi_{s'}^\dagger \chi_s. \end{aligned} \quad (\text{D.7})$$

and

$$\begin{aligned}
\langle B'(p') | \bar{J}(0) | B(p) \rangle &= \{F_1^B(q^2) + F_2^B(q^2)\} \bar{u}_{B'}(p') \bar{\gamma} u_B(p) \\
&= \{F_1^B(q^2) + F_2^B(q^2)\} \chi_{s'}^\dagger \frac{i\bar{\sigma}_B \times \bar{q}}{2m_B} \chi_s \\
&= G_M^B(Q^2) \chi_{s'}^\dagger \frac{i\sigma_B \times \bar{q}}{2m_B} \chi_s.
\end{aligned} \tag{D.8}$$

by using the free Dirac equation to get the solution:

$$\bar{u}_{B'}(p') \gamma^0 u_B(p) = \chi_{s'}^\dagger \chi_s \tag{D.9}$$

$$\bar{u}_{B'}(p') u_B(p) = \frac{E}{m_B} \chi_{s'}^\dagger \chi_s \tag{D.10}$$

$$\bar{u}_{B'}(p') \gamma^i u_B(p) = \chi_{s'}^\dagger \frac{i\bar{\sigma} \times \bar{q}}{2m_B} \chi_s. \tag{D.11}$$

where

$$\begin{aligned}
u_B(p) &= N \begin{pmatrix} 1 \\ \frac{\bar{\sigma} \cdot (-\bar{q}/2)}{E + m_B} \end{pmatrix} \chi_s, \\
\bar{u}_B(p) &= N \chi_{s'}^\dagger \begin{pmatrix} 1 & -\bar{\sigma} \cdot (\bar{q}/2) \\ & E + m_B \end{pmatrix}, \quad N = \sqrt{\frac{E + m_B}{2m_B}}.
\end{aligned} \tag{D.12}$$

Therefore

$$\begin{aligned}
\bar{u}_{B'}(p')\gamma^0 u_B(p) &= N^2 \chi_{s'}^\dagger \begin{pmatrix} 1 & \frac{-\bar{\sigma} \cdot (\bar{q}/2)}{E + m_B} \end{pmatrix} \begin{pmatrix} 1 & 0 \\ 0 & -1 \end{pmatrix} \begin{pmatrix} 1 \\ \frac{\bar{\sigma} \cdot (-\bar{q}/2)}{E + m_B} \end{pmatrix} \chi_s \\
&= \left(\frac{E + m_B}{2m_B} \right) \chi_{s'}^\dagger \left(1 - \frac{(\bar{\sigma} \cdot \bar{q}/2)^2}{E + m_B} \right) \chi_s \\
&= \frac{m_B^2 + 2Em_B + (E^2 - \bar{q}^2/4)}{2m_B(E + m_B)} \chi_{s'}^\dagger \chi_s \\
&= \frac{m_B^2 + 2Em_B + m_B^2}{2m_B(E + m_B)} \chi_{s'}^\dagger \chi_s \\
&= \chi_{s'}^\dagger \chi_s.
\end{aligned} \tag{D.13}$$

and

$$\begin{aligned}
\bar{u}^{B'}(p')u_B(p) &= N^2 \chi_{s'}^\dagger \begin{pmatrix} 1 & \frac{-\bar{\sigma} \cdot (\bar{q}/2)}{E + m_B} \end{pmatrix} \begin{pmatrix} 1 \\ \frac{\bar{\sigma} \cdot (-\bar{q}/2)}{E + m_B} \end{pmatrix} \chi_s \\
&= \left(\frac{E + m_B}{2m_B} 1 + \frac{(\bar{\sigma} \cdot \bar{q}/2)^2}{(E + m_B)^2} \right) \chi_{s'}^\dagger \chi_s \\
&= \frac{E^2 + 2m_BE + (m_B^2 + (\bar{q}/2)^2)}{2m_B(E + m_B)} \chi_{s'}^\dagger \chi_s \\
&= \frac{2E(E + m_B)}{2m_B(E + m_B)} \chi_{s'}^\dagger \chi_s \\
&= \frac{E}{m_B} \chi_{s'}^\dagger \chi_s.
\end{aligned} \tag{D.14}$$

and

$$\begin{aligned}
\bar{u}_{B'}(p')\gamma^i u_B(p) &= N^2 \chi_{s'}^\dagger \begin{pmatrix} 1 & \frac{-\bar{\sigma} \cdot (\bar{q}/2)}{E + m_B} \end{pmatrix} \begin{pmatrix} 0 & \sigma^i \\ -\sigma^i & 0 \end{pmatrix} \begin{pmatrix} 1 \\ \frac{\bar{\sigma} \cdot (-\bar{q}/2)}{E + m_B} \end{pmatrix} \chi_s \\
&= N^2 \chi_{s'}^\dagger \left(\sigma^i \frac{\bar{\sigma} \cdot \bar{q}/2}{E + m_B} + \sigma^i \frac{\bar{\sigma} \cdot (-\bar{q}/2)}{E + m_B} \right) \chi_s \\
&= \left(\frac{E + m_B}{2m_B} \right) \left(\sigma^i \frac{\bar{\sigma} \cdot \bar{q}/2}{E + m_B} + \sigma^i \frac{\bar{\sigma} \cdot (-\bar{q}/2)}{E + m_B} \right) \chi_{s'}^\dagger \chi_s \\
&= \frac{1}{4m_B} \chi_{s'}^\dagger \{ -\sigma^i (\bar{\sigma} \cdot \bar{q}) + \sigma^i (\bar{\sigma} \cdot \bar{q}) \} \chi_s \\
&= \frac{1}{4m_B} \chi_{s'}^\dagger \{ -\sigma^i \sigma^j q_j + \sigma^j q_j \sigma^i \} \chi_s \\
&= \frac{1}{4m_B} \chi_{s'}^\dagger \{ -\sigma^i \sigma^j + \sigma^j \sigma^i \} q_j \chi_s \\
&= \frac{1}{4m_B} \chi_{s'}^\dagger \{ -i\epsilon^{ijk} \sigma^k + i\epsilon^{jik} \sigma^k \} q_j \chi_s \\
&= \frac{1}{4m_B} \chi_{s'}^\dagger \{ -i\epsilon^{ijk} \sigma^k - i\epsilon^{ijk} \sigma^k \} q_j \chi_s \\
&= \frac{1}{4m_B} \chi_{s'}^\dagger (-2i\epsilon^{ijk} \sigma^k) q_j \chi_s \\
&= -\frac{i}{2m_B} \chi_{s'}^\dagger \epsilon^{ijk} \sigma^k q_j \chi_s \\
&= \frac{1}{2m_B} \chi_{s'}^\dagger i (\bar{\sigma} \times \bar{q})^i \chi_s. \tag{D.15}
\end{aligned}$$

The analytical expression of the electromagnetic form factors relevant the diagrams.

Three-quark diagram [Fig. D.1]:

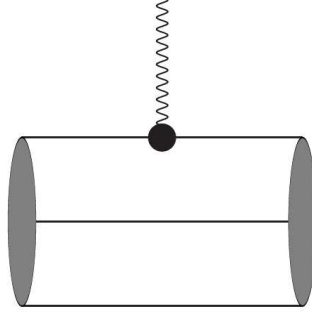


Figure D.1 Three-quark diagram

$$G_E^p(Q^2)|_{3q} = G_E^p(Q^2)|_{3q}^{LO} + G_E^p(Q^2)|_{3q}^{NLO}, G_E^n(Q^2)|_{3q} \equiv 0,$$

$$G_M^p(Q^2)|_{3q} = G_M^p(Q^2)|_{3q}^{LO} + G_M^p(Q^2)|_{3q}^{NLO}, G_M^n(Q^2)|_{3q} \equiv -\frac{2}{3}G_M^p(Q^2)|_{3q}, \quad (\text{D.16})$$

where

$$G_E^p(Q^2)|_{3q}^{LO} = \exp\left(-\frac{Q^2 R^2}{4}\right) \left(1 - \frac{\rho^2}{1 + \frac{2}{3}\rho^2} \frac{Q^2 R^2}{4}\right),$$

$$G_E^p(Q^2)|_{3q}^{NLO} = \exp\left(-\frac{Q^2 R^2}{4}\right) \hat{m}^r \frac{Q^2 R^3 \rho}{4(1 + \frac{3}{2}\rho^2)^2} \times \left(\frac{1 + 7\rho^2 + \frac{15}{4}\rho^4}{1 + \frac{3}{2}\rho^2} - \frac{Q^2 R^2}{4} \rho^2\right),$$

$$G_M^p(Q^2)|_{3q}^{LO} = \exp\left(-\frac{Q^2 R^2}{4}\right) \frac{2m_N \rho R}{1 + \frac{3}{2}\rho^2},$$

$$G_M^p(Q^2)|_{3q}^{NLO} = G_M^p(Q^2)|_{3q}^{LO} \cdot \hat{m}^r \frac{R\rho}{1 + \frac{3}{2}\rho^2} \times \left(\frac{Q^2 R^2}{4} - \frac{2 - \frac{2}{3}\rho^2}{1 + \frac{3}{2}\rho^2}\right). \quad (\text{D.17})$$

Three-quark counterterm (CT) [Fig. D.2]:

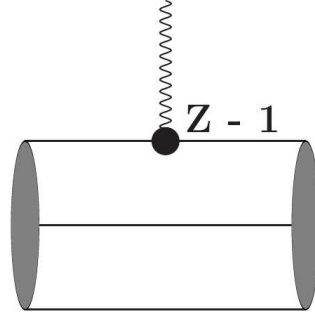


Figure D.2 Three-quark counter-term diagram

$$G_E^p(Q^2)|_{CT} \equiv (\hat{Z} - 1)G_E^p(Q^2)|_{3q}^{LO}, G_E^n(Q^2)|_{CT} \equiv 0,$$

$$G_M^p(Q^2)|_{CT} \equiv (\hat{Z} - 1)G_M^p(Q^2)|_{3q}^{LO},$$

$$G_M^n(Q^2)|_{CT} \equiv -\frac{2}{3}G_M^p(Q^2)|_{CT}. \quad (D.18)$$

Meson-cloud diagram (MC) [Fig. D.3]:

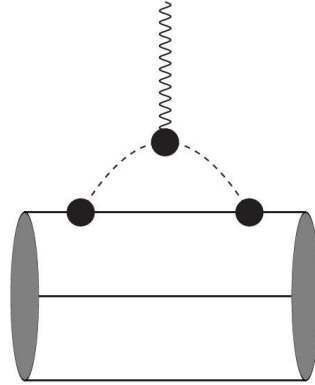


Figure D.3 Meson cloud diagram

$$\begin{aligned}
G_E^N(Q^2)|_{MC} &= \frac{9}{400} \left(\frac{g_A}{\pi F} \right)^2 \int_0^\infty dp p^2 \int_{-1}^1 dx (p^2 + p\sqrt{Q^2}x) \\
&\quad \times \mathcal{F}_{\pi NN}(p^2, Q^2, x) t_E^N(p^2, Q^2, x)|_{MC}, \\
G_M^N(Q^2)|_{MC} &= \frac{3}{400} m_N \left(\frac{g_A}{\pi F} \right)^2 \int_0^\infty dp p^4 \int_{-1}^1 dx (1 - x^2) \\
&\quad \times \mathcal{F}_{\pi NN}(p^2, Q^2, x) t_M^N(p^2, Q^2, x)|_{MC}, \tag{D.19}
\end{aligned}$$

where

$$\begin{aligned}
\mathcal{F}_{\pi NN}(p^2, Q^2, x) &= F_{\pi NN}(p^2) F_{\pi NN}(p^2 + Q^2 + 2p\sqrt{Q^2}x), \\
t_E^p(p^2, Q^2, x)|_{MC} &= C_\pi^{11}(p^2, Q^2, x) + 2C_K^{11}(p^2, Q^2, x), \\
t_E^n(p^2, Q^2, x)|_{MC} &= -C_\pi^{11}(p^2, Q^2, x) + C_K^{11}(p^2, Q^2, x), \\
t_M^p(p^2, Q^2, x)|_{MC} &= D_\pi^{22}(p^2, Q^2, x) + \frac{4}{5}D_K^{11}(p^2, Q^2, x), \\
t_M^n(p^2, Q^2, x)|_{MC} &= -D_\pi^{22}(p^2, Q^2, x) - \frac{1}{5}D_K^{22}(p^2, Q^2, x), \\
D_\Phi^{n_1, n_2}(p^2, Q^2, x) &= \frac{1}{w_\Phi^{n_1}(p^2) w_\Phi^{n_2}(p^2 + Q^2 + 2p\sqrt{Q^2}x)}, \\
C_\Phi^{n_1, n_2}(p^2, Q^2, x) &= \frac{2D_\Phi^{n_1, n_2}}{w_\Phi(p^2) + w_\Phi(p^2 + Q^2 + 2p\sqrt{Q^2}x)}. \tag{D.20}
\end{aligned}$$

Vertex-correction diagram (VC) [Fig. D.4]:

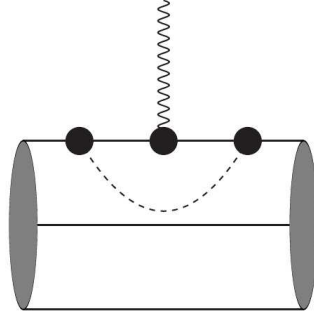


Figure D.4 Vertex correction diagram

$$\begin{aligned}
 G_{E(M)}^N(Q^2)|_{VC} &= G_{E(M)}^p(Q^2)|_{3q}^{LO} \frac{9}{200} \left(\frac{g_a}{\pi F}\right)^2 \int_0^\infty dp p^4 \\
 &\times F_{\pi NN}^2(p^2) t_{E(M)}^N(p^2)|_{VC}.
 \end{aligned}
 \tag{D.21}$$

where

$$\begin{aligned}
 t_E^p(p^2)|_{VC} &= \frac{1}{2}W_\pi - W_K(p^2) + \frac{1}{6}W_\eta(p^2), \\
 t_E^n(p^2)|_{VC} &= W_\pi - W_K(p^2), \\
 t_M^p(p^2)|_{VC} &= \frac{1}{6}W_\pi - \frac{1}{3}W_K(p^2) - \frac{1}{6}W_\eta(p^2), \\
 t_M^n(p^2)|_{VC} &= -\frac{2}{3}W_\pi + \frac{1}{3}W_K(p^2) + \frac{1}{9}W_\eta(p^2).
 \end{aligned}
 \tag{D.22}$$

$$W_\Phi(p^2) = \frac{1}{w_\Phi^3(p^2)}.
 \tag{D.23}$$

Meson-in-flight diagram (MF) [Fig. D.5] :

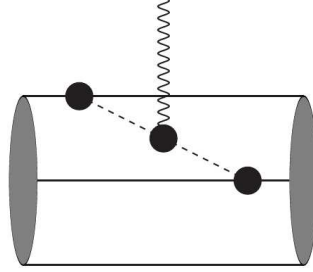


Figure D.5 Meson-in-flight diagram

$$G_E^p(Q^2)|_{MF} \equiv 0, G_E^n(Q^2)|_{MF} \equiv 0,$$

$$G_M^n(Q^2)|_{MF} \equiv -G_M^p(Q^2)|_{MF}, \quad (\text{D.24})$$

$$G_M^p(Q^2)|_{MF} = \frac{9}{100} m_N \left(\frac{g_A}{\pi F} \right) \int_0^\infty dp p^4 \int_{-1}^1 dx (1-x^2) \\ \times \mathcal{F}_{\pi NN}(p^2, Q^2, x) D_\pi^{22}(p^2, Q^2, x). \quad (\text{D.25})$$

Appendix E

PUBLICATION PAPER

Dependence of nucleon properties on pseudoscalar meson masses

Amand Faessler^{1,3}, Thomas Gutsche¹, Valery E Lyubovitskij^{1,3}
and Chalump Oonariya^{1,2}

¹ Institut für Theoretische Physik, Universität Tübingen, Auf der Morgenstelle 14,
D-72076 Tübingen, Germany

² School of Physics, Suranaree University of Technology, 111 University Avenue,
Nakhon Ratchasima 30000, Thailand

E-mail: amand.faessler@uni-tuebingen.de, thomas.gutsche@uni-tuebingen.de,
valeri.lyubovitskij@uni-tuebingen.de and chalump@tphys.physik.uni-tuebingen.de

Received 6 November 2007

Published 10 January 2008

Online at stacks.iop.org/JPhysG/35/025005

Abstract

We discuss the sensitivity of nucleon properties (mass, magnetic moments and electromagnetic form factors) on the variation of the pseudoscalar meson masses in the context of the perturbative chiral quark model. The obtained results are compared to data and other theoretical predictions.

(Some figures in this article are in colour only in the electronic version)

1. Introduction

In recent years nucleon properties have been in the focus of manifestly Lorentz covariant chiral perturbation theory (ChPT), improved lattice QCD computations and chiral extrapolations (see, e.g., [1–23]). The lattice formulation of QCD is well established and is a powerful tool for studying the structure of nucleons. The computation of nucleon properties in lattice QCD is progressing with steadily increasing accuracy [4–8]. Accurate computations of the nucleon mass with dynamical fermions and two active flavors are now possible [9, 10] in lattice QCD. In practice, these computations are so far limited to relatively large quark masses. Direct simulations of QCD for light current quark masses, near the chiral limit, remain computationally intensive. To extract predictions for observables, lattice data generated at high current quark masses have to be extrapolated to the point of physical quark or pion mass. Therefore, one of the current aims in lattice QCD is to establish the quark mass dependence of quantities of physical interest, such as the nucleon mass, magnetic moments and form factors. The major tool in establishing the current quark mass dependence of lattice QCD results is methods based on chiral effective field theory. Recent extrapolation studies of lattice results concern the nucleon mass [4, 5, 11, 12, 14], its axial vector coupling constant and

³ On leave of absence from the Department of Physics, Tomsk State University, 634050 Tomsk, Russia.

magnetic moments [11–13], the pion–nucleon sigma term, charge radii [15], form factors [16–18], and moments of structure functions [19]. The chiral expansion in the chiral effective field theory (χ EFT) has been used to study the quark mass (pion mass) dependence of the magnetic moments, magnetic form factors and the axial–vector coupling constant [20, 21] of the nucleon for extrapolations of lattice QCD results, so far determined at relatively large quark masses corresponding to pion masses of $m_\pi \geq 0.6$ GeV, down to physical values of m_π . In the chiral limit, with $m_\pi \rightarrow 0$, QCD at low energies is realized in the form of an effective field theory with spontaneously broken chiral symmetry, with massless pions as the primary active degrees of freedom. The coupling of the chiral Goldstone bosons to these spin-1/2 matter fields produces the so-called pion-cloud of the nucleon, an important component of nucleon structure at low energy and low momentum scales.

In the present paper, we investigate the dependence of nucleon properties (mass, magnetic moments and electromagnetic form factors) on pseudoscalar meson masses applying the perturbative chiral quark model (PCQM) [24–26]. In the PCQM baryons are described by three relativistic valence quarks confined in a static potential, which are supplemented by a cloud of pseudoscalar Goldstone bosons, as required by chiral symmetry. This simple phenomenological model has already been successfully applied to the charge and magnetic form factors of baryons, sigma terms, ground-state masses of baryons, the electromagnetic $N \rightarrow \Delta$ transition, and other baryon properties [24–26]. Note that in [27, 28] we extend this approach by constructing a framework which is manifestly Lorentz covariant and aims for consistency with ChPT.

In this work, our strategy is as follows. First, we discuss the nucleon properties (mass, magnetic moments and electromagnetic form factors) in dependence on the pion mass in the two-flavor sector. Second, we extend our formalism to the three-flavor sector including kaon and η -meson degrees of freedom with fixed masses. All calculations are performed at one loop. The chiral limit, where current quark masses approach zero with $\hat{m}, m_s \rightarrow 0$, is well defined. We compare the obtained quark mass dependence of the nucleon observables to the results of other approaches (lattice QCD, chiral extrapolations).

This paper is organized as follows. In section 2, we give a short overview of our approach. In section 3, we discuss dependence of nucleon properties on the variation of the pion mass in the two- and three-flavor picture in the context of the PCQM and compare them to other theoretical approaches. In section 4, we give our conclusions.

2. The perturbative chiral quark model

The perturbative chiral quark model [24–26] is based on an effective chiral Lagrangian describing baryons by a core of three valence quarks, moving in a central Dirac field with $V_{\text{eff}}(r) = S(r) + \gamma^0 V(r)$, where $r = |\vec{x}|$. In order to respect chiral symmetry, a cloud of Goldstone bosons (π , K and η) is included, which are treated as small fluctuations around the three-quark core. The model Lagrangian is

$$\begin{aligned} \mathcal{L}(x) = & \bar{\psi}(x)[i\not{\partial} - \gamma^0 V(r) - \mathcal{M}]\psi(x) + \frac{F^2}{4} \text{Tr}[\partial^\mu U(x)\partial^\mu U^\dagger(x) + 2\mathcal{M}B(U(x) + U^\dagger(x))] \\ & - \bar{\psi}(x)S(r)\left[\frac{U(x) + U^\dagger(x)}{2} + \gamma^5 \frac{U(x) - U^\dagger(x)}{2}\right]\psi(x), \end{aligned} \quad (1)$$

where $\psi = (u, d, s)$ is the triplet of quark fields, $U = \exp[i\hat{\Phi}/F]$ is the chiral field in the exponential parametrization, $F = 88$ MeV is the pion decay constant in the chiral limit [29], $\mathcal{M} = \text{diag}\{m_u, m_d, m_s\}$ is the mass matrix of current quarks and $B = -\langle 0|\bar{u}u|0\rangle/F^2 = -\langle 0|\bar{d}d|0\rangle/F^2$ is the quark condensate constant. In the numerical calculations we restrict

to the isospin symmetry limit $m_u = m_d = \hat{m}$. We rely on the standard picture of chiral symmetry breaking [30] and for the masses of pseudoscalar mesons we use the leading term in their chiral expansion (i.e. linear in the current quark mass). By construction, our effective chiral Lagrangian is consistent with the known low-energy theorems (Gell–Mann–Okubo and Gell–Mann–Oakes–Renner relations, partial conservation of axial current (PCAC), Feynman–Hellmann relation between pion–nucleon σ -term and the derivative of the nucleon mass, etc). The electromagnetic field is included into the effective Lagrangian (1) using the standard procedure, i.e. the interaction of quarks and charged mesons with photons is introduced using minimal substitution.

To derive the properties of baryons, which are modeled as bound states of valence quarks surrounded by a meson cloud, we formulate perturbation theory and restrict the quark states to the ground-state contribution with $\psi(x) = b_0 u_0(\vec{x}) \exp(-i\mathcal{E}_0 t)$, where b_0 is the corresponding single-quark annihilation operator. The quark wavefunction $u_0(\vec{x})$ belongs to the basis of potential eigenstates used for expanding the quark field operator $\psi(\vec{x})$. In our calculation of matrix elements, we project quark diagrams on the respective baryon states. The baryon states are conventionally set up by the product of the SU(6) spin-flavor and SU(3)_c color wavefunctions, where the nonrelativistic single quark spin wavefunction is simply replaced by the relativistic solution $u_0(\vec{x})$ of the Dirac equation

$$[-i\gamma^0 \vec{\gamma} \cdot \vec{\nabla} + \gamma^0 S(r) + V(r) - \mathcal{E}_0]u_0(\vec{x}) = 0, \quad (2)$$

where \mathcal{E}_0 is the single-quark ground-state energy.

For the description of baryon properties, we use the effective potential $V_{\text{eff}}(r)$ with a quadratic radial dependence [24, 25]:

$$S(r) = M_1 + c_1 r^2, \quad V(r) = M_2 + c_2 r^2 \quad (3)$$

with the particular choice

$$M_1 = \frac{1 - 3\rho^2}{2\rho R}, \quad M_2 = \mathcal{E}_0 - \frac{1 + 3\rho^2}{2\rho R}, \quad c_1 \equiv c_2 = \frac{\rho}{2R^3}. \quad (4)$$

Here, R and ρ are parameters related to the ground-state quark wavefunction u_0 :

$$u_0(\vec{x}; i) = N_0 \exp\left[-\frac{\vec{x}^2}{2R^2}\right] \left(i\rho \vec{\sigma}(i) \cdot \vec{x}/R \right) \chi_s(i) \chi_f(i) \chi_c(i), \quad (5)$$

where $N_0 = [\pi^{3/2} R^3 (1 + 3\rho^2/2)]^{-1/2}$ is a normalization constant; χ_s, χ_f, χ_c are the spin, flavor and color quark wavefunctions, respectively. The index ‘ i ’ stands for the i th quark. The constant part of the scalar potential M_1 can be interpreted as the constituent mass of the quark, which is simply the displacement of the current quark mass due to the potential $S(r)$. The parameter ρ is related to the axial charge g_A of the nucleon calculated in the zeroth-order (or 3 q -core) approximation:

$$g_A = \frac{5}{3} \left(1 - \frac{2\rho^2}{1 + \frac{3}{2}\rho^2} \right). \quad (6)$$

Therefore, ρ can be replaced by g_A using the matching condition (6). The parameter R is related to the charge radius of the proton in the zeroth-order approximation as

$$\langle r_{E/\text{LO}}^2 \rangle^P = \int d^3x u_0^\dagger(\vec{x}) \vec{x}^2 u_0(\vec{x}) = \frac{3R^2}{2} \frac{1 + \frac{5}{2}\rho^2}{1 + \frac{3}{2}\rho^2}. \quad (7)$$

In our calculations we use the value $g_A = 1.25$. Therefore, we have only one free parameter in our model, that is R or $\langle r_{E/\text{LO}}^2 \rangle^P$. In previous publications R was varied in the region from

0.55 fm to 0.65 fm, which corresponds to a change of $\langle r_E^2 \rangle_{\text{LO}}^p$ from 0.5 to 0.7 fm². Note that for the given form of the effective potential (3) the Dirac equation (2) can be solved analytically (for the ground state see equation (5), for excited states see [26]).

The expectation value of an operator \hat{A} is then set up as:

$$\langle \hat{A} \rangle = {}^B \langle \phi_0 | \sum_{n=1}^{\infty} \frac{i^n}{n!} \int d^4x_1 \dots \int d^4x_n T[\mathcal{L}_I(x_1) \dots \mathcal{L}_I(x_n) \hat{A}] | \phi_0 \rangle_c^B, \quad (8)$$

where the state vector $|\phi_0\rangle$ corresponds to the unperturbed three-quark state (3q-core). Superscript ‘B’ in the equation indicates that the matrix elements have to be projected onto the respective baryon states, whereas subscript ‘c’ refers to contributions from connected graphs only. Here $\mathcal{L}_I(x)$ is the appropriate interaction Lagrangian. For the purpose of the present paper, we include in $\mathcal{L}_I(x)$ the linearized coupling of pseudoscalar fields with quarks and the corresponding coupling of quarks and mesons to the electromagnetic field (see details in [24]):

$$\begin{aligned} \mathcal{L}_I(x) = & -\bar{\psi}(x) i\gamma^5 \frac{\hat{\Phi}(x)}{F} S(r) \psi(x) - e A_\mu(x) \bar{\psi}(x) \gamma^\mu Q \psi(x) \\ & - e A_\mu(x) \sum_{i,j=1}^8 \left[f_{3ij} + \frac{f_{8ij}}{\sqrt{3}} \right] \Phi_i(x) \partial^\mu \Phi_j(x) + \dots, \end{aligned} \quad (9)$$

where f_{ijk} are the SU(3) antisymmetric structure constants.

For the evaluation of equation (8) we apply Wick’s theorem with the appropriate propagators for the quarks and pions. For the quark propagator we use the vacuum Feynman propagator for a fermion in a binding potential restricted to the ground-state quark wavefunction with

$$iG_0(x, y) = u_0(\vec{x}) \bar{u}_0(\vec{y}) e^{-i\mathcal{E}_0(x_0 - y_0)} \theta(x_0 - y_0). \quad (10)$$

For the meson field we use the free Feynman propagator for a boson field with

$$i\Delta_{ij}(x - y) = \langle 0 | T \{ \Phi_i(x) \Phi_j(y) \} | 0 \rangle = \delta_{ij} \int \frac{d^4k}{(2\pi)^4 i} e^{-ik(x-y)} \Delta_\Phi(k), \quad (11)$$

where $\Delta_\Phi(k) = [M_\Phi^2 - k^2 - i0^+]^{-1}$ is the meson propagator in momentum space and M_Φ is the meson mass.

The physical nucleon mass at one loop is given by

$$m_N = m_N^{\text{core}} + \Delta m_N \quad (12)$$

where

$$m_N^{\text{core}} = 3\{\mathcal{E}_0 + \gamma \hat{m}\} = 3 \left\{ \mathcal{E}_0 + \frac{\gamma}{2B} M_\pi^2 \right\} \quad (13)$$

is the contribution of the three-quark core (the second term on the rhs of equation (13) is the contribution of the current quark mass) and

$$\Delta m_N = \Pi^{\text{MC}} + \Pi^{\text{ME}} \quad (14)$$

is the nucleon mass shift due to the meson-cloud contribution. The diagrams that contribute to the nucleon mass shift Δm_N at one loop are shown in figure 1 (see details in [24, 25]). Figure 1(a) corresponds to the so-called meson-cloud (MC) contribution and figure 1(b) is the meson-exchange (ME) contribution. The operators Π^{MC} and Π^{ME} are functions of the meson masses and are expressed in terms of the universal self-energy operator

$$\Pi(M_\Phi^2) = -I_\Phi^{24}, \quad \Phi = \pi, K, \eta. \quad (15)$$

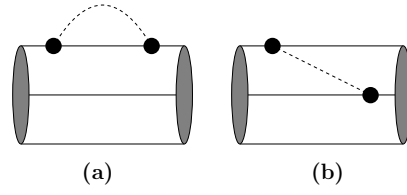


Figure 1. Diagrams contributing to the nucleon mass shift.

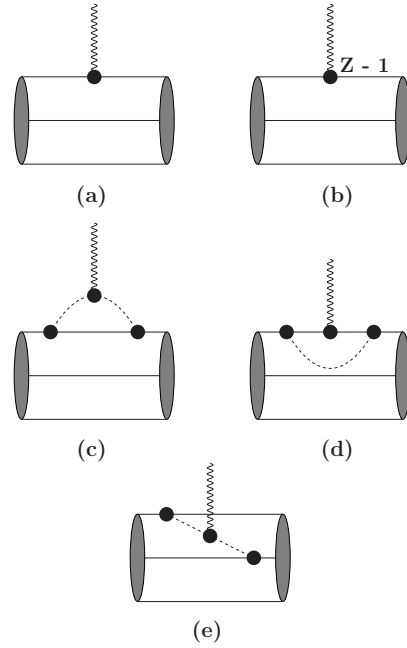


Figure 2. Diagrams contributing to the nucleon electromagnetic form factors.

Here we introduce a notation for the structure integral in terms of which all further formulae can be expressed:

$$I_{\Phi}^{MN} = \left(\frac{g_A}{\pi F} \right)^2 \int_0^{\infty} dp p^N \frac{F_{\pi NN}^2(p^2)}{(M_{\Phi}^2 + p^2)^{\frac{M}{2}}}, \quad M, N = 0, 1, 2, \dots \quad (16)$$

and

$$I_{\Phi}^{0N} \equiv I_N \equiv \left(\frac{g_A}{\pi F} \right)^2 \int_0^{\infty} dp p^N F_{\pi NN}^2(p^2) = \left(\frac{g_A}{\pi F} \right)^2 \left(\frac{2}{R^2} \right)^{\frac{N+1}{2}} \times \Gamma\left(\frac{N+1}{2}\right) \left(\frac{1}{2} - \frac{N+1}{4}\beta + \frac{(N+1)(N+3)}{32}\beta^2 \right), \quad (17)$$

where $\beta = 2\rho^2/(2 - \rho^2)$. The function $F_{\pi NN}(p^2)$ is the πNN form factor normalized to unity at zero recoil ($p^2 = 0$):

$$F_{\pi NN}(Q^2) = \exp\left(-\frac{Q^2 R^2}{4}\right) \left\{ 1 - \frac{Q^2 R^2}{4}\beta \right\}. \quad (18)$$

The meson-cloud contributions to the mass shift are then given

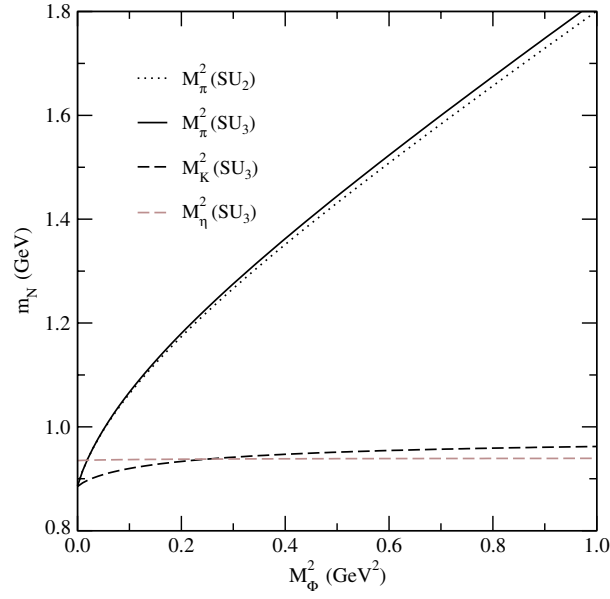


Figure 3. Dependence of nucleon mass m_N on meson mass M_Φ^2 : $m_N(M_\pi^2)$ in SU(2) (dotted line) and $m_N(M_\pi^2)$, $m_N(M_K^2)$, $m_N(M_\eta^2)$ in SU(3) (the other lines).

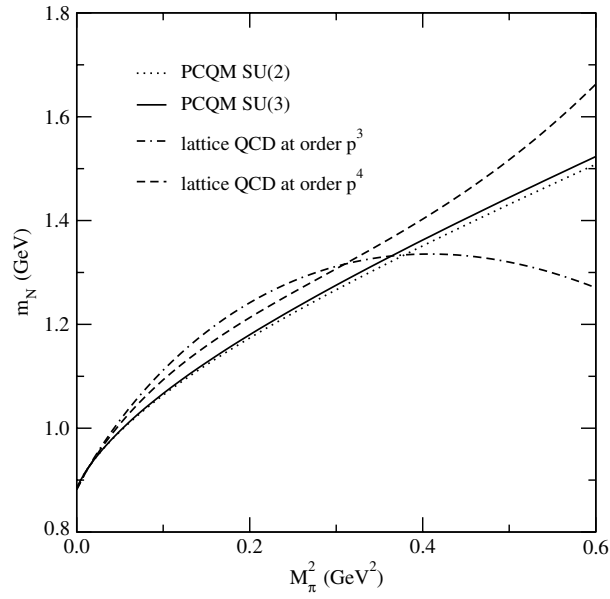


Figure 4. Dependence of nucleon mass m_N on pion mass M_π^2 : $m_N(M_\pi^2)$ in SU(2) (dotted line), SU(3) (solid line) and from lattice QCD [4] (the others) at orders p^3 and p^4 .

(1) in SU(2) as

$$\Pi^{\text{MC}} = \frac{81}{400} \Pi(M_\pi^2), \quad \Pi^{\text{ME}} = \frac{90}{400} \Pi(M_\pi^2), \quad (19)$$

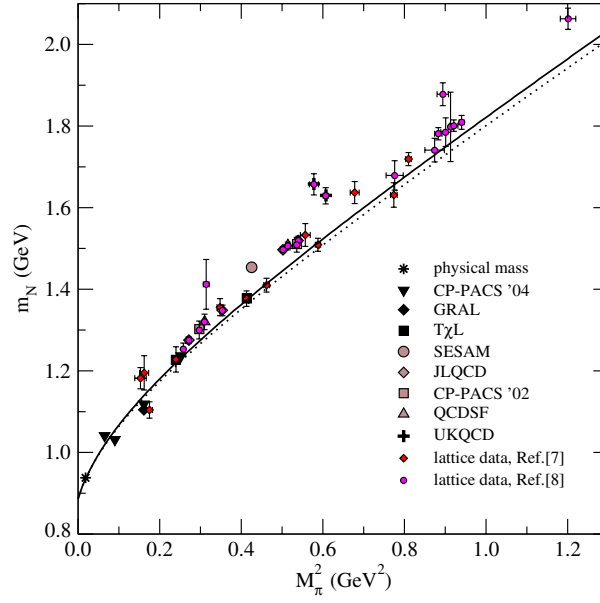


Figure 5. Nucleon dependences $m_N(M_\pi^2)$ in SU(2) (dotted line) and in SU(3) (solid line) are compared to data from various collaborations as a function of M_π^2 .

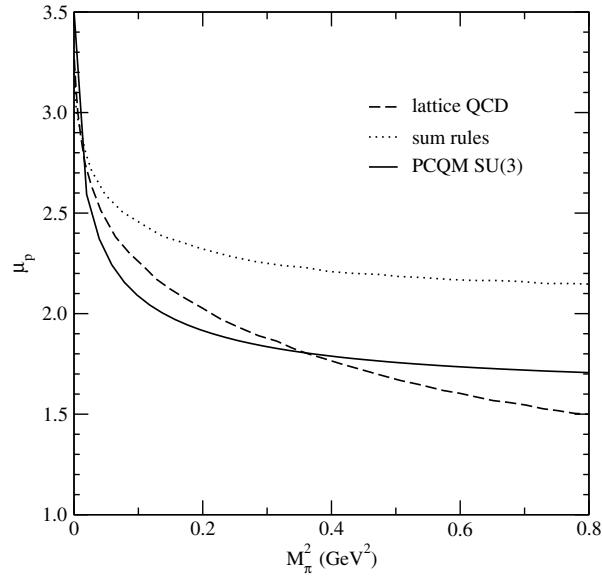


Figure 6. M_π^2 -dependence of the proton magnetic moment $\mu_p(M_\pi^2)$ to one-loop from sum rules [13] (dotted curve), lattice QCD [18] (dashed curve) and our results in SU(3) (solid curve).

(2) in SU(3) as

$$\begin{aligned}\Pi^{\text{MC}} &= \frac{81}{400} \Pi(M_\pi^2) + \frac{54}{400} \Pi(M_K^2) + \frac{9}{400} \Pi(M_\eta^2), \\ \Pi^{\text{ME}} &= \frac{90}{400} \Pi(M_\pi^2) - \frac{6}{400} \Pi(M_\eta^2).\end{aligned}\tag{20}$$

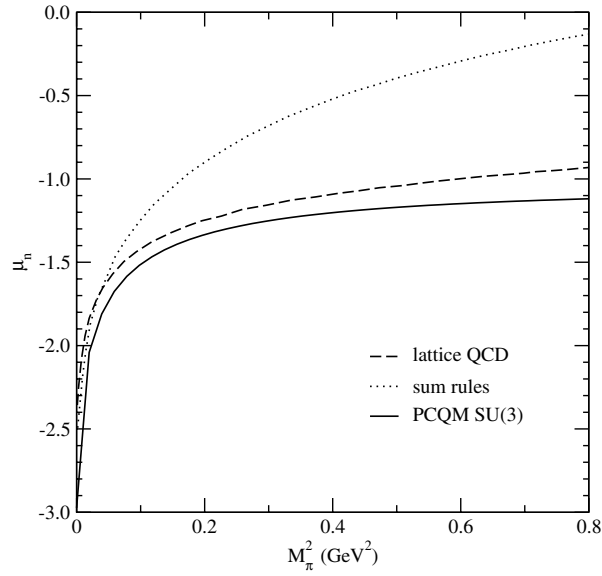


Figure 7. M_π^2 -dependence of the neutron magnetic moment $\mu_n(M_\pi^2)$ to one-loop from sum rules [13] (dotted curve), lattice QCD [18] (dashed curve) and our results in SU(3) (solid curve).

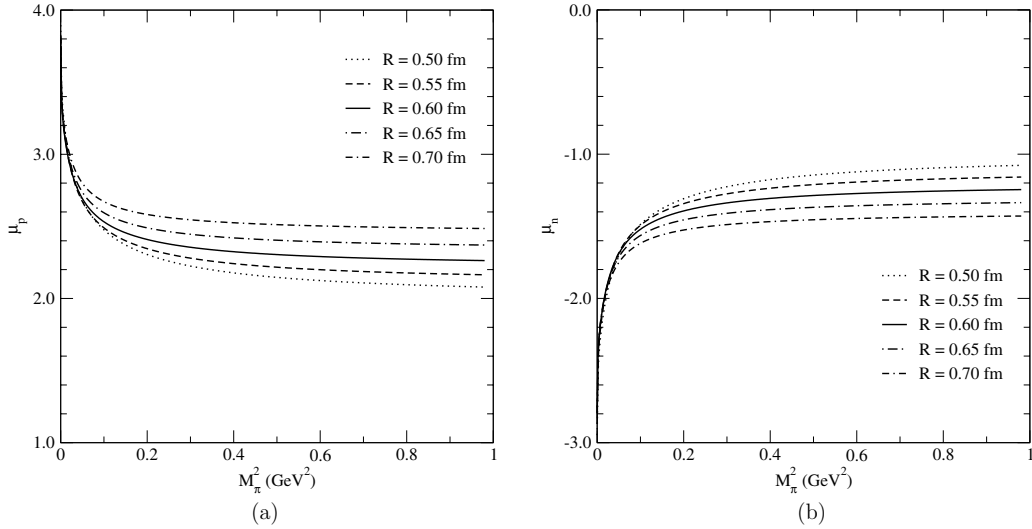


Figure 8. μ_N at $M_\pi^2 = 0-1 \text{ GeV}^2$ and $R = 0.5-0.7 \text{ fm}$ in SU(2).

Exact expressions for the nucleon electromagnetic form factors can be found in [24]. Diagrams contributing to these quantities are shown in figure 2. Here we just present the typical results for the magnetic moments in SU(2) and SU(3). The two-flavor result is obtained from the three-flavor one when neglecting kaon and η -meson contributions. The magnetic moments of the nucleons, μ_p and μ_n , are given by the expressions

$$\begin{aligned} \mu_p &= \mu_p^{LO} \left[1 + \delta - \frac{1}{400} \{ 26I_\pi^{34} + 16I_K^{34} + 4I_\eta^{34} \} \right] + \frac{m_N}{50} \{ 11I_\pi^{44} + I_K^{44} \}, \\ \mu_n &= -\frac{2}{3} \mu_p^{LO} \left[1 + \delta - \frac{1}{400} \{ 21I_\pi^{34} + 21I_K^{34} + 4I_\eta^{34} \} \right] - \frac{m_N}{50} \{ 11I_\pi^{44} + I_K^{44} \}, \end{aligned} \quad (21)$$

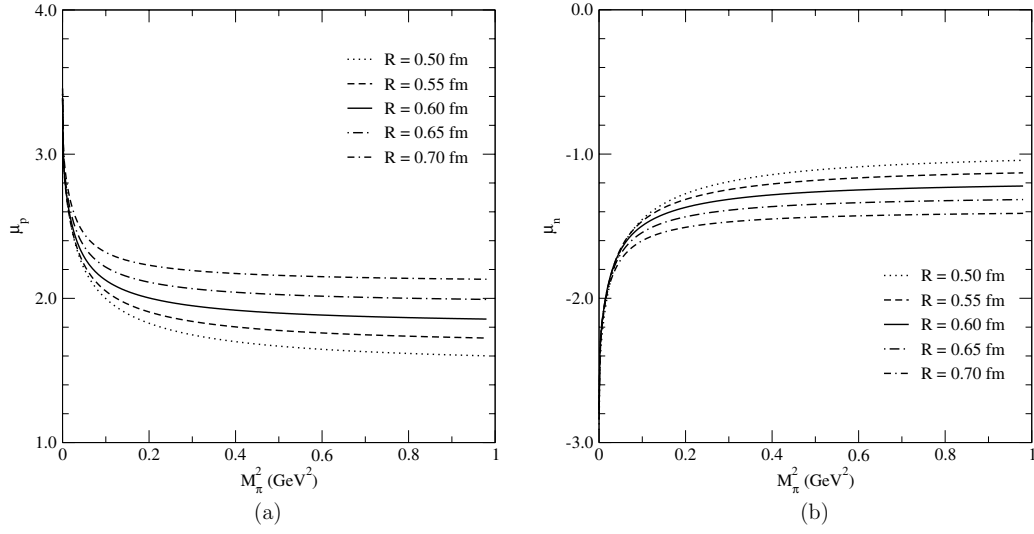


Figure 9. μ_N at $M_\pi^2 = 0-1 \text{ GeV}^2$ and $R = 0.5-0.7 \text{ fm}$ in SU(3).

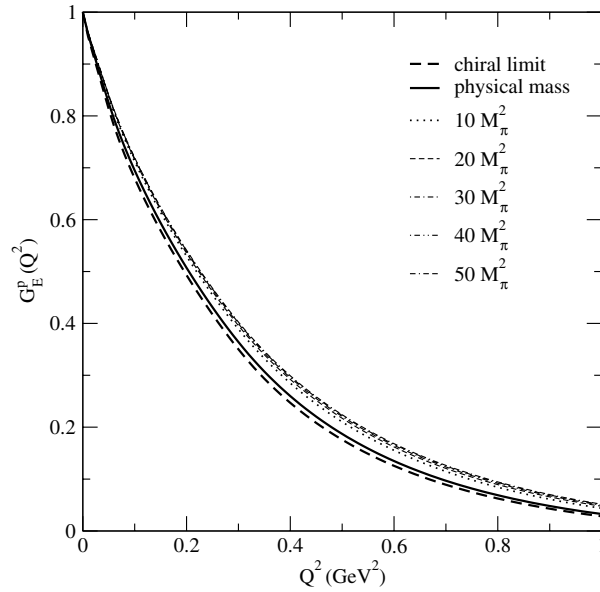


Figure 10. Proton charge form factor $G_E^p(Q^2)$ as function of M_π^2 in SU(2).

where

$$\mu_p^{LO} = \frac{2m_N \rho R}{1 + \frac{3}{2}\rho^2} \quad (22)$$

is the leading-order contribution to the proton magnetic moment. The factor

$$\delta = - \left(\hat{m} + \frac{\Pi^{\text{MC}}}{3} \cdot \frac{1 + \frac{3}{2}\rho^2}{1 - \frac{3}{2}\rho^2} \right) \frac{2 - \frac{3}{2}\rho^2}{(1 + \frac{3}{2}\rho^2)^2} R \rho \quad (23)$$

defines the NLO correction to the nucleon magnetic moments due to the modification of the quark wavefunction [24].

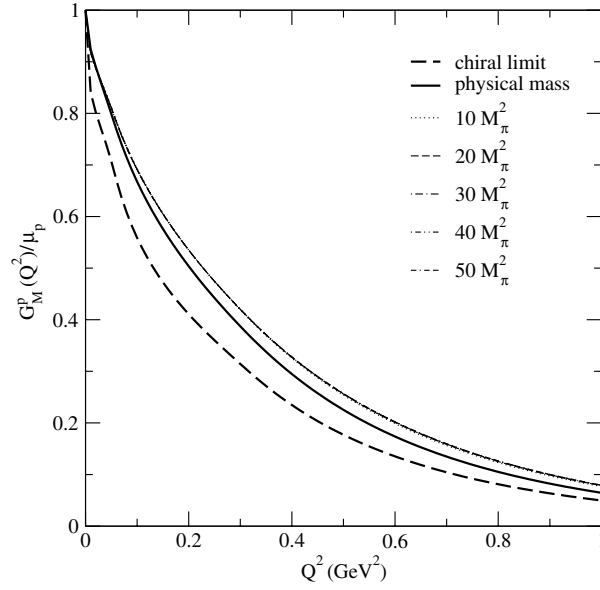


Figure 11. Proton magnetic form factor $G_M^p(Q^2)$ as function of M_π^2 in SU(2).

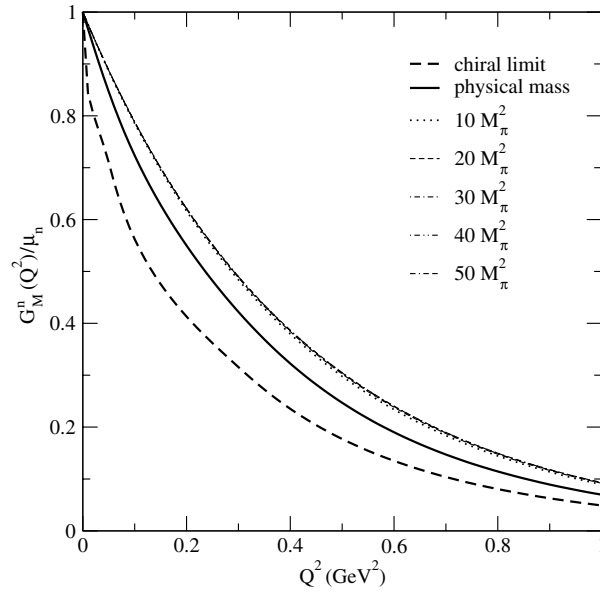


Figure 12. Neutron magnetic form factor $G_M^n(Q^2)$ as function of M_π^2 in SU(2).

3. Numerical results

In this section, we discuss the numerical results for the dependence of nucleon properties on a variation of the pseudoscalar meson masses.

In table 1, we present our results for the nucleon mass in dependence on the pion mass. Both the SU(2) version, considering only the pion cloud contribution, and the SU(3) variant, including in addition kaon and η -meson cloud contributions, are indicated. The total result

Table 1. Nucleon mass (in GeV) in the SU(2) and SU(3) versions and at different values for M_π^2 .

Nucleon mass	SU(2)	SU(3)	Other approaches
$3q$ -core	1.203	1.247	–
Meson loops (total)	–0.265	–0.309	–
π loops	–0.265	–0.265	–
K loops	–	–0.042	–
η loops	–	–0.002	–
Total	0.938 27	0.938 27	–
Chiral limit	0.887	0.831	0.880 [5, 12], 0.883 [4], 0.770(110) [31], 0.890(180) [14], 0.832 [27]
M_π^2 (in GeV ²)			
0.153	1.122	1.128	1.182(26) [7]
0.162	1.133	1.138	1.195(42) [7]
0.175	1.148	1.154	1.104(20) [7]
0.240	1.212	1.220	1.228(31) [7]
0.348	1.310	1.320	1.356(21) [7]
0.413	1.360	1.371	1.377(19) [7]
0.462	1.400	1.412	1.410(17) [7]
0.557	1.475	1.490	1.533(28) [7]
0.588	1.500	1.515	1.509(16) [7]
0.678	1.566	1.582	1.637(27) [7]
0.774	1.638	1.656	1.631(30) [7]
0.810	1.664	1.682	1.619(16) [7]
0.258	1.231	1.239	1.253(15) [8]
0.271	1.240	1.248	1.275(82) [8]
0.297	1.266	1.275	1.300(22) [8]
0.310	1.275	1.284	1.320(19) [8]
0.314	1.280	1.288	1.412(61) [8]
0.354	1.314	1.324	1.348(13) [8]
0.502	1.431	1.444	1.497(77) [8]
0.514	1.442	1.456	1.506(94) [8]
0.536	1.458	1.742	1.509(18) [8]
0.540	1.462	1.476	1.519(11) [8]
0.578	1.493	1.507	1.657(26) [8]
0.607	1.515	1.530	1.629(20) [8]
0.776	1.640	1.658	1.679(36) [8]
0.874	1.710	1.730	1.741(29) [8]
0.883	1.717	1.736	1.781(15) [8]
0.894	1.725	1.744	1.878(28) [8]
0.901	1.730	1.749	1.785(35) [8]
0.913	1.738	1.758	1.798(85) [8]
0.921	1.744	1.764	1.801(14) [8]
0.940	1.758	1.778	1.809(17) [8]
1.201	1.943	1.965	2.063(26) [8]

is normalized to the physical value (coinciding with the proton mass treated as the reference point) $m_N \equiv m_p = 938.27$ MeV by fixing the ground-state quark energy to $\mathcal{E}_0 \simeq 397$ MeV [in case of SU(2)] and $\mathcal{E}_0 \simeq 411$ MeV [in case of SU(3)]. We also indicate the separate contributions of the $3q$ -core and the meson cloud, and, in addition, the value obtained in the

Table 2. Nucleon magnetic moments in SU(2).

R (fm)	μ_p		μ_n	
	$M_\pi = 0$	M_π^{phys}	$M_\pi = 0$	M_π^{phys}
0.50	3.896	2.984	-2.948	-2.015
0.55	3.828	2.947	-2.871	-1.970
0.60	3.796	2.945	-2.823	-1.952
0.65	3.792	2.969	-2.797	-1.954
0.70	3.803	3.012	-2.789	-1.973

Table 3. Nucleon magnetic moments in SU(3) for fixed masses M_K^2 and M_η^2 .

R (fm)	μ_p		μ_n	
	$M_\pi = 0$	M_π^{phys}	$M_\pi = 0$	M_π^{phys}
0.50	3.512	2.598	-2.976	-2.043
0.55	3.466	2.585	-2.984	-1.993
0.60	3.456	2.605	-2.843	-1.972
0.65	3.471	2.648	-2.815	-1.972
0.70	3.505	2.709	-2.804	-1.988

chiral limit, consistent with the values of [14, 27, 31]. For the dependence on the pion mass we choose mass values in the range of $M_\pi^2 \simeq 0.15\text{--}1.2 \text{ GeV}^2$ and the resulting nucleon mass is directly compared to either chiral extrapolations or lattice data [7, 8]. In both comparisons our results are consistent with the corresponding values of either the extrapolations or the lattice data. In figures 3 and 4, we indicate the full functional dependence of the nucleon mass on M_π^2 , M_K^2 and M_η^2 , respectively, and compare them (in the case of the SU(2) M_π^2 -dependence) to results of lattice QCD at orders p^3 and p^4 of [4]. In figure 5, we compare the results for the nucleon mass both in SU(2) and SU(3) to lattice QCD data from various collaborations [7, 8] as functions of M_π^2 .

In table 2, we present our results for the nucleon magnetic moments in the SU(2) version for different values of the model scale parameter R at $M_\pi = 0$ and at the physical pion mass M_π^{phys} . In table 3, we give the analogous results for SU(3). In figures 6 and 7, we draw the curves for the nucleon magnetic moments as functions of M_π^2 and compare them to results of lattice QCD [13, 18]. Note that the nucleon magnetic moments are not sensitive to a variation of the strange current quark mass m_s . In figures 8 and 9, we demonstrate the sensitivity of the nucleon magnetic moments as functions of M_π^2 on the variation of the scale parameter R .

Finally, in figures 10–12 we present results for the nucleon form factors $G_E^p(Q^2)$, $G_M^p(Q^2)/\mu_p$ and $G_M^n(Q^2)/\mu_n$ at different values of M_π^2 . A larger pion mass leads to an increase of the normalized (at $Q^2 = 0$) form factors.

4. Conclusions

In this work, we apply the perturbative chiral quark model at one loop to describe the dependence of nucleon properties on the meson masses. It has been previously verified that the model is successful in the explanation of many aspects of nucleon properties [23–25], such as magnetic moments, the axial vector form factor, the $N \rightarrow \Delta$ transition amplitude, the meson–nucleon sigma-term and πN nucleon scattering. Here we demonstrate that the meson

mass dependence of nucleon properties such as the mass, magnetic moments, electromagnetic form factors, both for the two- and three-flavor variants, is reasonably described in comparison to present lattice data and extrapolations of these results. Given also the simplicity of this model approach, the evaluation at one loop seems sufficient to correctly describe the pion mass dependence of the discussed observables.

Acknowledgments

This work was supported by the DFG under contracts FA67/31-1 and GRK683. This research is also part of the EU Integrated Infrastructure Initiative Hadronphysics project under contract number RII3-CT-2004-506078 and President grant of Russia ‘Scientific Schools’ No. 5103.2006.2. The stay in Tübingen of Chalump Oonariya was supported by the DAAD under PKZ:A/05/57631.

References

- [1] Becher T and Leutwyler H 1999 *Eur. Phys. J. C* **9** 643 (Preprint [hep-ph/9901384](#))
Becher T and Leutwyler H 2001 *J. High Energy Phys.* JHEP06(2001)017 (Preprint [hep-ph/0103263](#))
Ellis P J and Tang H B 1998 *Phys. Rev. C* **57** 3356 (Preprint [hep-ph/9709354](#))
Kubis B and Meissner U G 2001 *Nucl. Phys. A* **679** 698 (Preprint [hep-ph/0007056](#))
Kubis B and Meissner U G 2001 *Eur. Phys. J. C* **18** 747 (Preprint [hep-ph/0010283](#))
Schindler M R, Gegelia J and Scherer S 2004 *Phys. Lett. B* **586** 258 (Preprint [hep-ph/0309005](#))
Schindler M R, Gegelia J and Scherer S 2004 *Eur. Phys. J. A* **19** 35 (Preprint [hep-ph/0309234](#))
Schindler M R, Gegelia J and Scherer S 2005 *Eur. Phys. J. A* **26** 1 (Preprint [nucl-th/0509005](#))
Lehnhart B C, Gegelia J and Scherer S 2005 *J. Phys. G: Nucl. Part. Phys.* **31** 89 (Preprint [hep-ph/0412092](#))
Schindler M R, Djukanovic D, Gegelia J and Scherer S 2007 *Phys. Lett. B* **649** 390 (Preprint [hep-ph/0612164](#))
Schindler M R, Fuchs T, Gegelia J and Scherer S 2007 *Phys. Rev. C* **75** 025202 (Preprint [nucl-th/0611083](#))
Bernard V 2008 *Prog. Part. Nucl. Phys.* **60** 82 (Preprint [0706.0312](#))
- [2] Leinweber D B, D H Lu and Thomas A W 1999 *Phys. Rev. D* **60** 034014 (Preprint [hep-lat/9810005](#))
- [3] Leinweber D B, Thomas A W and Young R D 2004 *Phys. Rev. Lett.* **92** 242002 (Preprint [hep-lat/0302020](#))
- [4] Procura M, Musch B U, Wollenweber T, Hemmert T R and Weise W 2006 *Phys. Rev. D* **73** 114510 (Preprint [hep-lat/0603001](#))
- [5] Procura M, Hemmert T R and Weise W 2004 *Phys. Rev. D* **69** 034505 (Preprint [hep-lat/0309020](#))
- [6] Procura M, Musch B U, Hemmert T R and Weise W 2007 *Phys. Rev. D* **75** 014503 (Preprint [hep-lat/0610105](#))
- [7] Orth B, Lippert T and Schilling K 2005 *Phys. Rev. D* **72** 014503 (Preprint [hep-lat/0503016](#))
- [8] Ali Khan A *et al* 2004 (QCDSF-UKQCD Collaboration) *Nucl. Phys. B* **689** 175 (Preprint [hep-lat/0312030](#))
- [9] Ali Khan A *et al* 2002 (CP-PACS Collaboration) *Phys. Rev. D* **65** 054505
Ali Khan A *et al* 2003 (CP-PACS Collaboration) *Phys. Rev. D* **67** 059901 (Preprint [hep-lat/0105015](#)) (erratum)
- [10] Aoki S *et al* 2003 (JLQCD Collaboration) *Phys. Rev. D* **68** 054502 (Preprint [hep-lat/0212039](#))
- [11] Young R D, Leinweber D B and Thomas A W 2003 *Prog. Part. Nucl. Phys.* **50** 399 (Preprint [hep-lat/0212031](#))
- [12] Bernard V, Hemmert T R and Meissner U G 2004 *Nucl. Phys. A* **732** 149 (Preprint [hep-ph/0307115](#))
- [13] Holstein B R, Pascalutsa V and Vanderhaeghen M 2005 *Phys. Rev. D* **72** 094014 (Preprint [hep-ph/0507016](#))
- [14] Frink M, Meissner U G and Scheller I 2005 *Eur. Phys. J. A* **24** 395 (Preprint [hep-lat/0501024](#))
- [15] Hackett-Jones E J, Leinweber D B and Thomas A W 2000 *Phys. Lett. B* **494** 89 (Preprint [hep-lat/0008018](#))
- [16] Hemmert T R and Weise W 2002 *Eur. Phys. J. A* **15** 487 (Preprint [hep-lat/0204005](#))
Hemmert T R, Procura M and Weise W 2003 *Phys. Rev. D* **68** 075009 (Preprint [hep-lat/0303002](#))
- [17] Leinweber D B, Thomas A W, Tsushima K and Wright S V 2000 *Phys. Rev. D* **61** 074502 (Preprint [hep-lat/9906027](#))
- [18] Wang P, Leinweber D B, Thomas A W and Young R D 2007 *Phys. Rev. D* **75** 073012 (Preprint [hep-ph/0701082](#))
- [19] Detmold W, Melnitchouk W, Negele J W, Renner D B and Thomas A W 2001 *Phys. Rev. Lett.* **87** 172001 (Preprint [hep-lat/0103006](#))
- [20] Hemmert T R, Procura M and Weise W 2003 *Phys. Rev. D* **68** 075009 (Preprint [hep-lat/0303002](#))
- [21] Procura M, Musch B U, Hemmert T R and Weise W 2006 *AIP Conf. Proc.* **842** 240
- [22] Hackett-Jones E J, Leinweber D B and Thomas A W 2000 *Phys. Lett. B* **489** 143 (Preprint [hep-lat/0004006](#))
- [23] Hemmert T R, Procura M and Weise W 2003 *Nucl. Phys. A* **721** 938 (Preprint [hep-lat/0301021](#))

- [24] Lyubovitskij V E, Gutsche T and Faessler A 2001 *Phys. Rev. C* **64** 065203 (Preprint [hep-ph/0105043](#))
- [25] Lyubovitskij V E, Gutsche T, Faessler A and Drukarev E G 2001 *Phys. Rev. D* **63** 054026 (Preprint [hep-ph/0009341](#))
Lyubovitskij V E, Gutsche T, Faessler A and Vinh Mau R 2001 *Phys. Lett. B* **520** 204 (Preprint [hep-ph/0108134](#))
Lyubovitskij V E, Gutsche T, Faessler A and Vinh Mau R 2002 *Phys. Rev. C* **65** 025202 (Preprint [hep-ph/0109213](#))
Lyubovitskij V E, Wang P, Gutsche T and Faessler A 2002 *Phys. Rev. C* **66** 055204 (Preprint [hep-ph/0207225](#))
Simkovic F, Lyubovitskij V E, Gutsche T, Faessler A and Kovalenko S 2002 *Phys. Lett. B* **544** 121 (Preprint [hep-ph/0112277](#))
- [26] Cheedket S, Lyubovitskij V E, Gutsche T, Faessler A, Pumsa-Ard K and Yan Y 2004 *Eur. Phys. J. A* **20** 317 (Preprint [hep-ph/0212347](#))
Pumsa-Ard K, Lyubovitskij V E, Gutsche T, Faessler A and Cheedket S 2003 *Phys. Rev. C* **68** 015205 (Preprint [hep-ph/0304033](#))
Inoue T, Lyubovitskij V E, Gutsche T and Faessler A 2004 *Phys. Rev. C* **69** 035207 (Preprint [hep-ph/0311275](#))
Khosonthongkee K, Lyubovitskij V E, Gutsche T, Faessler A, Pumsa-Ard K, Cheedket S and Yan Y 2004 *J. Phys. G: Nucl. Part. Phys.* **30** 793 (Preprint [hep-ph/0403119](#))
- [27] Faessler A, Gutsche T, Lyubovitskij V E and Pumsa-Ard K 2006 *Phys. Rev. D* **73** 114021 (Preprint [hep-ph/0511319](#))
- [28] Faessler A, Gutsche T, Holstein B R, Lyubovitskij V E, Nicmorus D and Pumsa-Ard K 2006 *Phys. Rev. D* **74** 074010 (Preprint [hep-ph/0608015](#))
Faessler A, Gutsche T, Lyubovitskij V E and Pumsa-Ard K 2005 *Prog. Part. Nucl. Phys.* **55** 12
Faessler A, Gutsche T, Lyubovitskij V E and Pumsa-Ard K 2007 *AIP Conf. Proc.* **884** 43
Faessler A, Gutsche T, Holstein B R, Lyubovitskij V E, Nicmorus D and Pumsa-Ard K 2006 Preprint [hep-ph/0612246](#)
Faessler A, Gutsche T, Holstein B R and Lyubovitskij V E (in preparation)
- [29] Gasser J, Sainio M E and Svarc A 1988 *Nucl. Phys. B* **307** 779
- [30] Gasser J and Leutwyler H 1982 *Phys. Rep.* **87** 77
Gasser J and Leutwyler H 1985 *Nucl. Phys. B* **250** 465
- [31] Borasoy B and Meissner U G 1997 *Ann. Phys.* **254** 192 (Preprint [hep-ph/9607432](#))

CURRICULUM VITAE

NAME: Chalump Oonariya.

GENDER: Male.

NATIONALITY: Thai.

DATE OF BIRTH: September 3, 1972.

EMPLOYEE

- The Meteorological Department, Bangkok, Thailand (1999-present)

EDUCATIONAL BACKGROUND:

- B.Sc. in Physics, Ramkhamhaeng University, Bangkok, Thailand, 1995.

- M.Sc. in Nuclear Tech., Chulalongkorn University, Bangkok, Thailand, 2000.

PUBLICATIONS:

- Amand Faessler, Thomas Gutsche, Vasily E. Lyubovitskij and Chalump Oonariya, "**Dependence of Nucleon Properties on Pseudoscalar Meson Masses**", *J. Phys. G: Nucl. Part. Phys.* 35 025005 (14pp)

PRESENTATIONS:

- C. Oonariya, P. Suebka, C. Kobdaj and Y. Yan, " **$\pi\pi$ Reaction in Non-Relativistic Quark Mode**", *The 31st Congress on Science and Technology of Thailand*, Nakhon Ratchasima, Thailand

- C. Oonariya, C. Kobdaj, Y. Yan, A. Faessler, T. Gutsche and V. E. Lyubovitskij, "**Dependence of Baryon Octet Properties on Pseudoscalar Meson Masses**", *The 3rd Siam Physics Congress 2008*, Nakhon Ratchasima, Thailand.

FELLOWSHIPS:

- Deutscher Akademischer Austausch Dienst(DAAD), 2006-2007.

SKILL:

- Computer: Unix, ANSI C, C++, FORTRAN, Mathematica, Maple

- Language: Thai, English, German